UNCLASSIFIED

AD NUMBER
AD329725
CLASSIFICATION CHANGES
TO: **UNCLASSIFIED**
FROM: **CONFIDENTIAL**
LIMITATION CHANGES
TO: **Approved for public release; distribution is unlimited.**
FROM: **Distribution authorized to U.S. Gov't. agencies and their contractors; Administrative/Operational Use; OCT 1961. Other requests shall be referred to Office of the Naval Research, Arlington, VA 22303.**
AUTHORITY
31 Oct 1973, DoDD 5200.10 ; ONR ltr 30 Apr 1974

THIS PAGE IS UNCLASSIFIED

AD 329 725

Reproduced
by the

ARMED SERVICES TECHNICAL INFORMATION AGENCY
ARLINGTON HALL STATION
ARLINGTON 12, VIRGINIA

NOTICE: When government or other drawings, specifications or other data are used for any purpose other than in connection with a definitely related goyernment procurement operation, the U. S. Government thereby incurs no responsibility, nor any obligation whatsoever; and the fact that the Government may have formulated, furnished, or in any way supplied the said drawings, specifications, or other data is not to be regarded by implication or otherwise as in any manner licensing the holder or any other person or corporation, or conveying any rights or permission to manufacture, use or sell any patented invention that may in any way be related thereto.

329 725

SUBIC

Submarine Integrated Control

OFFICE OF
NAVAL
RESEARCH

GENERAL DYNAMICS CORPORATION
ELECTRIC BOAT DIVISION
GROTON, CONNECTICUT

Mathematical Concepts of the Automatic Statistical Processing Fire Control Computer (U)

This material contains information affecting the national defense of the United States within the meaning of the espionage laws, title 18, U.S.C., secs. 793 and 794, the transmission or revelation of which in any manner to an unauthorized person is prohibited by law.

DOWNGRADED AT 3 YEAR INTERVALS;
DECLASSIFIED AFTER 12 YEARS
DOD DIR 5200.10

Mathematical Concepts of the Automatic Statistical Processing Fire Control Computer (U)

by

Claude R. Gagnon
Frances R. Callanan

GENERAL DYNAMICS/ELECTRIC BOAT
Research and Development Department

Examined: _____
C. R. DeVoe
Computer Applications Supervisor

Approved: _____
Dr. A. J. van Woerkom
Chief Computer Scientist

ASTIA
JUN 28 1962
TISIA

C417-61-011
October 1961

CONFIDENTIAL

FOREWORD

This report was prepared by the Computer Applications Section of General Dynamics/Electric Boat as part of the Submarine Integrated Control Program (SUBIC) of the Office of Naval Research. Electric Boat is coordinator, under Contract Nonr 2512(00), of this program; Cdr. F. R. Haselton, Jr., USN, is Project Officer for ONR; Dr. H. E. Sheets is Project Coordinator for Electric Boat; and Dr. A. J. van Woerkom is Chief Computer Scientist.

The program is divided into several parts: ship control, weapon and tactical control, engineering control, communications, environmental control, and command control. This report is one of a series dealing with tactical control.

ABSTRACT
(Unclassified)

This report consists of a mathematical model of a simple, statistical fire control scheme. The equations are developed for the determination of relative target motion parameters, a complete bearings-only solution and complete solutions based upon hypothesized inputs of target speed, course, or range. The statistical properties of some of the results are analyzed and compared to Mark 113 results and idealized manual plots. A method of detecting target zigs is described and statistically evaluated. Methods of improving some of the present Mark 113 fire control system computational schemes are presented.

SUMMARY

Purposes

Automatic Statistical Processing (ASP) is a fire control computational scheme that has been developed to provide all available tactical data rapidly and accurately and, ultimately, to provide a fire control solution for a target employing evasive tactics.

Techniques

1. Bearing-time Curve and Relative Motion Analysis

ASP's basic technique consists of statistically smoothing bearings to a mathematical approximation to the bearing-time curve. By using a digital computer for rigorous statistical processing, the best possible curve (least-square fit) is produced. The smoothed curve used in manual plotting is obtained by eye and, in general, only approximates the least-square fit.

The equation of the least-square bearing-time curve yields the bearing (B), bearing-rate ($\dot{B}$) and bearing acceleration ($\ddot{B}$) as functions of time. These parameters contain all the essential information contained in the raw bearing-time data. The following relative motion parameters can be deduced from this information:

1. relative angle-on-the-bow (α)
2. relative course (θ)
3. ratio of relative speed to initial range (U/R_o)
4. minimum target speed ($V_{min}^{(2)}$)

In order to obtain a meaningful approximation to the bearing-time curve and the resulting parameters, it is necessary for own-ship to travel with uniform, rectilinear motion. This is true for both ASP and manual plotting techniques.

ASP also has the capacity to produce hypothetical solutions on any single leg of own-ship track by introducing values of target speed, course or range into the computer. The values introduced may be estimated, hypothesized or based on physical limitations. By displaying the resulting "solutions", qualitative information about possible tactical situations is provided.

2. Zig Detection

The initial step toward ultimate solution of the passive maneuvering target problem is the detection of target zigs. ASP includes a technique whereby a computer calculates the probability that a target has zigged. The principle used is fundamentally the same as that used in the Barnard plot. A least-square bearing-time curve is extrapolated to obtain an estimate of the expected future bearings. The occurrence of a target zig is then indicated by systematic deviations of the measured bearings from the predicted bearings. Since deviations will result from bearing noise even when a target zig has not occurred, only the probability of a target zig can be determined. Probabilities in excess of 95% are, however, usually interpreted as certainty. Comparison of the expected bearings to the measured bearings is continued for approximately two minutes whence the bearing data obtained in the two minute interval are automatically combined with the bearing history to form a new least-square fit. The next two minute interval is then scanned in the same manner. When a zig is detected, the history prior to detection is disregarded (zig detection reset) and a new history is collected on the next leg of target track for the purpose of detecting possible subsequent target zigs. Since the zig detector is also sensitive to own-ship zigs, it must be reset when own-ship maneuvers.

Two types of bearing-time curve-fitting have been investigated for purposes of zig detection: a curved line (quadratic scheme) and a straight line (linear scheme). The extrapolation and deviation caused by a target zig are illustrated in Fig. C-1-1 on page 116 for the quadratic scheme and in Fig. C-5-2 on page 126 for the linear scheme.

3. Bearings-only Complete Solution

When the zig detector indicates that the target is straight running, a complete bearings-only target localization solution is possible. To obtain the solution, own-ship travels on a straight leg and collects bearing-time data, then changes course and/or speed and collects a second set of bearing-time data. By combining the information contained in the resulting two statistically-smoothed bearing-time curves, the range, course and speed of the target can be obtained.

Results

1. Statistical Error Analysis

Since all bearing data have random deviations, all parameters derived from bearing-time data are subject to statistical uncertainty. The curves in sections 3, 4, 5, and 6 of Appendix B illustrate the uncertainties in the relative motion parameters. The uncertainties in bearing, bearing-rate and bearing acceleration decreases as tracking-time increases. The uncertainties in the other relative motion parameters decrease with increasing bearing-rate and time and with decreasing range. Although no formal error analysis has been made for the hypothetical solutions, their accuracies are not expected to be very high. However, this type of solution can be used to furnish early information about possible tactical situations.

The percentage error in bearings-only range decreases as tracking times and the absolute difference in the bearing-rates on the two own-ship legs increase. Statistical evaluation of the bearings-only solution has also indicated the possibility that bearing-rate and its uncertainty can be used to determine the optimum time for own-ship zig. The details for establishing an own-ship zig time criterion are yet to be determined.

The linear zig detection scheme has been found to be more effective for long range targets. Figs. C-6-1 and C-6-2 and the accompanying tables contain quantative comparisons of the two schemes.

2. Comparison of ASP with Manual Plots

To quantatively compare ASP with manual plots, it is necessary to assume that manual plots are rigorously least-square fitted. Comparison can then be made directly because ASP's mathematics are implicit in manual plotting techniques.

The ASP scheme is superior because of the high data assimilation rate possible using digital computer processing. Parameters are obtained more accurately, more rapidly and at longer ranges. The curves of Section 6 of Appendix B (pages 82 through 106) compare the accuracies achieved by the two techniques for various geometries. A complete discussion of the assumptions and results of the comparison is contained in Sections 4.A and 4.B of Part II of this report (pages 29 through 31).

3. Comparison of ASP with Mark 113

The Mark 113 system includes relative motion analysis and a complete bearings-only solution (Churn).

Relative motion analysis in the present Mark 113 is similar to that in ASP in that bearing-time data are used as input and own-ship is constrained to uniform, rectilinear motion to obtain a meaningful relative motion analysis. However, the only parameters provided by the Mark 113 relative motion analysis are the initial angle-on-the-bow and the ratio of relative speed to initial range. Since no statistical error analysis has been made for the Mark 113 relative motion parameters, accuracies for the two techniques cannot be compared.

In the Mark 113 system, a hypothetical solution can be obtained for an input of target speed only. In the event that a dual solution exists (see Fig. A-4-2 c page 51), only the longer range solution is provided, whereas ASP furnishes both solutions.

The Mark 113 bearings-only solution uses bearing-time data and own-ship motion parameters for at least two own-ship legs to provide target range, course and speed. Although Churn theoretically allows

own-ship freedom of motion (with resulting mathematical complexity), in reality, an optimum tactic (two straight legs differing in course and/or speed) is necessary to produce adequate solutions at SUBROC ranges. Also, own-ship straight legs are required in order to detect target zigs. It is therefore apparent that the freedom of own-ship motion provided by the Mark 113 system is not a requirement in connection with SUBROC fire control solutions.

4. Bearing Pre-Smoothing

In addition to being complex, the mathematics in Churn include an inherent bias. It has been shown (reference 1) that this bias can be reduced to insignificance by pre-smoothing (averaging) groups of bearings. At present the averaging criterion is based on bearing-rate. The ASP study indicates that a better criterion, based on bearing acceleration and its uncertainty, can be developed.

CONTENTS

	Page
Foreword	i
Abstract	iii
Summary	v
Introduction	1
I - Target Localization Solutions	
1. Geometric Relations, Definitions, Symbols	5
2. Bearing-Time Relation and Approximation	9
3. Relative Motion Parameters	11
4. Requirements for a Complete Solution	13
5. Solution Using Speed Input	13
6. Solution Using Range Input	16
7. Solution Using Course Input	18
8. Bearings-Only Solution	18
II - Statistical Properties	
1. Variances and Covariances of Least-Square Coefficients	23
2. Variance in Relative Motion Parameters	25
3. Bearings-Only Range Variance	27
4. Examples for Particular Geometries and Comparison of ASP with Manual Plots	29
5. Bearing Pre-Smoothing	31
III - Long Range Bearings-Only Zig Detection	
1. Detection Scheme	33
2. Equations	33
3. Theoretical Results	36
IV - Conclusions and Areas Requiring Further Investigation	39
Appendix A - Derivation of Target Localization Equations	43
Appendix B - Derivation of Statistical Properties	63
Appendix C - Derivation of Zig Detection Equations	115
References	145

FIGURES

		Page
I-1-1	Earth-Fixed Coordinates	6
I-1-2	Own-Ship Coordinates	7
I-1-3	Velocity Vectors	8
I-2-1	Bearing-Time Curves	10
I-5-1	Speed Input Solution Possibilities	15
A-1-1	Own-Ship Coordinates	44
A-4-1	Velocity Vectors	50
A-4-2	Earth-Related Dual-Solution Illustration	51
A-4-3	First and Fourth Quadrant Solution Possibilities	52
A-4-4	Second and Third Quadrant Solution Possibilities	54
A-4-5	Speed Input Solution Possibilities	55
B-1-1	σ_a Versus Time	67
B-1-2	σ_b Versus Time	68
B-1-3	σ_c Versus Time	69
B-3-1	$\sigma_{\dot{B}}$ Versus Time	72
B-4-1	σ_α and σ_θ Versus Time	76
B-5-1	σ_{U/R_o} Versus Time for $U/R_o = 2$ hr^{-1}	78
B-5-2	σ_{U/R_o} Versus Time for $U/R_o = 1$ hr^{-1}	79
B-5-3	σ_{U/R_o} Versus Time for $U/R_o = 0.5$ hr^{-1}	80
B-6-1	Case 1 Geometry	82
B-6-2	Case 1 $\sigma_{U/R_o}/U/R_o$ Versus Time	83
B-6-3	Case 1 σ_α Versus Time	84
B-6-4	Case 1 $\sigma_{\dot{B}/\dot{B}}$ Versus Time	85
B-6-5	Case 1 $\sigma_{\ddot{B}/\ddot{B}}$ Versus Time	86
B-6-6	Case 2 Geometry	87
B-6-7	Case 2 $\sigma_{U/R_o}/U/R_o$ Versus Time	88
B-6-8	Case 2 σ_α Versus Time	89
B-6-9	Case 2 $\sigma_{\dot{B}/\dot{B}}$ Versus Time	90
B-6-10	Case 2 $\sigma_{\ddot{B}/\ddot{B}}$ Versus Time	91

		Page
B-6-11	Case 3 Geometry	92
B-6-12	Case 3 $\sigma_{U/R_o}/U/R_o$ Versus Time	93
B-6-13	Case 3 σ_{α} Versus Time	94
B-6-14	Case 3 $\sigma_{\dot{B}/\dot{B}}$ Versus Time	95
B-6-15	Case 3 $\sigma_{\ddot{B}/\ddot{B}}$ Versus Time	96
B-6-16	Case 4 Geometry	97
B-6-17	Case 4 $\sigma_{U/R_o}/U/R_o$ Versus Time	98
B-6-18	Case 4 σ_{α} Versus Time	99
B-6-19	Case 4 $\sigma_{\dot{B}/\dot{B}}$ Versus Time	100
B-6-20	Case 4 $\sigma_{\ddot{B}/\ddot{B}}$ Versus Time	101
B-6-21	Case 5 Geometry	102
B-6-22	Case 5 $\sigma_{U/R_o}/U/R_o$ Versus Time	103
B-6-23	Case 5 σ_{α} Versus Time	104
B-6-24	Case 5 $\sigma_{\dot{B}/\dot{B}}$ Versus Time	105
B-6-25	Case 5 $\sigma_{\ddot{B}/\ddot{B}}$ Versus Time	106
B-7-1	x-opt Versus y	110
B-7-2	z-opt Versus y	111
C-1-1	Bearing-Time Curves for a Zigging Target	116
C-3-1	Standard Deviation of Γ Versus Time for Quadratic Extrapolation	122
C-4-1	Standard Deviation of Γ Versus Time for Linear Extrapolation	123
C-5-1	Linear Bearing-Time Curve for a Zigging Target	126
C-5-2	Γ_j for $t_z < t_j$	126
C-5-3	Behavior of Linear Γ_j in Succeeding Scan Intervals	130
C-5-4	Zig Geometry No. 1	132
C-5-5	Zig Geometry No. 2	132
C-5-6	Γ Linear Versus Zig Time for Given Geometries	133
C-5-7	Γ Linear Versus Zig Time for Given Geometries	134
C-5-8	Γ Linear Versus Zig Time for Given Geometries	135
C-5-9	Behavior of Quadratic Γ_j in Succeeding Scan Interval	136
C-6-1	Γ_j Quadratic Versus Time	139
C-6-2	Γ_j Linear Versus Time	140

		Page
C-6-3	Γ Linear Versus Time for Two-Minute Scans - 20 Nautical Mile Target	141
C-6-4	Γ Linear Versus Time for Two-Minute Scans - 15 Nautical Mile Target	142
C-6-5	Γ Linear Versus Time for Two-Minute Scans - 10 Nautical Mile Target	143

INTRODUCTION

Automatic Statistical Processing (ASP) is a continuation of earlier SUBIC studies in the fire control area. The objective set forth for ASP (in addition to the more general SUBIC objectives) is to provide all useful tactical information which can be derived from available data as rapidly and accurately as possible.

It is felt that a significant portion of available tactical information is not now displayed in present automatic computing systems. For example, in the existing Mark 113 fire control system, the initial relative angle-on-the-bow and ratio of the relative target speed to initial range are the only quantities derived from the bearings on the first leg of own-ship maneuver. Range, course, and speed are available either upon entering a target speed estimate or after an own-ship zig. Other tactical information such as target zig indications, smoothed bearings and bearing-rate, a quantity often used to fire acoustic torpedoes, is obtained from manual plots which are severely limited in accuracy at the longer ranges.

The technique used to meet the ASP objective consists of smoothing, in the statistical sense, bearing data to a mathematical approximation to the bearing-time curve. This technique provides relative motion parameters during the first leg of own-ship maneuver, results in simplified solution equations, and makes zig detection possible. In order to achieve these ends, however, it is necessary to constrain own-ship to uniform rectilinear motion. Relative motion parameters can be obtained on any own-ship uniform rectilinear motion leg. Such legs will be referred to as single legs throughout this report; and relative motion analysis, or simply single leg analysis will be used to designate calculations leading to relative motion parameters.

The relative motion parameters which can be obtained from any single

leg analysis are:

1. relative angle-on-the-bow
2. relative course
3. statistically smoothed bearings
4. bearing-rate
5. change in bearing-rate
6. ratio of relative speed to initial range
7. minimum target speed

These quantities can be supplied continuously for the entire tracking period. It is also possible for the operator to introduce into the computer estimates or hypothetical values of target range, course or speed to obtain possible target localization solutions. The possible solutions can be geographically represented on a display similar to a strip plot for a qualitative "picture" of the possible tactical situations.

When confronted with a zigging target, as indicated by the zig detector, it may be possible to obtain a range estimate by obtaining parameters for each leg of the target track and, from these, selecting portions of the possible target tracks where zigs will not severely degrade range solutions. In the event that the target is sinuating, it may be possible to approximate the track by a series of straight legs and use the same technique as for a zigging target.

Thus, a leg-by-leg analysis, coupled with the ability of a trained operator, might possibly be used to partially overcome the difficulties presented by a zigging target so that a rough estimate of target range can be passively obtained. This range could be used to indicate whether the target is within weapon range and, if so, which weapon to use. Single ping techniques could then be used to obtain a more accurate range, if necessary. Thus, the possibility of pinging a target beyond weapon ranges could be reduced.

In addition to the objectives and capabilities mentioned above, the ASP fire control system can also be used to obtain a complete bearings-only solution. To obtain this solution, own-ship maneuver must consist of two straight legs differing in course and/or speed. Comparison of the bearings-only solution to the hypothetical solutions obtained on first leg of own-ship maneuver can serve to increase operator confidence in computer outputs.

This report is preliminary and represents the results of the study to date. Conclusions based on this work and an outline of the work considered for the future are contained in Part IV.

I

TARGET LOCALIZATION SOLUTIONS

1. Geometric Relations, Definitions, and Symbols

The expression target localization is used here to designate the data processing which provides information about the time-dependent position of the target relative to own-ship. Complete knowledge of the target's relative position as a function of time (subject to statistical uncertainties) will be called a complete solution. Thus, target range and bearing as functions of time; or target range, course and speed, and own-ship motion constitute a complete solution.

The geometry for an earth-fixed coordinate system is shown in Fig. I-1-1 where both own-ship and target are traveling with uniform motion*. Fig. I-1-2 depicts the same situation, but with the coordinate system origin fixed to own-ship. The velocity vector relations are illustrated in Fig. I-1-3.

The symbols used in the aforementioned figures are also used in the mathematical development. Vector quantities are designated by horizontal bars above the symbols; their magnitudes are designated by the symbols without the bars. Superscripts (1) and (2) refer to own-ship and target quantities, respectively. Inputs to the target localization computer other than bearing data and own-ship parameters are designated by an e subscript.

Equations appearing in Sections I, II, and III of this report are developed in the appendices and bear the same numbers. The useful equations for target localization solutions are enclosed in rectangles.

*This will be assumed throughout unless otherwise indicated.

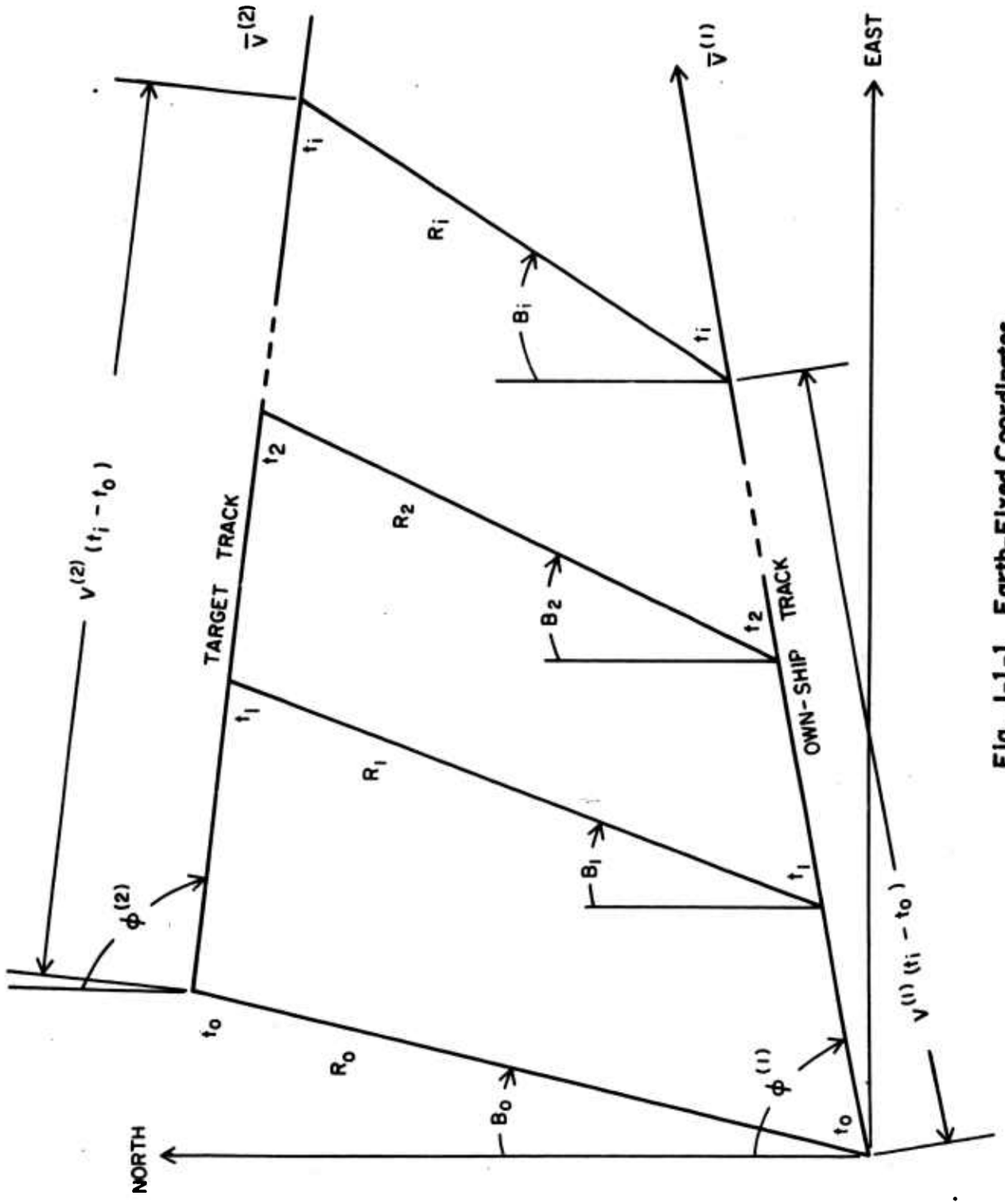

Fig. 1-1-1 Earth-Fixed Coordinates

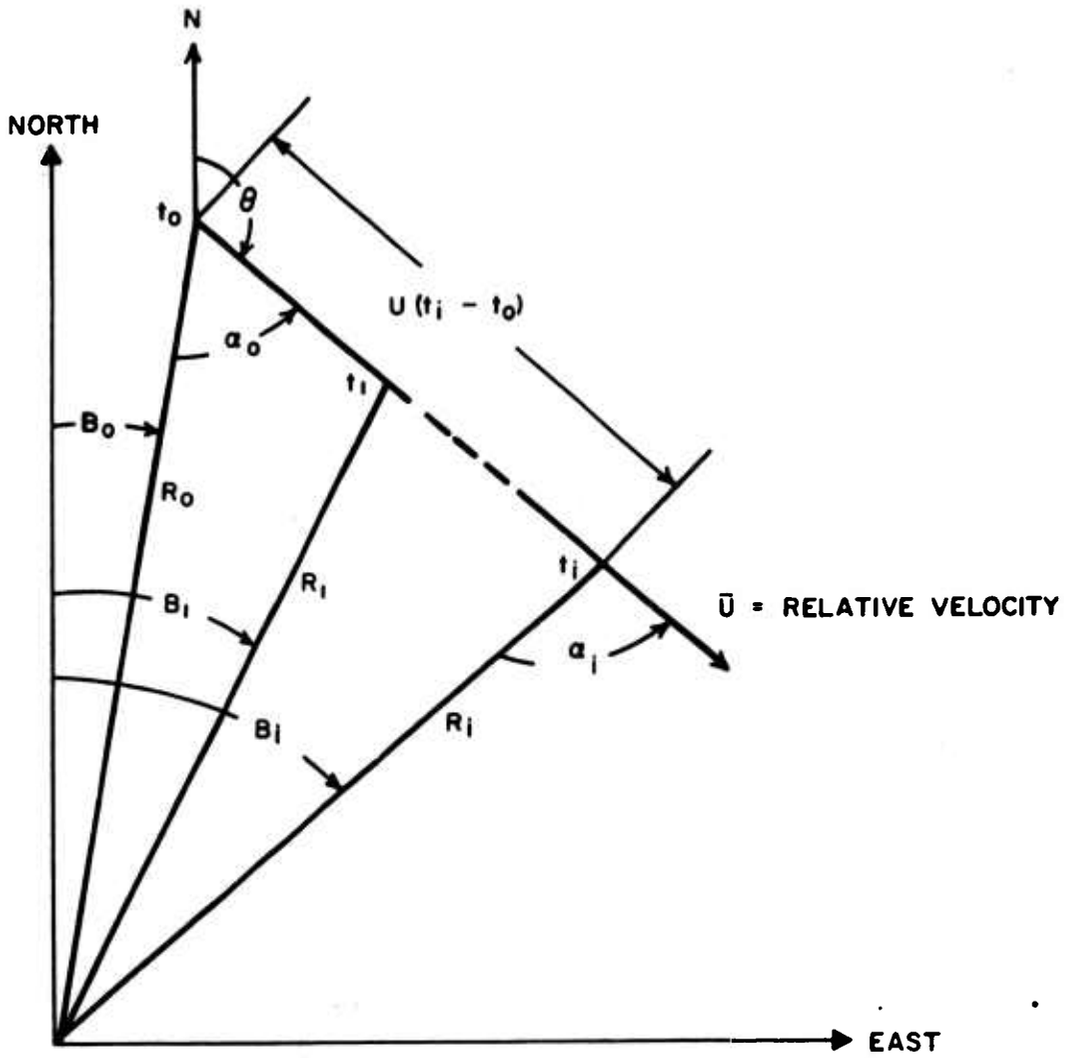

Fig. 1-1-2 Own-Ship Coordinates

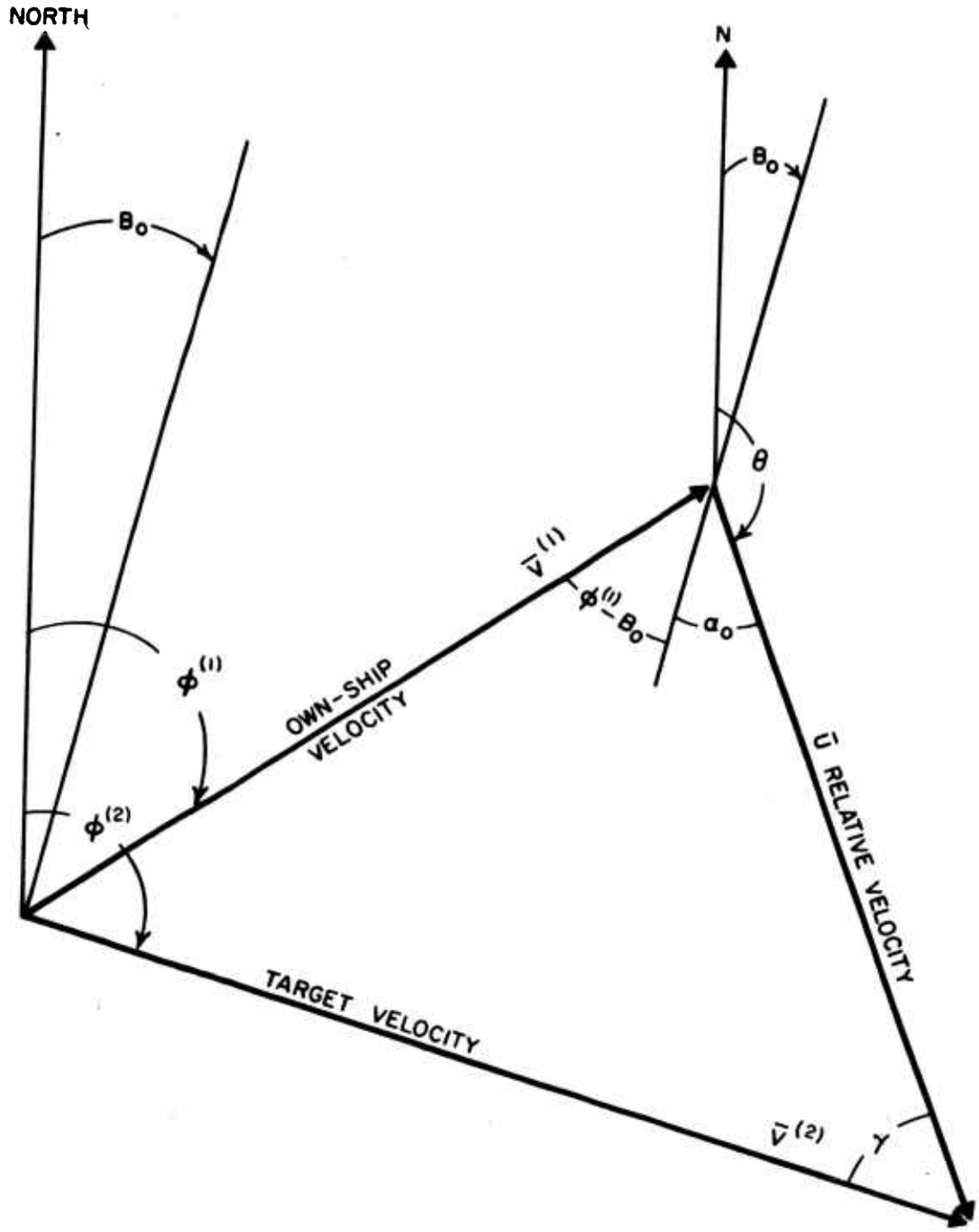

Fig. I-1-3 Velocity Vectors

2. Bearing-Time Relation and Approximation

Typical bearing-time relations are qualitatively represented by Fig. I-2-1 for U/R_o both small and large. The point of maximum bearing-rate is the closest point of approach (CPA) of the target.

It is shown in Section 1 of Appendix A that limited portions of the bearing-time relation can be approximated by

$$\boxed{B = a+b(t-t_o)+c(t-t_o)^2} \qquad \text{(A-1-2)}$$

in which

$$a = B_o, \qquad \text{(A-1-3)}$$

$$b = (U/R_o)\ \sin \alpha_o, \qquad \text{(A-1-4)}$$

and

$$c = (U/R_o)^2\ \sin \alpha_o \cos \alpha_o. \qquad \text{(A-1-5)}$$

The approximation to the bearing time curve (equation A-1-2) is more accurate at long ranges than at short ranges.

A least-square processing of bearings versus time using (A-1-2) yields the matrix equation

$$\boxed{u = C\ v} \qquad \text{(A-1-9)}$$

in which

$$\boxed{u = \begin{bmatrix} a \\ b \\ c \end{bmatrix}}, \qquad \text{(A-1-10)}$$

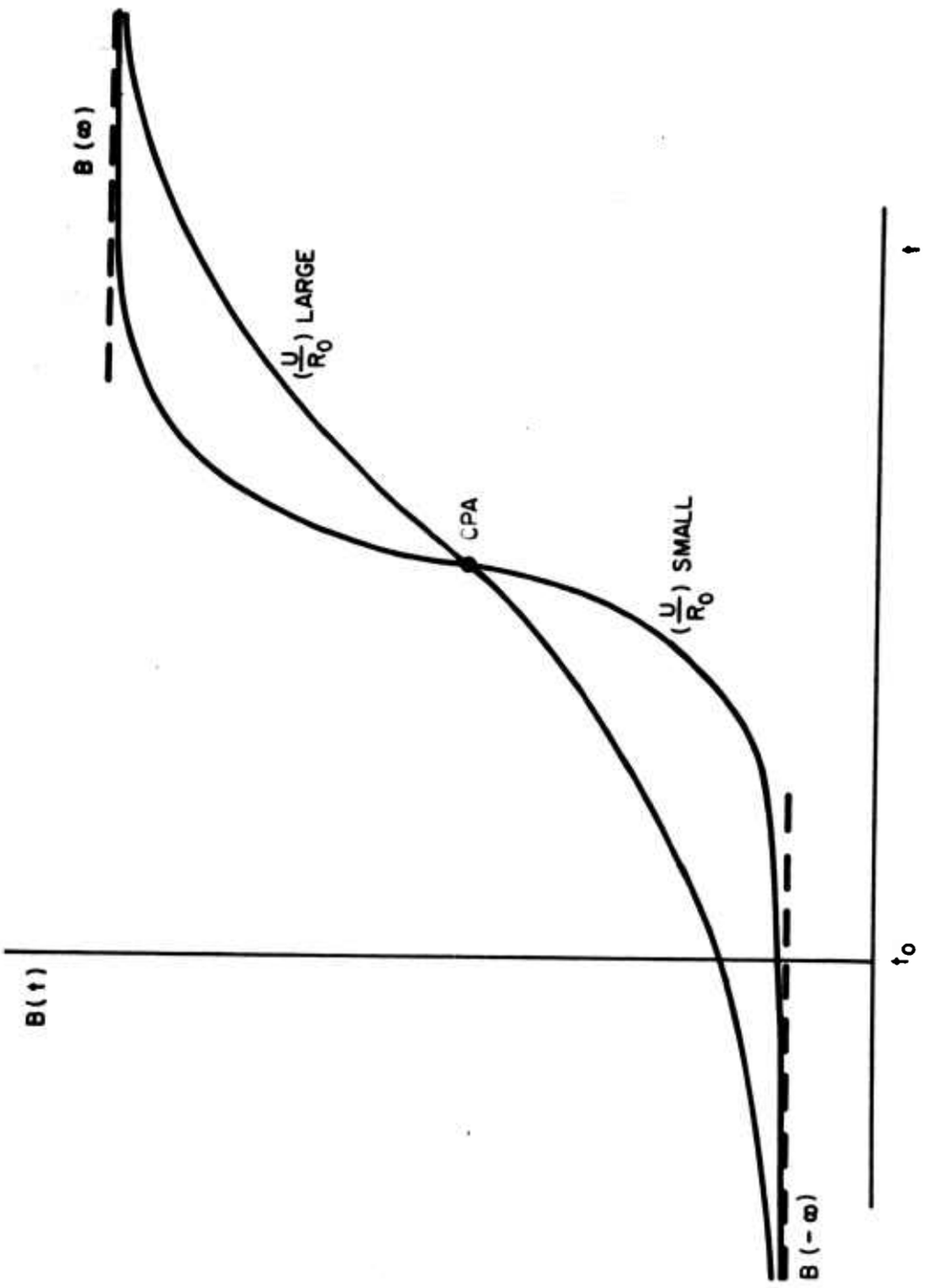

Fig. I-2-1 Bearing-Time Curves

$$v = \begin{bmatrix} \Sigma B_i \\ \Sigma B_i (t_i - t_o) \\ \Sigma B_i (t_i - t_o)^2 \end{bmatrix} , \qquad \text{(A-1-11)}$$

$$C = A^{-1} , \qquad \text{(A-1-12)}$$

$$A = \begin{bmatrix} n & \Sigma (t_i - t_o) & \Sigma (t_i - t_o)^2 \\ \Sigma (t_i - t_o) & \Sigma (t_i - t_o)^2 & \Sigma (t_i - t_o)^3 \\ \Sigma (t_i - t_o)^2 & \Sigma (t_i - t_o)^3 & \Sigma (t_i - t_o)^4 \end{bmatrix}$$

and B_i is the bearing obtained at time t_i.

The coefficients a, b, and c as obtained from equations (A-1-9, 10) are used in the subsequent section to obtain relative motion parameters.

3. Relative Motion Parameters

The relative motion parameters are those quantities which are obtainable on a single leg of own-ship maneuver.

The equations of this section are developed in Sections 2 and 3 of Appendix A.

Differentiating equation (A-1-2) with respect to time gives

$$\dot{B} = b + 2c(t-t_o) \qquad \text{(A-2-1)}$$

which when differentiated again gives

$$\ddot{B} = 2c \; . \qquad \text{(A-2-2)}$$

$\dot{B}$ and $\ddot{B}$ are bearing-rate and the change in bearing-rate, respectively. The change in bearing-rate indicates whether the target is opening or closing.

The relative angle-on-the-bow is obtained from the relation

$$\alpha_o = \tan^{-1}(b^2/c) \qquad \text{(A-3-1)}$$

for the initial value and from

$$\alpha(t) = \alpha_o + B(t) - a \qquad \text{(A-3-2)}$$

for any subsequent time (t).

Relative course can then be found from the relation

$$\theta = \pi - \alpha_o + a \; . \qquad \text{(A-3-3)}$$

The ratio of relative speed to initial range can also be obtained from bearing data alone. The relation is expressed by

$$\boxed{U/R_o = b/\sin \alpha_o}\ , \qquad \text{(A-3-4)}$$

or

$$\boxed{U/R_o = \left[\frac{c^2+b^4}{b^2}\right]^{1/2}}\ . \qquad \text{(A-3-5)}$$

4. Requirements for a Complete Solution

Bearing data alone is insufficient to obtain a complete solution when own-ship travels with uniform motion. It is possible, however, to obtain a complete solution when either range, course, or speed of target is specified (i.e., obtained externally). Occasionally, estimates of one or more of these parameters are available and can be used to obtain estimates of the remaining parameters. Alternatively, values can be hypothesized in order to obtain various possibilities for the remaining parameters. Thus, for example, a submariner might ask for possible ranges and courses under the hypotheses that the target speed is ten, twelve, and fifteen knots. Hypothesized parameters are perhaps more prevalent than estimated parameters in the manual and semi-automatic plotting systems.

5. Solution Using Speed Input

In this and the following sections, inputs to the target localization computer other than bearing data and own-ship parameters are designated by an e subscript.

The equations of this section provide a complete solution from bearing data and a given target speed ($V_e^{(2)}$). The development is in Section 4 of Appendix A.

Target course is given by

$$\boxed{\phi^{(2)} = \pi - \gamma + a - \alpha_o} \qquad \text{(A-4-1)}$$

in which

$$\boxed{\gamma = \sin^{-1}\left[\frac{V^{(1)}}{V_e^{(2)}} \sin(\phi^{(1)} - a + \alpha_o)\right]} \; . \qquad \text{(A-4-2)}$$

Equation (A-4-2) indicates the possibility of two solutions. This dual solution possibility is a property of the fire control geometry and is independent of the particular mathematical descriptions used (see Section 4 of Appendix A). It is also possible to enter a speed $V_e^{(2)}$ which is too small to provide a solution. This latter situation leads to a minimum target speed (subject to statistical uncertainties).

By examining the angle $(\phi^{(1)} - a + \alpha_o)$ and $V_e^{(2)}$, the various solution possibilities may be determined. Fig. I-5-1 summarizes the different possibilities.

When more than one solution exists, two values of γ exist. One is given by the principal value of equation (A-4-2) and the other by its complement. Thus

$$\boxed{\gamma_1 = \gamma} \qquad \text{(A-4-4)}$$

$$\boxed{\gamma_2 = \pi - \gamma} \qquad \text{(A-4-5)}$$

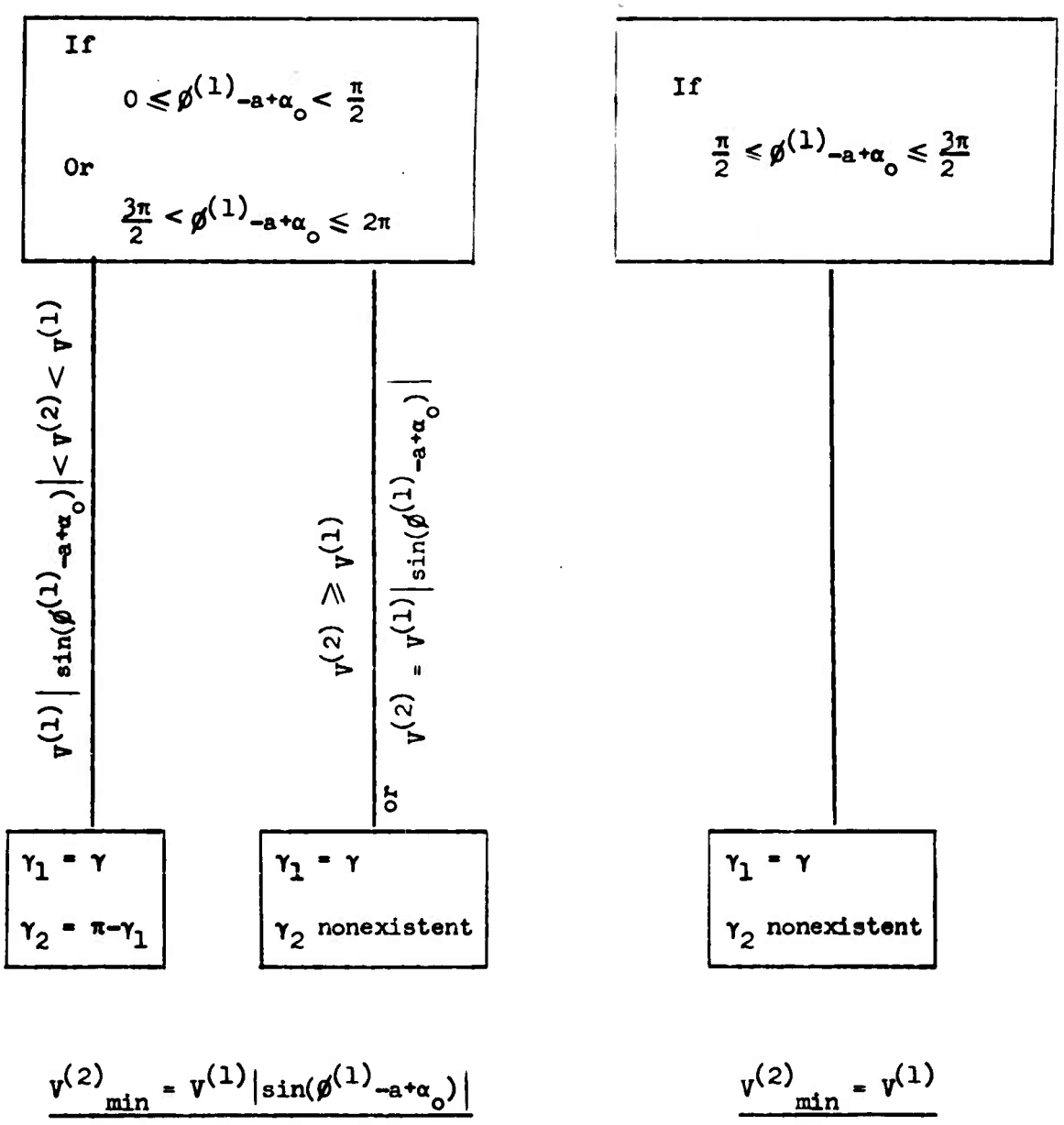

Fig. I-5-1 Speed Input Solution Possibilities

In the event that two γ angles are possible, equation (A-4-1) and those which follow will have to be duplicated to provide the two possible solutions. Thus,

$$\phi_j^{(2)} = \pi - \gamma_j + a - \alpha_o \qquad (j = 1 \text{ or } 1,2) \quad , \qquad \text{(A-4-7)}$$

$$U_j = \left[V^{(1)^2} + V_e^{(2)^2} - 2V^{(1)} V_e^{(2)} \cos(\phi_j^{(2)} - \phi^{(1)}) \right]^{1/2} \quad , \text{(A-4-8)}$$

$$R_{o_j} = bU_j/(c^2 + b^4)^{1/2} \quad , \text{and} \quad R(t)_j = \frac{R_{oj} b}{b + c(t - t_o)} \qquad \text{(A-4-9) and (A-4-10)}$$

in which R(t) is the range at any time t.

In many cases, one of the two solutions will be physically absurd although it is mathematically possible.

6. Solution Using Range Input

The equations of this section are derived in Section 5 of Appendix A.

Let $R_e(t_e)$ be a range input at time t_e, then

$$V_x^{(2)}(t_e) = V^{(1)} \sin \left[\phi^{(1)} - B(t_e) \right] + R_e(t_e) \left[b + 2c(t_e - t_o) \right] \qquad \text{(A-5-6)}$$

and

$$V_y^{(2)}(t_e) = V^{(1)}\cos\left[\phi^{(1)} - B(t_e)\right] - \frac{R_e(t_e)c}{b+c(t_e-t_o)} \qquad \text{(A-5-7)}$$

in which $V_x^{(2)}(t_e)$ and $V_y^{(2)}(t_e)$ are the cross-line-of-sight and along-line-of-sight speeds at t_e, respectively, and

$$B(t_e) = a+b(t_e-t_o)+c(t_e-t_o)^2 \qquad \text{(A-5-2)}$$

Target speed is then obtained by

$$V^{(2)} = \left[V_x^{(2)2}(t_e)+V_y^{(2)2}(t_e)\right]^{1/2} \qquad \text{(A-5-8)}$$

and the target course by

$$\phi^{(2)} = B(t_e)+\tan^{-1}\left[\frac{V_x^{(2)}(t_e)}{V_y^{(2)}(t_e)}\right] \qquad \text{(A-5-9)}$$

Range at any time other than t_e is then

$$R(t) = \frac{R_e(t_e)\left[b+c(t_e-t_o)\right]}{b+c(t-t_o)} \qquad \text{(A-5-10)}$$

7. Solution Using Course Input (See Section 6 of Appendix A for development)

For an estimate of target course ($\phi_e^{(2)}$), target speed is obtained from

$$V^{(2)} = \frac{V^{(1)} \sin(\phi^{(1)} - a + \alpha_o)}{\sin \gamma} \qquad \text{(A-6-2)}$$

in which

$$\gamma = \pi + a - \alpha_o - \phi_e^{(2)} \qquad \text{(A-6-1)}$$

Target range can then be found from

$$R(t) = \frac{R_o b}{b + c(t - t_o)} \qquad \text{(A-4-10)}$$

in which

$$R_o = \frac{\left[V^{(1)2} + V^{(2)2} - 2V^{(1)}V^{(2)} \cos(\phi_e^{(2)} - \phi^{(1)})\right]^{1/2} b}{(c^2 + b^4)^{1/2}} \qquad \text{(A-6-3)}$$

8. Bearings-Only Solution (See Section 7 of Appendix A for development)

For a bearings-only solution, own-ship travels for a time t' with uniform motion, then changes course and/or speed and travels with uniform motion until the end of the tracking time. The simplifying assumption is made that own-ship changes course and/or speed instantaneously at

t'.* Bearing data is collected and processed on each of these two "legs" of own-ship track. The subscripts 1 and 2 are used to indicate first and second leg parameters, respectively. The x and y subscripts are used to indicate the cross-line-of-sight and along-line-of-sight speeds, respectively.

At the time of own-ship zig (t'), it can be seen that two values of own-ship cross-line-of-sight speed and two values of bearing-rate are obtainable, one from each of the legs of own-ship track. Thus, for leg 1,

$$\boxed{V_{1x}^{(1)}(t') = V_1^{(1)}\sin\left[\phi_1^{(1)} - B(t')\right]}, \qquad \text{(A-7-4)}$$

and

$$\boxed{\dot{B}_1(t') = b_1 + 2c_1(t'-t_o)}. \qquad \text{(A-7-7)}$$

For leg 2,

$$\boxed{V_{2x}^{(1)}(t') = V_2^{(1)}\sin\left[\phi_2^{(1)} - B(t')\right]}, \qquad \text{(A-7-5)}$$

and

$$\boxed{\dot{B}_2(t') = b_2}. \qquad \text{(A-7-8)}$$

*See Section 2, Part IV.

The bearing B(t') is common to both legs and is calculated using the appropriate time weighing factors. Thus,

$$B(t') = \frac{t'}{t}\left[a_1+b_1(t'-t_o)+c_1(t'-t_o)^2\right]+\frac{t-t'}{t}a_2 \quad . \qquad \text{(A-7-6)}$$

The range at t' is then calculated from

$$R(t') = \frac{V_{1x}^{(1)}(t')-V_{2x}^{(1)}(t')}{\dot{B}_2(t')-\dot{B}_1(t')} \qquad \text{(A-7-3)}$$

and for any subsequent time (t),

$$R(t) = \frac{R(t')b_2}{b_2+c_2(t-t')} \quad . \qquad \text{(A-7-9)}$$

Target speed and course are constant by assumption and can, therefore, be calculated using information obtained on both legs of own-ship maneuver. Thus, for leg k (k = 1, 2),

$$V_{kx}^{(2)}(t') = V_k^{(1)}\sin\left[\phi_k^{(1)}-B(t')\right]+R(t')\dot{B}_k(t') \quad , \qquad \text{(A-7-10)}$$

and

$$V_{ky}^{(2)}(t') = V_k^{(1)}\cos\left[\phi_k^{(1)}-B(t')\right]+\dot{R}_k(t') \qquad \text{(A-7-11)}$$

in which B(t') is found by equation (A-7-6),

$$\dot{R}_1(t') = - \frac{R(t')c_1}{b_1+c_1(t'-t_o)} , \qquad \text{(A-7-12)}$$

and

$$\dot{R}_2(t') = - \frac{R(t')c_2}{b_2} . \qquad \text{(A-7-13)}$$

Using the above equations,

$$V_k^{(2)} = \left\{ \left[V_{kx}^{(2)}(t') \right]^2 + \left[V_{ky}^{(2)}(t') \right]^2 \right\}^{1/2} , \qquad \text{(A-7-14)}$$

and

$$\phi_k^{(2)} = B(t') + \tan^{-1} \left[\frac{V_{kx}^{(2)}(t')}{V_{ky}^{(2)}(t')} \right] . \qquad \text{(A-7-15)}$$

Introducing the appropriate weighing factors,

$$V^{(2)} = W_1 V_1^{(2)} + W_2 V_2^{(2)} \qquad \text{(A-7-16)}$$

and

$$\phi^{(2)} = W_3 \phi_1^{(2)} + W_4 \phi_2^{(2)} \qquad \text{(A-7-17)}$$

II
STATISTICAL PROPERTIES

1. Variances and Covariences of Least-Square Coefficients (See Section 1 of Appendix B for development)

The variances, covariances, and correlation coefficients of the coefficients a, b, and c are given by

$$\boxed{\begin{aligned} \sigma_a^2 &= c_{11}\sigma_B^2 \\ \sigma_b^2 &= c_{22}\sigma_B^2 \\ \sigma_c^2 &= c_{33}\sigma_B^2 \end{aligned}}, \qquad \text{(B-1-2)}$$

$$\boxed{\begin{aligned} \tau_{ab}\sigma_a\sigma_b &= c_{12}\sigma_B^2 \\ \tau_{bc}\sigma_b\sigma_c &= c_{23}\sigma_B^2 \\ \tau_{ac}\sigma_a\sigma_c &= c_{13}\sigma_B^2 \end{aligned}}, \qquad \text{(B-1-3)}$$

$$\boxed{\begin{aligned} \tau_{ab} &= \frac{c_{12}}{(c_{11}c_{22})^{1/2}} \\ \tau_{bc} &= \frac{c_{23}}{(c_{22}c_{33})^{1/2}} \\ \tau_{ac} &= \frac{c_{13}}{(c_{11}c_{33})^{1/2}} \end{aligned}} \qquad \text{(B-1-4)}$$

where the c_{ij}'s are the elements of the inverse of matrix A, which is obtained from the coefficients of a, b, and c of equations (A-1-7) or

$$A = \begin{bmatrix} n & \Sigma(t_i-t_o) & \Sigma(t_i-t_o)^2 \\ \Sigma(t_i-t_o) & \Sigma(t_i-t_o)^2 & \Sigma(t_i-t_o)^3 \\ \Sigma(t_i-t_o)^2 & \Sigma(t_i-t_o)^3 & \Sigma(t_i-t_o)^4 \end{bmatrix}.$$

The elements of A consist of somewhat cumbersome summations. Therefore, to facilitate calculations for analysis it is assumed that the bearings are obtained at equal time increments (T). The variances then become

$$\sigma_a^2 = \frac{9}{n}\sigma_B^2,$$

$$\sigma_b^2 = \frac{192}{T^2n^3}\sigma_B^2, \qquad \text{(B-1-12)}$$

$$\sigma_c^2 = \frac{180}{T^4n^5}\sigma_B^2.$$

in which σ_B is the standard deviation of sonar bearings and n is the number of bearings sampled.

The covariances are

$$\tau_{ab}\sigma_a\sigma_b = -\frac{36}{Tn^2}\sigma_B^2,$$

$$\tau_{bc}\sigma_b\sigma_c = -\frac{180}{T^3n^4}\sigma_B^2, \qquad \text{(B-1-13)}$$

$$\tau_{ac}\sigma_a\sigma_c = \frac{30}{T^2n^3}\sigma_B^2,$$

and the correlation coefficients are

$$\tau_{ab} = -\sqrt{3}/2 = -0.866,$$

$$\tau_{bc} = -\sqrt{15}/4 = -0.97, \qquad \text{(B-1-14)}$$

$$\tau_{ac} = \sqrt{5}/3 = 0.745.$$

Figs. B-1-1, B-1-2, and B-1-3 of Section 1, Appendix B, are plots of the standard deviations of the least square coefficients as functions of time. A bearing sampling interval of two seconds and a sonar bearing standard deviation of 0.2° are used.

2. Variance in Relative Motion Parameters (See Sections 3 and 4 of Appendix B for development)

The standard deviation in bearing rate is given by

$$\boxed{\sigma_{\dot{B}} \cong \sigma_b} \; . \qquad \text{(B-3-2)}$$

The standard deviation in the change in bearing rate is given by

$$\boxed{\sigma_{\ddot{B}} = 2\sigma_c} \; . \qquad \text{(B-3-3)}$$

The standard deviation in α_o is

$$\boxed{\sigma_{\alpha_o} \cong (U/R_o)^{-2}\sigma_c} \qquad \text{(B-4-2)}$$

and

$$\boxed{\sigma_\alpha = \sigma_{\alpha_o}} \quad . \tag{B-4-3}$$

Also, the standard deviation in θ is

$$\boxed{\sigma_\theta \cong (U/R_o)^{-2}\sigma_c \cong \sigma_\alpha} \quad . \tag{B-4-7}$$

The general expression for standard deviation in the parameter U/R_o is given by

$$\boxed{\sigma_{U/R_o} \cong \left| \left(\frac{\sin^2\alpha_o - \cos^2\alpha_o}{\sin \alpha_o} \right) \sigma_b - (U/R_o)^{-1} \cot \alpha_o \sigma_c \right|} \quad . \tag{B-5-1}$$

For $\alpha_o \cong \pi/2$, equation (B-5-1) reduces to

$$\sigma_{U/R_o} \cong \sigma_b . \tag{B-5-2}$$

For $\alpha_o \cong 0$,

$$\sigma_{U/R_o} \longrightarrow \infty \ , \tag{B-5-3}$$

but in this case bearing rate is zero and the only information which can be derived from the data is,

$$B = \text{constant}$$

and

$$\dot{B} = 0.$$

The figures in Sections 3, 4, and 5 of Appendix B illustrate the variation of the standard deviations of the relative motion parameters with tracking time.

3. Bearings-Only Range Variance

The equations of this section are developed in Section 7 of Appendix B.

The variance of the range at current time (t) is obtained from

$$\frac{\sigma_{R(t)}}{R(t)} = \left[\left(\frac{T_t}{T_1}\right)^3 + \left(\frac{T_t}{T_2}\right)^3\left(\frac{\dot{B}_1}{\dot{B}_2}\right)^2\right]^{1/2} \frac{8\sqrt{3}\, T^{1/2}\sigma_B}{T_t^{3/2}|\Delta \dot{B}|} \quad , \qquad \text{(B-7-3)}$$

and the variance of the range at zig time (t') is obtained from

$$\frac{\sigma_{R(t')}}{R(t')} = \left[\left(\frac{T_t}{T_1}\right)^3 + \left(\frac{T_t}{T_2}\right)^3\right]^{1/2} \frac{8\sqrt{3}\, T^{1/2}\sigma_B}{T_t^{3/2}|\Delta \dot{B}|} \qquad \text{(B-7-6)}$$

in which T_t is the total tracking time and the 1 and 2 subscripts refer to first and second leg quantities, respectively. The above two equations show that the range uncertainty decreases with the total tracking time and, for a given total time, is minimized by maximizing the change in bearing-rate ($\Delta\dot{B}$).

The change in bearing-rate can be very nearly maximized by running own-ship perpendicular to the initial bearing line for a period of time, and running in the opposite direction for the remainder of the tracking time. The terms within the brackets indicate how the ratios of the times on each leg to the total time affect the range uncertainty. The bracketed part of equation (B-7-6) is a minimum when $T_1 = T_2$. The

minimum for the bracketed part of equation (B-7-3) is, however, a function of both the times and the bearing-rates on each leg. When the bearing-rate on the second leg approaches zero, the uncertainty of the current range increases beyond bound. This is also a property of the Mark 113 (Mode 2) range solution as time on second leg increases beyond bound (Reference 1). A small $\dot{B}_2$ can be avoided by running own-ship in the direction of the bearing drift on the first leg and against the bearing drift on the second leg. If for some reason this is not done and $\dot{B}_2$ is small compared to $\dot{B}_1$, R(t') will be a much more reliable estimate than R(t). The Mark 113 system computes only R(t), (Reference 2).

The minimum for the bracketed expression of equation (B-7-3) and the comparable expression for Mode 2 is illustrated in Fig. B-7-1 of Appendix B. The x and y variables are defined by

$$x = \frac{T_2}{T_t}$$

and

$$y = \frac{\dot{B}_1}{\dot{B}_1 - \dot{B}_2} .$$

The ratio T_2/T_1 which minimizes the bracketed expression of equation (B-7-3) is designated by x-opt and represents the optimum time ratio for a given y. Positive y values correspond to $\dot{B}_2 < \dot{B}_1$.

The cusp of the ASP curve shown on Fig. B-6-1 does not extend to a zero value for x-opt since at this point T_2 and $\dot{B}_1$ would also be zero, causing the bracketed expression in equation (B-7-6) to become indeterminate. This expresses the fact that no solution can be obtained on a single leg (i.e., $T_2 \neq 0$).

The minimum value of the bracketed expression for various values of y is designated by z-opt. Fig. B-7-2 of Section 7, Appendix B, illustrates z-opt for both ASP and Mode 2. In general, the ASP range

uncertainty will be about 1.4 times larger than the Mode 2 uncertainty, but when $\dot{B}_1$ approaches zero, the range error will be the same for both systems.

The term optimum tactic is defined as the own-ship maneuver which will result in the smallest range uncertainty. Optimum tactic designates both the direction of travel and the length of time on each leg. The difference in the optimum tactics for ASP and Mode 2 lies only in the length of time on each leg. For ASP, the time on the first leg should, in general, be slightly more than half the total tracking time ($T_1 \cong .55\ T_t$; $T_2 \cong .45\ T_t$), but for Mode 2 (Reference 1) the time spent on the first leg should be only about thirty per cent of the total ($T_1 \cong .3T_t$; $T_2 \cong .7T_t$).

4. Examples for Particular Geometries and Comparisons of ASP with Manual Plots

A. Relative Motion Parameters

The figures of Section 6, Appendix B, show relative motion parameter accuracies

$$\sigma_\alpha,\ \frac{\sigma_{U/R_o}}{U/R_o},\ \frac{\sigma_{\dot{B}}}{\dot{B}},\ \text{and}\ \frac{\sigma_{\ddot{B}}}{\ddot{B}}$$

for both ASP and manual plotting as functions of time for the particular geometries illustrated. Although bearing-rate is the only one of these parameters presently obtained from the manual plots, the mathematical approach for obtaining all of the parameters is implicitly contained in plotting techniques. This fact is used to make a comparison of man versus computer. The comparison is idealized by assuming that the manual plots represent least-square fits of the data. The essential difference between the man and the computer is taken to be the data assimilation rate. One bearing per two seconds is assumed for ASP while one bearing per minute is assumed for the manual plots.

All sonar bearing errors are considered independent and normally distributed with a standard deviation of 0.2 degrees; but, since physical plotting of data introduces some error, the total standard deviation of bearing data for the manual plots is assumed to be 0.3 degrees. For these sampling intervals bearing-error correlation times of two seconds or less will not degrade the results (Reference 1). Likewise, a constant bearing offset will not degrade the results although the final least-square bearings will be offset by the same amount.

These graphical comparisons illustrate that

1. The standard deviations in the relative motion parameters are always approximately eight times less for ASP than for manual plotting when the same geometry and tracking time are assumed.

2. To achieve equal accuracy with manual plotting techniques longer tracking times are required.

   a. For $\sigma_{\dot{B}}$ the required time using manual plots is more than four times as great as that required for ASP.

   b. For σ_{α} and $\sigma_{\ddot{B}}$ the required time is about two and one-thirds greater than that required for ASP.

   c. Since σ_{U/R_O} is geometry dependent, the required time varies from two and one-third to about four times as great as that required for ASP.

B. Manual Plot vs. ASP Range Accuracy

For the same geometry and length of tracking time, the standard deviation of bearings-only range for the best least-square manual plot is approximately 8.2 times as great as the standard deviation obtained

employing the ASP system.* This difference in accuracy is a result of the ASP system's faster bearing sampling rate and freedom from errors incurred in physical plotting.

To obtain a manual plot range accuracy comparable to that obtained by the ASP solution the necessary tracking time is more than four times greater than that required for ASP.

The ratio $\sigma_{\dot{B}/\dot{B}}$ (see figures of Section 6 of Appendix B) gives the significance of bearing-rate as a function of tracking time. Since all bearings-only solutions are dependent on the change in bearing-rate resulting from an own-ship zig, the range uncertainty will be a function of $\sigma_{\dot{B}/\dot{B}}$ for each leg. This provides a basis for determining the length of time own-ship should track on a single leg, the details of which have not yet been determined. No such criterion is given in the present Mark 113 system.

5. Bearing Pre-Smoothing

The ratio $\sigma_{\ddot{B}/\ddot{B}}$ indicates the significance of curvature in the bearing-time curve. It has been shown (Reference 1) that the inherent bias in the Mark 113 bearings-only solution can be reduced to insignificance by averaging (pre-smoothing) groups of bearings and using the resulting weighed averages as single bearings for the least-square processing. No information is lost by this scheme provided the bearing-time curve has no significant curvature within the averaging intervals. The present Mark 113 criterion for establishing the widths of the averaging intervals (Reference 2) is based on the bearing-rate. This criterion should be based on the $\sigma_{\ddot{B}/\ddot{B}}$ ratio.

A valid criterion is obtained by establishing a level of significance (K) for the curvature. Thus, when

---

*Using the assumptions of the preceding paragraph.

$$\sigma_{\ddot{B}/\ddot{\dot{B}}} > K \qquad \text{(K a constant)}$$

significant curvature is present. The first qn bearings are averaged ($q < 1$ and n is the total number of bearings) and the least-square process is applied to the remaining bearings and the incoming bearings until $\sigma_{\ddot{B}/\ddot{\dot{B}}} > K$ when the entire process is repeated.

Since it is necessary to have at least four bearings for a solution, an upper limit is set for the smoothing time. Thus, if

$$\sigma_{\ddot{B}/\ddot{\dot{B}}} < K$$

when the time interval is N minutes, the bearings in the N minute interval should be averaged and a new interval started.

III

LONG RANGE BEARINGS-ONLY ZIG DETECTION

1. Detection Scheme

All present bearings-only range finding methods are based on the assumption that the target track consists of uniform rectilinear motion. Thus, the usefulness of these bearings-only solutions depends on the ability to detect target zigs.

A zigging target is defined here as one which does not conform to the aforementioned hypothesis. This definition includes sinuating targets.

The equations of this section represent a zig-detection technique which is fundamentally the same as that used in the manual plots. In this technique bearing data are collected for a time interval and least-square fitted to a function of time. Estimates of the expected future bearings are obtained from the least-square fit (bearing history). The occurrence of a target zig is then indicated by systematic deviations of the measured bearings from the predicted bearings. When systematic deviations are not discernible, the bearing measurements obtained in the prediction interval are combined with the history bearings to form a new history from which a new least-square fit is obtained. Bearings are then predicted for the next interval and the entire process is repeated. The entire bearing-time curve is scanned in this manner.

2. Equations

The tracking time is divided into intervals t_o, t_1, ... t_j, t_{j+1}, ... such that

$$(t_i - t_{i-1}) = \Delta t$$

for (i = 1,2,...). Each Δt interval contains p bearing sampling points. The absolute value of the sum of the deviations of the predicted bearings from the measured bearings in the interval (t_j, t_{j+1}) is

$$\boxed{r_j = \left| \sum_{i=m_j+1}^{m_j+1+P} (B^*_{ij} - B_{ij}) \right|} \qquad \text{(C-1-3)}$$

in which the B_{ij}'s are measured bearings at times t_i and the B^*_{ij}'s are predicted bearings for times t_i.

Two schemes have been considered for bearing prediction. In the first, the predicted bearings are obtained from the quadratic expression

$$B^*_{ij} = a_j + b_j(t_i - t_o) + c_j(t_i - t_o)^2 \qquad \text{(C-1-1)}$$

in which a_j, b_j, and c_j are obtained from a least square fit of the m_j bearings in the interval (t_o, t_j).

The random part of the deviation r_j for the quadratic extrapolation is

$$\boxed{\sigma_j = \sigma_B \left\{ \begin{matrix} c_{11}p^2 + c_{22}T^2_{j1} + c_{33}T^2_{j2} + 2c_{12}T_{j1}p \\ +2c_{13}T_{j2}p + 2c_{23}T_{j1}T_{j2} + p \end{matrix} \right\}^{1/2}} \qquad \text{(C-3-5)}$$

in which the c_{ij}'s are as given in equations (A-1-12) with t_i replaced

by t_j, and T_{j1} and T_{j2} are

$$T_{j1} = \sum_{t_i=t_j+T}^{t_{j+1}} (t_i - t_o) \,, \tag{C-3-4}$$

$$T_{j2} = \sum_{t_i=t_j+T}^{t_{j+1}} (t_i - t_o)^2 \,.$$

The alternate scheme is based on linear prediction from

$$B^*_{ij} = a'_j + b'_j (t_i - t_o) \tag{C-1-2}$$

in which a'_j and b'_j are obtained from a linear least-square fit of the m_j bearings. The interval considered must, of course, be limited such that equation (C-1-2) is a sufficiently accurate description. The standard deviation for the linear extrapolation is

$$\sigma_j = \sigma_B \left\{ c'_{11} p^2 + c'_{22} T_{j1}^2 + 2c'_{12} T_{j1} p + p \right\}^{1/2} \tag{C-4-3}$$

in which

$$c'_{11} = \frac{\Sigma(t_i-t_o)^2}{\text{Det } A'}, \quad c'_{22} = \frac{n}{\text{Det } A'}, \quad c'_{12} = -\frac{\Sigma(t_i-t_o)}{\text{Det } A'},$$

and

(C-2-8)

$$\text{Det } A' = n\Sigma(t_i-t_o)^2 - \left[\Sigma(t_i-t_o)\right]^2 .$$

The sums in the above are from $t_i = t_o$ to t_j. The linear least-square fit is obtained by

$$a' = c'_{11}\Sigma B_i + c'_{12}\Sigma B_i(t_i-t_o)$$

and

$$b' = c'_{12}\Sigma B_i + c'_{22}\Sigma B_i(t_i-t_o) .$$

The probability of a target zig (P_z) is found by

$$P_z = \frac{1}{\sqrt{2\pi}\sigma_j}\int_{-\Gamma_j}^{\Gamma_j} \exp\left\{-\frac{x^2}{2\sigma_j^2}\right\}dx . \qquad \text{(C-1-4)}$$

3. Theoretical Results

The theoretical results of Section 6 of Appendix C indicate that, at least for long range targets, the linear prediction scheme is superior to the quadratic scheme. Further study at the shorter ranges is needed especially where the time for executing the zig is long. The quadratic scheme might be better in such cases. It is quite possible, however, that less sophisticated schemes such as visual inspection of

a bearing-time curve would be completely adequate for these short ranges.

Figs. C-6-1 through C-6-5 (see Section 6 of Appendix C) and the accompanying tables give comparisons of Γ_j and σ_j for various geometries. Approximate expressions for Γ_j and σ_j were used to obtain these figures. The theoretical expressions used to determine Γ_j are based on the following assumptions:

1. Range does not change appreciably during the time intervals considered.

2. Bearing-rate for each leg of the target track is approximately constant.

3. Target zigs occur instantaneously and without changes in speed.

Assumptions 1 and 2 above are not unrealistic for long ranges, i.e., ten nautical miles or more. The effects of assumption 3 can be partially reduced by applying the following interpretations for "zig time":

1. The "time of zig" (as used in the diagrams and tables) should be considered to lie approximately midway between the beginning of the zig and the end of the zig.

2. Speed reductions resulting from course zigs advance or retard the "time of zig" depending on whether the speed reductions increase or decrease the change in bearing-rate caused by the change in course. Thus, apart from the correction in 1 above, "zig time" should be interpreted as the time at which the bearing-rate changes abruptly.

The values of σ_j and consequently the zig probabilities are based on

an assumed raw bearing standard deviation of 0.2 degrees and a bearing sampling interval of 2 seconds. Larger standard deviations will degrade the results somewhat whereas a constant bearing off-set will have no effect.

The geometries considered (Figs. C-6-1 through C-6-5) represent zigs which are particularly difficult to detect. In all cases, a 15 degree counterclockwise rotation of the target track would make the zig impossible to detect. In such cases, however, the zig would not affect the bearings-only range solutions. Zigs which cause larger changes in bearing-rates will, of course, result in larger zig probabilities at a given time.

Figs. C-6-1 and C-6-2 and the corresponding tables illustrate the superiority of the linear zig detection scheme over the quadratic scheme at a relatively long range. Since the assumptions used for determining r_j are not valid at short ranges, a similar comparison cannot be made for the short range cases; computer simulations will be used for this latter situation. The zigs for these two figures were assumed to occur at the beginning of the scan intervals.

Figs. C-6-3 through C-6-5 and their respective tables illustrate the growth of the zig probability with subsequent scans. Thus, if the zig is not detected (zig probability too small) in the interval in which it occurred, it will be easier to detect in the subsequent intervals. This will not, in general, be true for the quadratic scheme.

Analysis is needed to determine the effects of undetected target zigs on the range estimate.

IV .

CONCLUSIONS AND AREAS REQUIRING FURTHER INVESTIGATION

1. Conclusions

A. The ASP relative-motion analysis is superior to manual plotting analysis in the following respects:

1. Accurate relative-motion parameters are obtained in less time for ASP than that required for manual plotting.

2. The ASP system can analyze targets at longer ranges than are possible using manual plots.

B. The ASP relative-motion analysis is superior to the present Mark 113 system analysis in the following respects:

1. More relative-motion parameters are obtained as outputs from the ASP analysis than from the present Mark 113 system analysis.

2. The ASP system has the capacity to produce "if-therefore" solutions based upon relative-motion parameters and an hypothesized input of target range, course or speed. The Mark 113 system can obtain this type of solution only for an input of target speed. Also, the possibility of a dual solution is recognized by the ASP system, but ignored by the present Mark 113 system.

C. Automatic target zig detection is possible within the ASP fire control computer.

D. The linear zig detection technique is superior to the quadratic technique at the longer ranges.

E. The significance of curvature criterion for establishing the widths of bearing pre-smoothing intervals is superior to the bearing-rate criterion presently employed in the Mark 113 system.

F. As presently formulated, the ASP bearings-only complete solution is inferior to that of the Mark 113 system.

2. Areas Requiring Further Investigation

A. A criterion is needed whereby the interval over which the bearing-time expansion is applied is such that the expansion is indeed an adequate approximation to the true bearing-time function. In the event that the total interval can only be adequately approximated by two or more separate expansions, it would be desirable to combine the information obtained from the separate intervals in such a manner that no useful information is discarded. The need for such a criterion is, as previously indicated, more important at the shorter ranges.

B. The bearings-only solution as presented here represents a "first look" at the system. The assumption that own-ship zig occurs instantaneously must be replaced by a realistic maneuver.

C. The combination of the first and second leg information has not been fully exploited. The scheme presented here treats the six parameters (a's, b's, and c's) as independent whereas only four can truly be independent (x, y, $\dot{x}$, and $\dot{y}$ of the

target). It would be desirable to find relations describing dependence if such can be obtained without introducing the complexity of the previous SUBIC schemes.

D. Variance expressions for many of the parameters have yet to be derived.

E. A method of introducing additional measurements (e.g., range from PUFFS or single ping) into the bearings-only complete solution is necessary to obtain the best possible solution from all of the data which might be available.

F. Analysis of the zig detection schemes must be continued and extended. Further study at shorter ranges is needed, especially where the zig is extended in time. Analysis is also needed to determine the effects of undetected target zigs on the range estimate.

G. The ASP approach to fire control has been designed to permit more effective communication between the man and his computer. The next step is to investigate how this communication can be accomplished and to evaluate the increase of tactical effectiveness resulting from this communication. In order to accomplish this, it is planned to connect a research console to a computer to determine those parameters which should be under operator control and those parameters which should be under computer control.

APPENDIX A
DERIVATION OF TARGET LOCALIZATION EQUATIONS

1. Least-Square Approximation to the Bearing-Time Relation

The bearing-time relation,

$$B = B_o + \tan^{-1}\left[\frac{(U/R_o)(t-t_o)\sin\alpha_o}{1-(U/R_o)(t-t_o)\cos\alpha_o}\right] \qquad (A\text{-}1\text{-}1)$$

is obtained from Fig. A-1-1 (which for convenience is reproduced here from Fig. I-1-2). An approximation to this relation is obtained by taking a Taylor expansion of

$$\tan(B-B_o)$$

and

$$\frac{(U/R_o)(t-t_o)\sin\alpha_o}{1-(U/R_o)(t-t_o)\cos\alpha_o}$$

to get

$$B = a+b(t-t_o)+c(t-t_o)^2 \qquad (A\text{-}1\text{-}2)$$

in which

$$a = B_o, \qquad (A\text{-}1\text{-}3)$$

$$b = (U/R_o)\sin\alpha_o, \qquad (A\text{-}1\text{-}4)$$

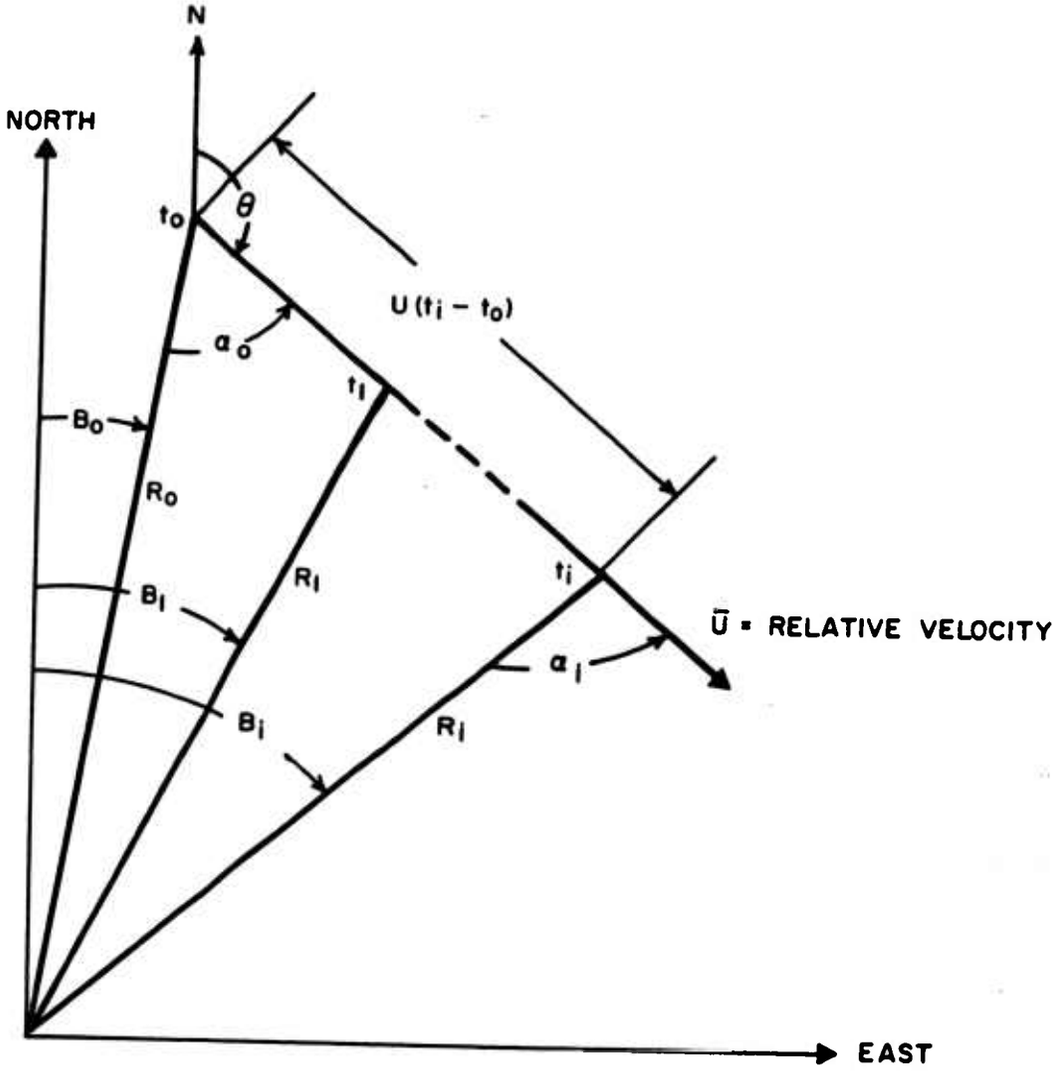

Fig. A-1-1 Own-Ship Coordinates

and

$$c = (U/R_o)^2 \sin \alpha_o \cos \alpha_o. \qquad \text{(A-1-5)}$$

When the quadratic expansion (equation (A-1-2)) is sufficiently accurate and when the bearings have random variations, a least-square processing of the bearing equation will yield unbiased estimates of the coefficients a, b, and c.

Assuming that the error in time is insignificant, the sum of the squares of the residuals is expressed by

$$G = \Sigma\left[a+b(t_i-t_o)+c(t_i-t_o)^2-B_i\right]^2 \qquad \text{(A-1-6)}$$

which is minimized with respect to the coefficients to give

$$\begin{aligned} an+b\Sigma(t_i-t_o)+c\Sigma(t_i-t_o)^2 &= \Sigma B_i, \\ a\Sigma(t_i-t_o)+b\Sigma(t_i-t_o)^2+c\Sigma(t_i-t_o)^3 &= \Sigma B_i(t_i-t_o), \qquad \text{(A-1-7)} \\ a\Sigma(t_i-t_o)^2+b\Sigma(t_i-t_o)^3+c\Sigma(t_i-t_o)^4 &= \Sigma B_i(t_i-t_o)^2. \end{aligned}$$

Let the coefficients of a, b, and c be designated by the matrix A, then

$$[A]\begin{bmatrix} a \\ b \\ c \end{bmatrix} = \begin{bmatrix} \Sigma B_i \\ \Sigma B_i(t_i-t_o) \\ \Sigma B_i(t_i-t_o)^2 \end{bmatrix} \qquad \text{(A-1-8)}$$

which can be written as

$$u = Cv \tag{A-1-9}$$

in which

$$u = \begin{bmatrix} a \\ b \\ c \end{bmatrix}, \tag{A-1-10}$$

$$v = \begin{bmatrix} \Sigma B_i \\ \Sigma B_i(t_i-t_o) \\ \Sigma B_i(t_i-t_o)^2 \end{bmatrix}, \tag{A-1-11}$$

and

$$C = A^{-1} \tag{A-1-12}$$

Then

$$a = c_{11}v_1+c_{12}v_2+c_{13}v_3,$$

$$b = c_{21}v_1+c_{22}v_2+c_{23}v_3,$$

$$c = c_{31}v_1+c_{32}v_2+c_{33}v_3.$$

Explicitly, these equations are

$$\text{Det } |A| = n\Sigma(t_i-t_o)^2\Sigma(t_i-t_o)^4+2\Sigma(t_i-t_o)\Sigma(t_i-t_o)^2\Sigma(t_i-t_o)^3+$$

$$-\left[\Sigma(t_i-t_o)^2\right]^3-n\left[\Sigma(t_i-t_o)^3\right]^2-\Sigma(t_i-t_o)^4\left[\Sigma(t_i-t_o)\right]^2$$

$$a\ \text{Det}\ |A| = \Sigma B_i \Sigma(t_i-t_o)^2 \Sigma(t_i-t_o)^4 + \Sigma B_i (t_i-t_o) \Sigma(t_i-t_o)^2 \Sigma(t_i-t_o)^3 +$$

$$+\Sigma B_i (t_i-t_o)^2 \Sigma(t_i-t_o) \Sigma(t_i-t_o)^3 - \Sigma B_i (t_i-t_o)^2 \left[\Sigma (t_i-t_o)^2\right]^2 +$$

$$-\Sigma B_i \left[\Sigma(t_i-t_o)^3\right]^2 - \Sigma B_i (t_i-t_o) \Sigma (t_i-t_o) \Sigma (t_i-t_o)^4,$$

$$b\ \text{Det}\ |A| = n\Sigma B_i (t_i-t_o) \Sigma(t_i-t_o)^4 + \Sigma B_i (t_i-t_o)^2 \Sigma(t_i-t_o) \Sigma(t_i-t_o)^2 +$$

$$+\Sigma B_i \Sigma(t_i-t_o)^2 \Sigma(t_i-t_c)^3 - \Sigma B_i (t_i-t_o) \left[\Sigma (t_i-t_o)^2\right]^2 +$$

$$-n\Sigma B_i (t_i-t_o)^2 \Sigma (t_i-t_o)^3 - \Sigma B_i \Sigma (t_i-t_o) \Sigma (t_i-t_o)^4,$$

and

$$c\ \text{Det}\ |A| = n\Sigma B_i (t_i-t_o)^2 \Sigma(t_i-t_o)^2 + \Sigma B_i \Sigma(t_i-t_o) \Sigma(t_i-t_o)^3 +$$

$$+\Sigma B_i (t_i-t_o) \Sigma (t_i-t_o) \Sigma(t_i-t_o)^2 - \Sigma B_i \left[\Sigma(t_i-t_o)^2\right]^2 +$$

$$-n\Sigma B_i (t_i-t_o) \Sigma(t_i-t_o)^3 - \Sigma B_i (t_i-t_o)^2 \left[\Sigma(t_i-t_o)\right]^2.$$

2. Bearing-Rate and Change in Bearing-Rate

Bearing-rate, the time-rate-of-change of bearing, is found by differentiating equation (A-1-2) with respect to time. Thus,

$$\dot{\beta} = \frac{\Sigma B_i (t_i-t_o)}{\Delta}. \qquad (A-2-1)$$

Similarly, the change in bearing-rate is given by

$$\ddot{B} = 2c. \qquad \text{(A-2-2)}$$

3. Determination of α, θ and U/R_o

From equations (A-1-4) and (A-1-5),

$$\alpha_o = \tan^{-1}(b^2/c) \qquad \text{(A-3-1)}$$

and from Fig. A-1-2,

$$\alpha(t) = \alpha_o + B(t) - a. \qquad \text{(A-3-2)}$$

This angle is referred to as the relative angle-on-the-bow.

The relative course (θ), see Fig. A-1-1, is seen to be

$$\theta = \pi - \alpha_o + a. \qquad \text{(A-3-3)}$$

From equation (A-1-4),

$$U/R_o = b/\sin \alpha_o \qquad \text{(A-3-4)}$$

and from equations (A-3-1) and (A-3-4),

$$U/R_o = \left[\frac{c^2+b^4}{b^2}\right]^{1/2}. \qquad \text{(A-3-5)}$$

4. Development of Solution Using Speed Input

Bearing data, own-ship motion parameters and a given target speed ($V_e^{(2)}$) are used to determine a complete solution.

From Fig. A-4-1 (which is Fig. I-1-3 reproduced here for convenience) target course is given by

$$\phi^{(2)} = \pi - \gamma + a - \alpha_o \qquad \text{(A-4-1)}$$

in which

$$\gamma = \sin^{-1}\left[\frac{v^{(1)}}{V_e^{(2)}} \sin(\phi^{(1)} - a + \alpha_o)\right]. \qquad \text{(A-4-2)}$$

The foregoing equation indicates the possibility of two solutions (this is a property of all target localization solutions based on bearing data). Fig. A-4-2 illustrates the fact that when bearing lines converge, two possible target tracks exist for a given target speed. By examining the angle ($\phi^{(1)} - a + \alpha_o$) the various solution possibilities may be determined.

Fig. A-4-3 (a) and (b) is a vector velocity diagram in which the angle ($\phi^{(1)} - a + \alpha_o$) is in the first and fourth quadrants, respectively. It can be seen that

$$V_{min}^{(2)} = V^{(1)} \left|\sin(\phi^{(1)} - a + \alpha_o)\right|. \qquad \text{(A-4-3)}$$

When $V_e^{(2)}$ exceeds $V_{min}^{(2)}$ but is less than $V^{(1)}$, two values of γ exist. One is given by the principal value of equation (A-4-2) and the other by its complement. Thus,

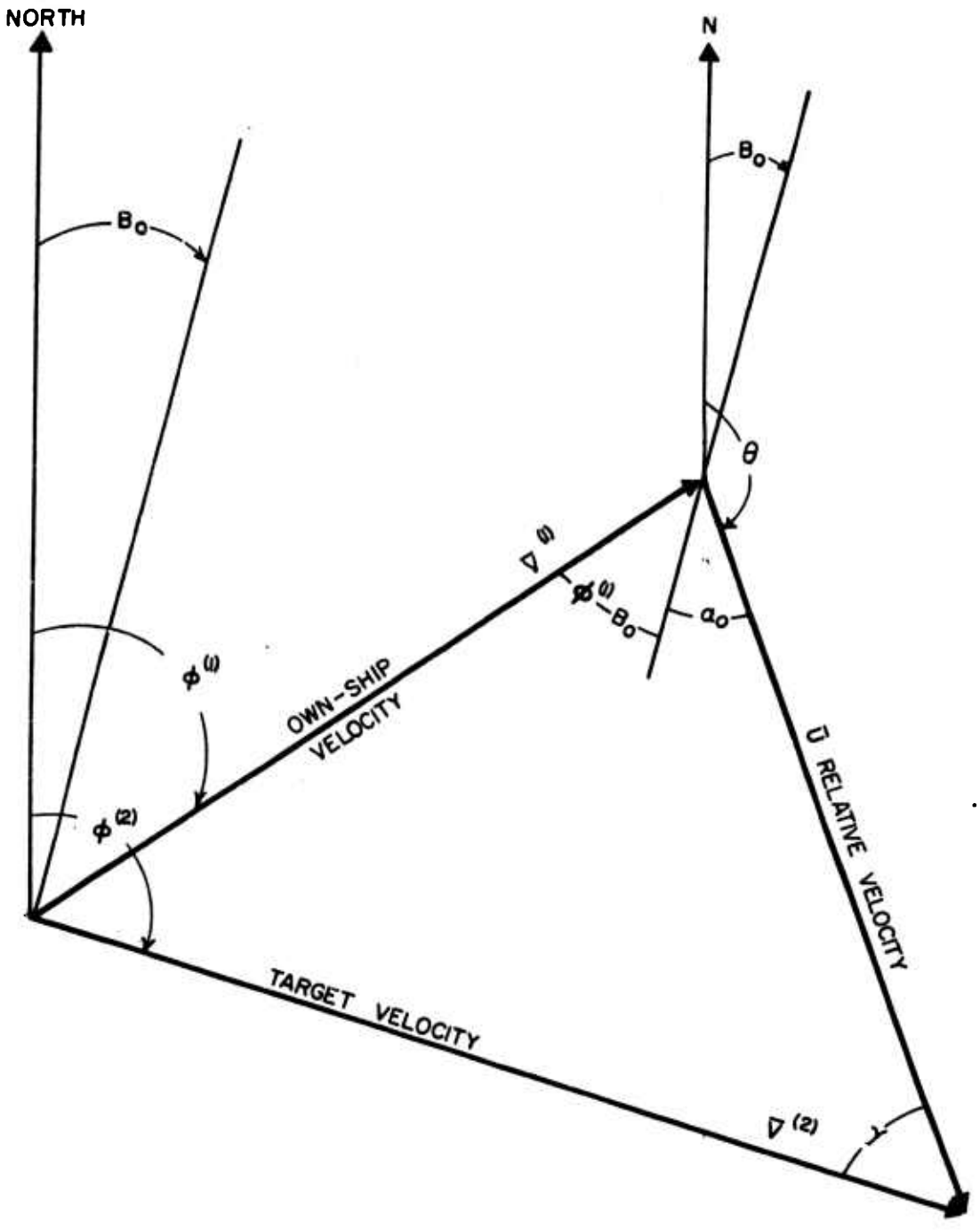

Fig. A-4-1 Velocity Vectors

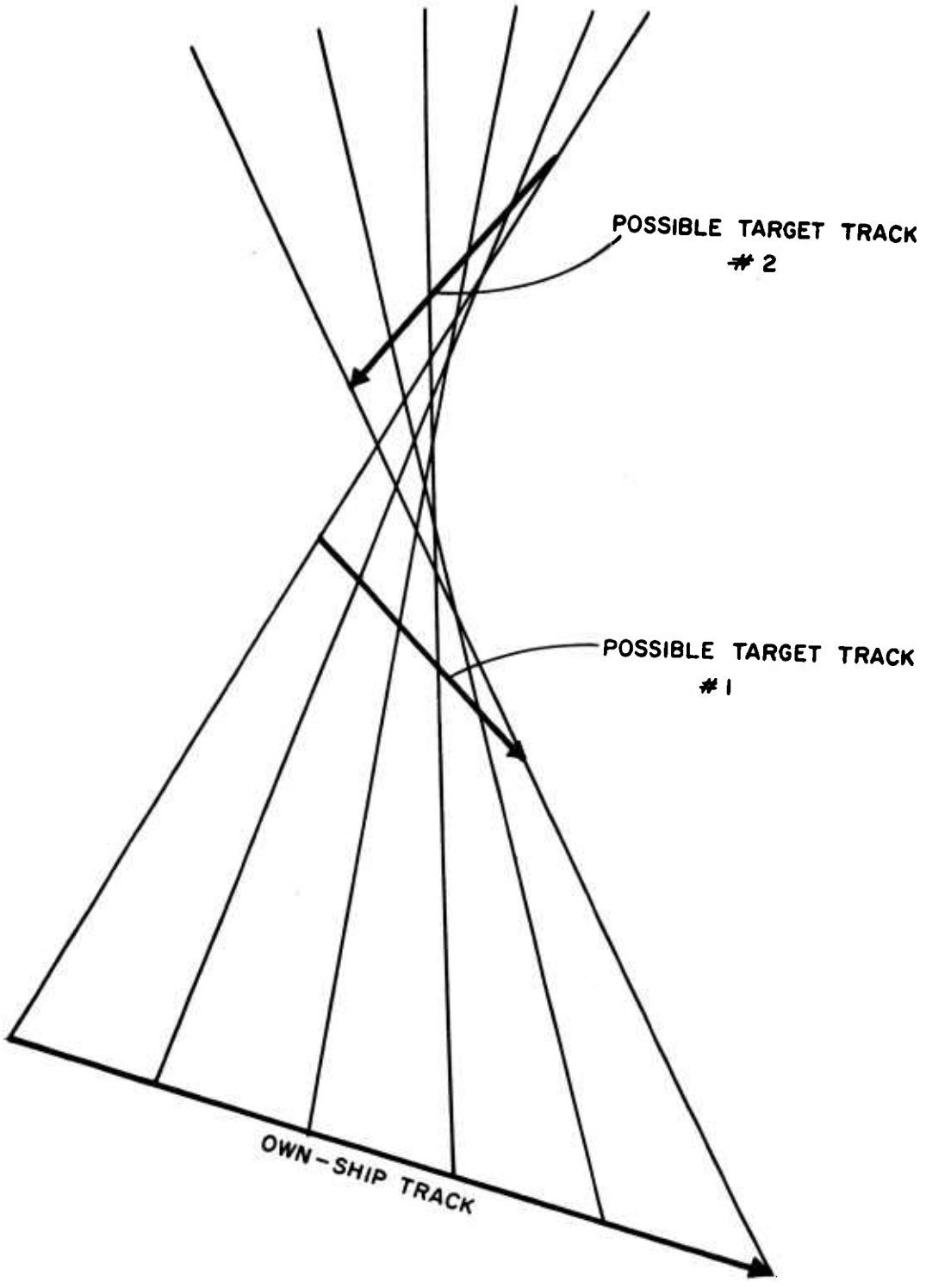

Fig. A-4-2 Earth-Related Dual-Solution Illustration

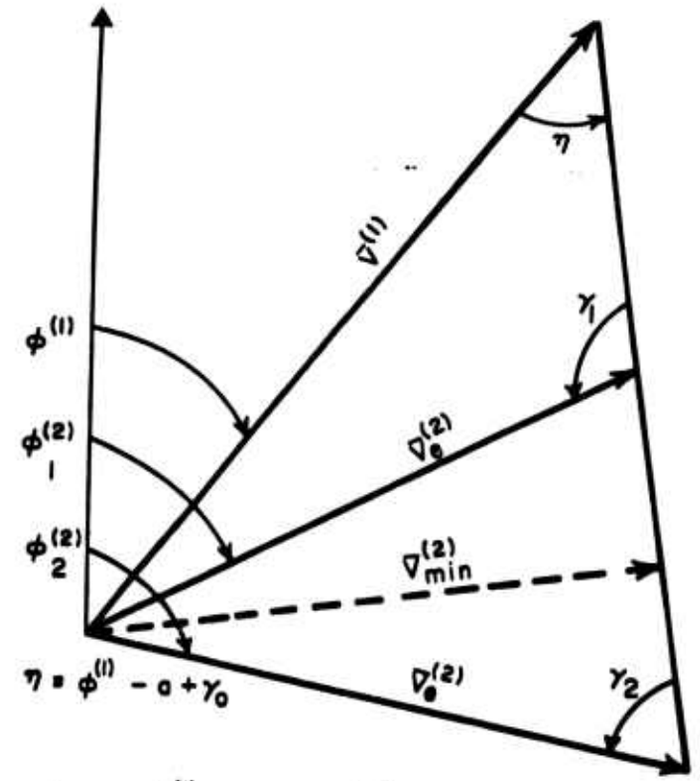

a) $0 \leq \phi^{(1)} - a + a_0 < \frac{\pi}{2}$

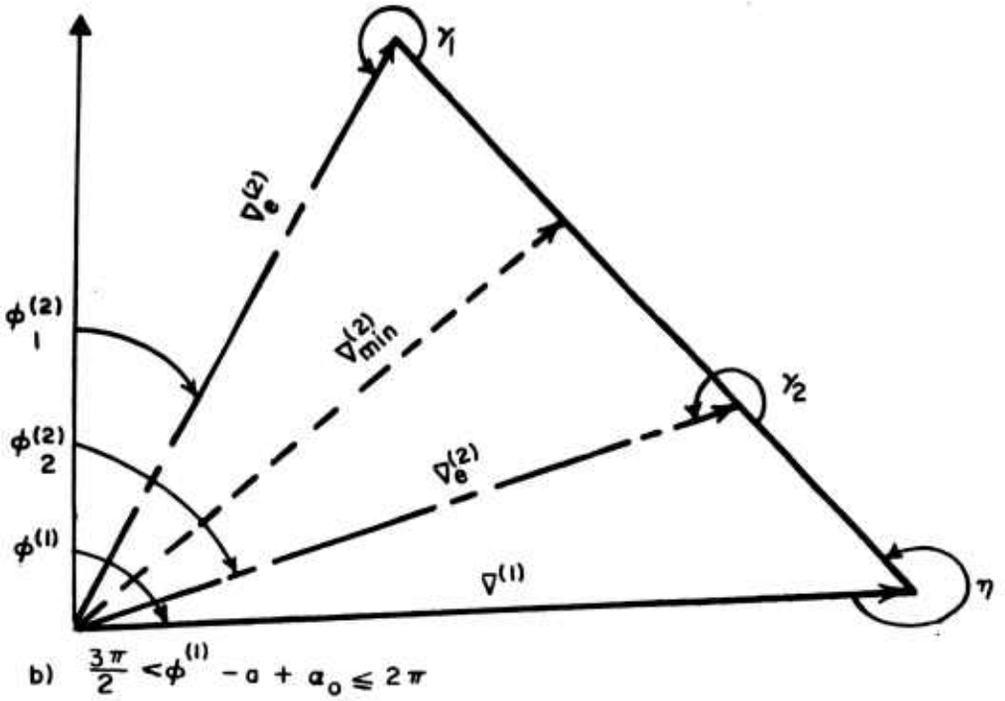

b) $\frac{3\pi}{2} < \phi^{(1)} - a + a_0 \leq 2\pi$

Fig. A-4-3 First and Fourth Quadrant Solution Possibilities

$$\gamma_1 = \gamma \qquad \text{(A-4-4)}$$

$$\gamma_2 = \pi - \gamma. \qquad \text{(A-4-5)}$$

When $V^{(2)} \geq V^{(1)}$, only γ_1 exists and there is a unique solution.

Fig. A-4-4 (a) and (b) depict the situations in which the angle $(\phi^{(1)} - a + \alpha_o)$ lies within the second or third quadrants, respectively. The minimum target speed is given by

$$V_{min}^{(2)} = V^{(1)}. \qquad \text{(A-4-6)}$$

For any larger value of $V_e^{(2)}$ a unique solution exists and γ_1 (principal value of equation (A-4-2)) alone exists.

Fig. A-4-5 summarizes the various solution possibilities.

When two values of γ exist, the entire solution must be performed in duplicate. Thus, equation (A-4-1) becomes

$$\phi_j^{(2)} = \pi - \gamma_j + a - \alpha_o \qquad (j = 1 \text{ or } 1, 2). \qquad \text{(A-4-7)}$$

From the law of cosines

$$U_j = \left[V^{(1)^2} + V_e{}^{(2)^2} - 2V^{(1)} V_e{}^{(2)} \cos(\phi_j{}^{(2)} - \phi^{(1)})\right]^{1/2}, \qquad \text{(A-4-8)}$$

and, from equation (A-3-5)

$$R_{oj} = bU_j / (c^2 + b^4)^{1/2}. \qquad \text{(A-4-9)}$$

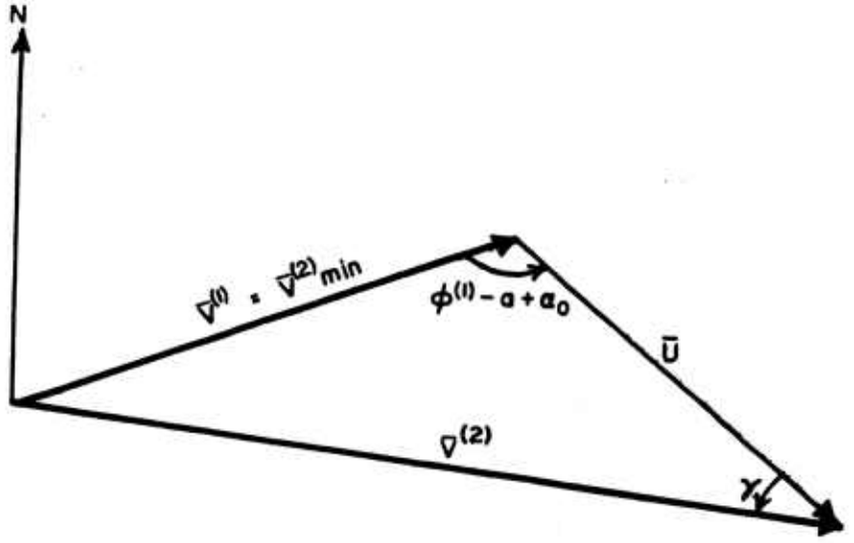

a) $\frac{\pi}{2} \leq \phi^{(1)} - a + \alpha_0 \leq \pi$

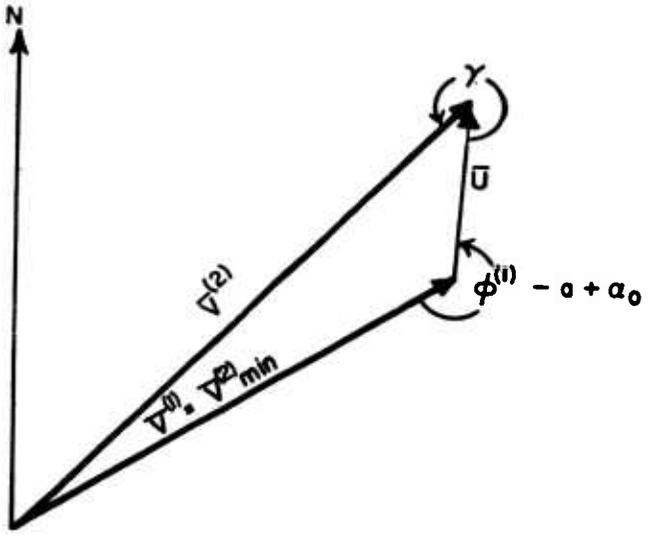

b) $\pi \leq \phi^{(1)} - a + \alpha_0 \leq \frac{3\pi}{2}$

Fig. A-4-4 Second and Third Quadrant Solution Possibilities

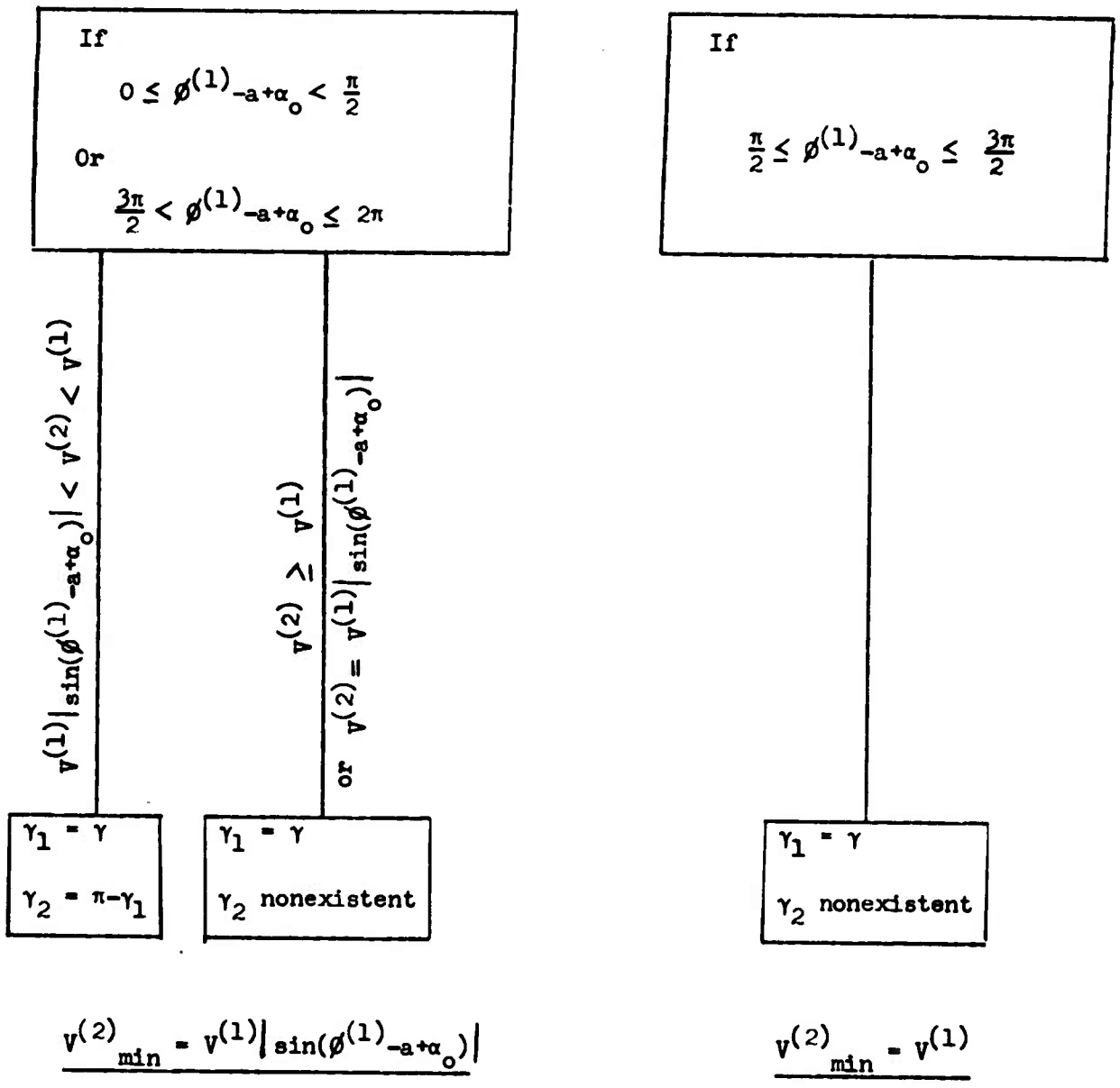

Fig. A-4-5 Speed Input Solution Possibilities

For range at any time (t), it can be seen from Fig. A-1-1 that

$$U \sin \alpha_o(t-t_o) = R(t)\sin\left[B(t)-a\right].$$

Thus, assuming (B-a) to be small

$$R(t)_j = \frac{R_{oj}b}{b+c(t-t_o)}. \qquad \text{(A-4-10)}$$

It is possible that one of the two solutions will be physically absurd, although mathematically possible.

5. Development of Solution Using Range Input

At any time (t_e), consider a coordinate system with the x axis perpendicular to the bearing line and the y axis along the bearing line. The components of target speed at this particular time can then be written in terms of known parameters and a range input at the given time, $R_e(t_e)$. The cross-line-of-sight component of target speed at t_e is then given by

$$V_x^{(2)}(t_e) = V^{(1)}\sin\left[\phi^{(1)}-B(t_e)\right]+R_e(t_e)\dot{B}(t_e), \qquad \text{(A-5-1)}$$

in which

$$B(t_e) = a+b(t_e-t_o)+c(t_e-t_o)^2 \qquad \text{(A-5-2)}.$$

and

$$\dot{B}(t_e) = b+2c(t_e-t_o). \qquad \text{(A-5-3)}$$

The along-line-of-sight component of target speed is given by

$$V_y^{(2)}(t_e) = V^{(1)}\cos\left[\phi^{(1)} - B(t_e)\right] + \dot{R}_e(t_e) \qquad \text{(A-5-4)}$$

in which the quantity $\dot{R}_e(t_e)$ can be developed as follows.

From equation (A-4-10)

$$R_e(t_e) = \frac{R_o b}{b+c(t_e-t_o)} .$$

Thus,

$$\dot{R}_e(t_e) = -\frac{R_o bc}{\left[b+c(t_e-t_o)\right]^2} ,$$

or

$$\dot{R}_e(t_e) = -\frac{R_e(t_e)c}{b+c(t_e-t_o)} . \qquad \text{(A-5-5)}$$

Equations (A-5-1) and (A-5-4) can then be written as

$$V_x^{(2)}(t_e) = V^{(1)}\sin\left[\phi^{(1)} - B(t_e)\right] + R_e(t_e)\left[b+2c(t_e-t_o)\right] \qquad \text{(A-5-6)}$$

and

$$V_y^{(2)}(t_e) = V^{(1)}\cos\left[\phi^{(1)} - B(t_e)\right] - \frac{R_e(t_e)c}{b+c(t_e-t_o)} . \qquad \text{(A-5-7)}$$

Total target speed is found from its components,

$$V^{(2)} = \left[V_x^{(2)^2}(t_e) + V_y^{(2)^2}(t_e)\right]^{1/2} . \qquad \text{(A-5-8)}$$

From Fig. A-4-1, it can be seen that target course is given by

$$\phi^{(2)} = B(t_e)+\tan^{-1}\left[\frac{V_x^{(2)}(t_e)}{V_y^{(2)}(t_e)}\right]. \qquad \text{(A-5-9)}$$

From equation (A-4-10)

$$R_o = \frac{R_e(t_e)\left[b+c(t_e-t_o)\right]}{b}$$

and for any time (t) other than (t_e)

$$R(t) = \frac{R_o b}{b+c(t-t_o)}\ .$$

Thus, range at any time is given by

$$R(t) = \frac{R_e(t_e)\left[b+c(t_e-t_o)\right]}{b+c(t-t_o)}\ . \qquad \text{(A-5-10)}$$

6. Development of Solution Using Course Input

Bearing data, own-ship motion parameters and a given target course ($\phi_e^{(2)}$) are used to determine a complete solution.

From equation (A-4-1)

$$\gamma = \pi+a-\alpha_o-\phi_e^{(2)}. \qquad \text{(A-6-1)}$$

Then, rearranging equation (A-4-2)

$$V^{(2)} = \frac{V^{(1)}\sin(\phi^{(1)}-a+\alpha_o)}{\sin\gamma} . \qquad \text{(A-6-2)}$$

Target range can then be obtained from equation (A-4-10) in which

$$R_o = \left| \frac{\left[V^{(1)^2}+V^{(2)^2}-2V^{(1)}V^{(2)}\cos(\phi_e^{(2)}-\phi^{(1)})\right]^{1/2} b}{(c^2+b^4)^{1/2}} \right| . \qquad \text{(A-6-3)}$$

7. Development of Bearings-Only Solution

Own-ship travels and collects bearing data on two distinct "legs", each consisting of uniform motion, but differing in speed and/or course. The simplifying assumption is made that own-ship zig (change of course and/or speed) occurs instantaneously. The subscripts 1 and 2 indicate first and second leg parameters, respectively. The x and y subscripts indicate the cross-line-of-sight and along-line-of-sight speeds, respectively. The initial time is designated by t_o, the time of own-ship zig by t', and current time on the second leg by t.

At the time of own-ship zig, the relation existing between range, relative cross-line-of-sight speeds and bearing-rate is

$$R(t')\dot{B}(t') = U_x(t') = V_x^{(2)}(t')-V_x^{(1)}(t'). \qquad \text{(A-7-1)}$$

For a uniform target track,

$$R(t')\Delta\dot{B}(t') = -\Delta V_x^{(1)}(t'). \qquad \text{(A-7-2)}$$

Thus,

$$R(t') = \frac{V_{1x}^{(1)}(t') - V_{2x}^{(1)}(t')}{\dot{B}_2(t') - \dot{B}_1(t')}, \qquad \text{(A-7-3)}$$

in which

$$V_{1x}^{(1)}(t') = V_1^{(1)} \sin\left[\phi_1^{(1)} - B(t')\right], \qquad \text{(A-7-4)}$$

$$V_{2x}^{(1)}(t') = V_2^{(1)} \sin\left[\phi_2^{(1)} - B(t')\right], \qquad \text{(A-7-5)}$$

and the bearing at time t' is the time-weighted mean of the two bearings (one from each of own-ship's "legs") obtained at time t'. Thus,

$$B(t') = \frac{t'}{t}\left[a_1 + b_1(t'-t_o) + c_1(t'-t_o)^2\right] + \frac{t-t'}{t} a_2. \qquad \text{(A-7-6)}$$

The two bearing-rates at time t' are given by

$$\dot{B}_1(t') = b_1 + 2c_1(t'-t_o) \qquad \text{(A-7-7)}$$

and

$$\dot{B}_2(t') = b_2. \qquad \text{(A-7-8)}$$

Range at any time on the second leg (t) is then calculated from

$$R(t) = \frac{R(t')b_2}{b_2 + c_2(t-t')}. \qquad \text{(A-7-9)}$$

By assumption, target course and speed are constant. Therefore, information obtained on each leg of own-ship track can be used to calculate target course and speed by the method used in the range input solution. Thus, for leg k (k = 1, 2),

$$V_{kx}^{(2)}(t') = V_k^{(1)} \sin\left[\phi_k^{(1)} - B(t')\right] + R(t')\dot{B}_k(t') \qquad \text{(A-7-10)}$$

and

$$V_{ky}^{(2)}(t') = V_k^{(1)} \cos\left[\phi_k^{(1)} - B(t')\right] + \dot{R}_k(t') \qquad \text{(A-7-11)}$$

in which B(t') is given by equation (A-7-6),

$$\dot{R}_1(t') = - \frac{R(t')c_1}{b_1 + c_1(t' - t_o)} , \qquad \text{(A-7-12)}$$

and

$$\dot{R}_2(t') = - \frac{R(t')c_2}{b_2} \qquad \text{(A-7-13)}$$

Target speed is then given by

$$V_k^{(2)} = \left\{ \left[V_{kx}^{(2)}(t')\right]^2 + \left[V_{ky}^{(2)}(t')\right]^2 \right\}^{1/2} , \qquad \text{(A-7-14)}$$

and target course is given by

$$\phi_k^{(2)} = B(t') + \tan^{-1}\left[\frac{V_{kx}^{(2)}(t')}{V_{ky}^{(2)}(t')} \right] . \qquad \text{(A-7-15)}$$

The results of equations (A-7-14) and (A-7-15) are then weighed to obtain the best values of target speed and course. Thus,

$$V^{(2)} = W_1 V_1^{(2)} + W_2 V_2^{(2)} \qquad \text{(A-7-16)}$$

and

$$\phi^{(2)} = W_3 \phi_1^{(2)} + W_4 \phi_2^{(2)} \qquad \text{(A-7-17)}$$

in which the W's are the appropriate weighing factors.

APPENDIX B
DERIVATION OF STATISTICAL PROPERTIES

1. Coefficient Variances and Covariances

By definition,

$$C = \text{Adj } A / \text{Det} \mid A \mid \qquad \text{(B-1-1)}$$

in which A is the coefficient matrix of equation (A-1-8) and let c_{ij} be the ij^{th} element of C. Since $A = \tilde{A}$, $C = \tilde{C}$, i.e., both matrices are symmetric, or $c_{ij} = c_{ji}$, then,

variances

$$\begin{cases} \sigma_a^2 = c_{11}\sigma_B^2 \\ \sigma_b^2 = c_{22}\sigma_B^2 \\ \sigma_c^2 = c_{33}\sigma_B^2 \end{cases} \qquad \text{(B-1-2)}$$

covariances

$$\begin{cases} \tau_{ab}\sigma_a\sigma_b = c_{12}\sigma_B^2 \\ \tau_{bc}\sigma_b\sigma_c = c_{23}\sigma_B^2 \\ \tau_{ac}\sigma_a\sigma_c = c_{13}\sigma_B^2 \end{cases} \qquad \text{(B-1-3)}$$

in which σ_B^2 is the variance in the bearing data and the τ_{mn}'s are the correlation coefficients which, from equations (B-1-2) and (B-1-3) are

$$\tau_{ab} = \frac{c_{12}}{(c_{11}c_{22})^{1/2}}, \quad \tau_{bc} = \frac{c_{23}}{(c_{22}c_{33})^{1/2}}, \text{ and } \tau_{ac} = \frac{c_{13}}{(c_{11}c_{33})^{1/2}}. \quad \text{(B-1-4)}$$

The elements of A from which the c_{ij}'s are calculated consist of relatively cumbersome summations. Simplified approximations are presented here to facilitate calculations. Let the bearings be obtained at equal time increments (T), then

$$t_i = Ti \quad \text{(B-1-5)}$$

in which t_i is the time at which the $\underline{i}^{th}$ bearing is obtained. Also,

$$\sum_{i=o}^{n} t_i = \sum_{i=o}^{n} Ti = T \sum_{i=o}^{n} i$$

or

$$\Sigma t_i = T\, n/2\, (n+1).$$

Similarly,

$$\Sigma t_i^2 = T^2\, n/6\, (n+1)(2n+1),$$

$$\Sigma t_i^3 = T^3\, n^2/4\, (n+1)^2, \quad \text{(B-1-6)}$$

and

$$\Sigma t_i^4 = T^4\, n^2/10\, (n+1)^2(2n+1).$$

For n large,

$$\Sigma t_i \cong T\, n^2/2, \qquad \Sigma t_i^2 \cong T^2\, n^3/3,$$

$$\Sigma t_i^3 \cong T^3\, n^4/4, \quad \text{and} \quad \Sigma t_i^4 \cong T^4\, n^5/5. \quad \text{(B-1-7)}$$

Relating equations (B-1-7) and (A-1-7), the elements (a_{ij}) of A are:

$$a_{11} = n,$$

$$a_{12} = a_{21} = T\,n^2/2,$$

$$a_{13} = a_{31} = a_{22} = T^2\,n^3/3, \qquad \text{(B-1-8)}$$

$$a_{23} = a_{32} = T^3\,n^4/4, \text{ and}$$

$$a_{33} = T^4\,n^5/5.$$

The determinant of A is

$$\text{Det}\,|A| = na_{22}a_{33} + a_{12}a_{23}a_{31} + a_{21}a_{32}a_{13} +$$

$$- a_{31}a_{22}a_{13} - a_{32}a_{23}n - a_{21}a_{12}a_{33}$$

and using (B-1-8),

$$\text{Det}\,|A| = T^6\,n^9/(2160). \qquad \text{(B-1-9)}$$

The elements of C are,

$$c_{11} = (a_{22}a_{33} - a_{32}a_{23})/\text{Det}\,|A|,$$

$$c_{22} = (a_{11}a_{33} - a_{31}a_{13})/\text{Det}\,|A|, \qquad \text{(B-1-10)}$$

$$c_{33} = (a_{11}a_{22} - a_{12}a_{21})/\text{Det}\,|A|,$$

$$c_{21} = c_{12} = (a_{31}a_{23} - a_{21}a_{33})/\text{Det } |A|,$$

$$c_{32} = c_{23} = (a_{31}a_{12} - a_{11}a_{32})/\text{Det } |A|, \qquad \text{(B-1-10)}$$

and

$$c_{13} = c_{31} = (a_{12}a_{23} - a_{22}a_{13})/\text{Det } |A|.$$

Using equations (B-1-8) and (B-1-9),

$$\begin{aligned} c_{11} &= 9/n, \\ c_{22} &= 192/T^2\, n^3, \\ c_{33} &= 180/T^4\, n^5, \\ c_{21} &= c_{12} = -36/T\, n^2, \\ c_{23} &= c_{32} = -180/T^3\, n^4, \end{aligned} \qquad \text{(B-1-11)}$$

and

$$c_{13} = c_{31} = 30/T^2\, n^3.$$

Combining equations (B-1-2), (B-1-3), and (B-1-11),

$$\begin{aligned} \sigma_a{}^2 &= (9/n)\sigma_B{}^2, \\ \sigma_b{}^2 &= (192/T^2n^3)\sigma_B{}^2, \\ \sigma_c{}^2 &= (180/T^4n^5)\sigma_B{}^2, \end{aligned} \qquad \text{(B-1-12)}$$

and

$$\begin{aligned} \tau_{ab}\sigma_a\sigma_b &= (-36/Tn^2)\sigma_B{}^2, \\ \tau_{bc}\sigma_b\sigma_c &= (-180/T^3n^4)\sigma_B{}^2, \\ \tau_{ac}\sigma_a\sigma_c &= (30/T^2n^3)\,\sigma_B{}^2. \end{aligned} \qquad \text{(B-1-13)}$$

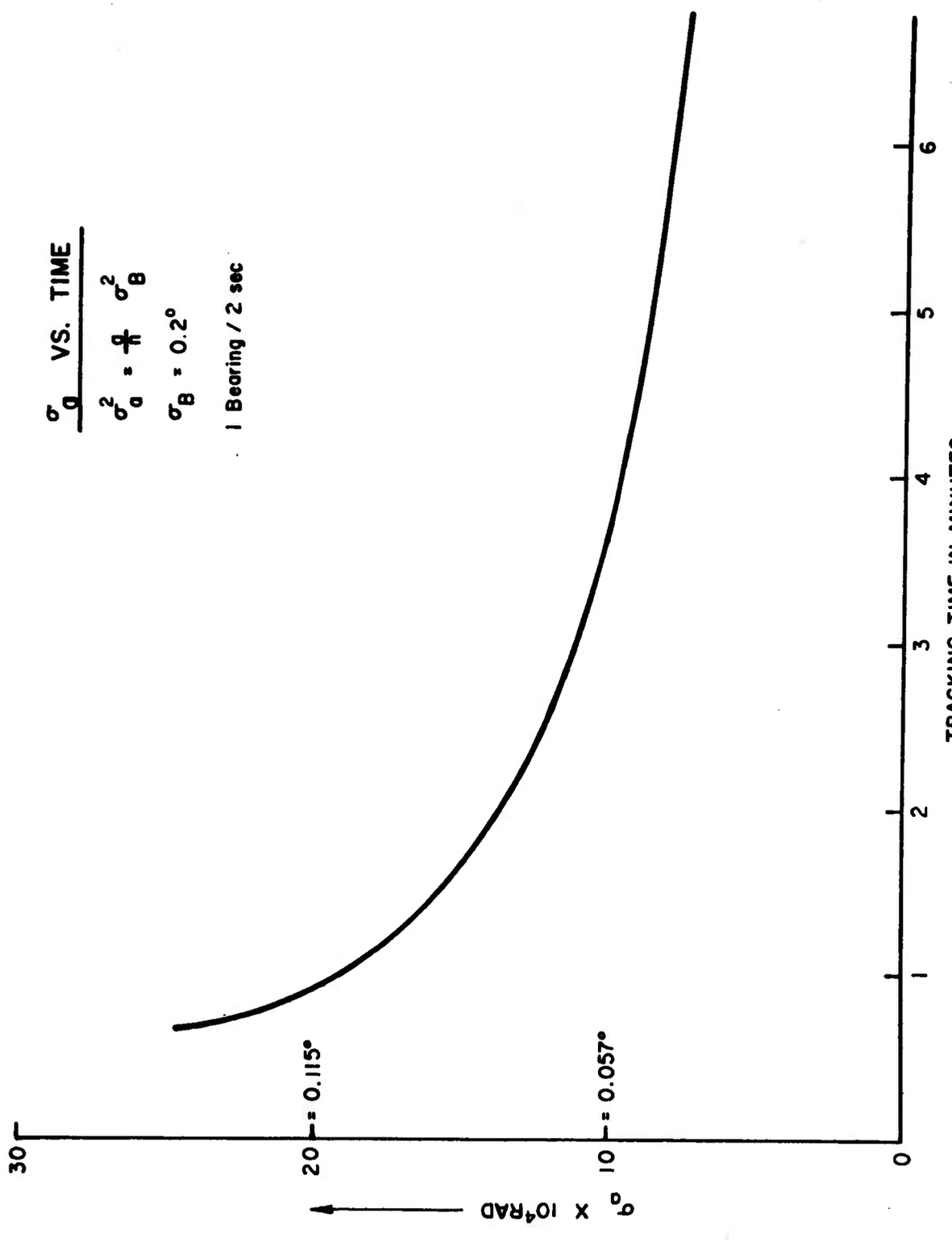

Fig. B-1-1 σ_a Versus Time

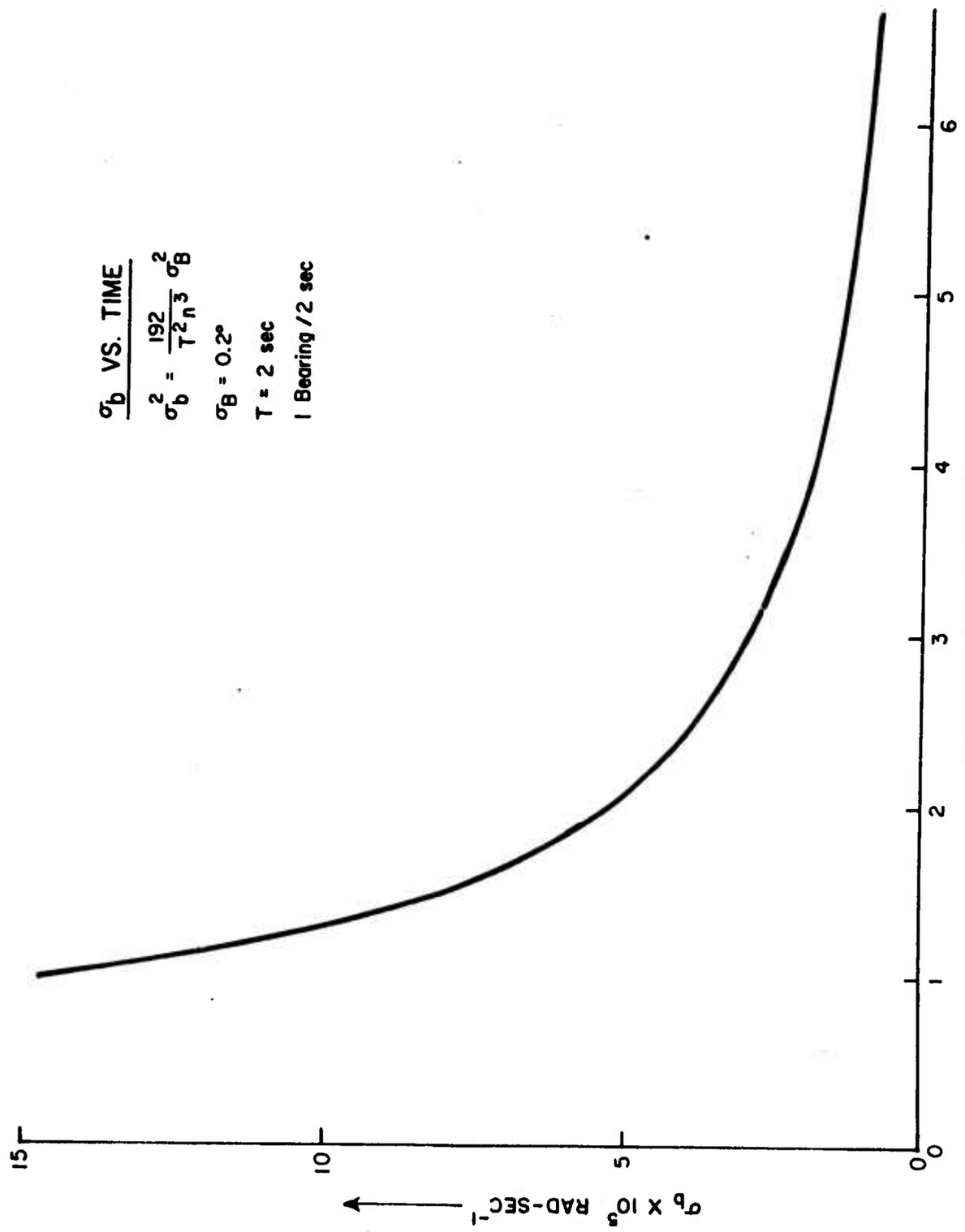

Fig. B-1-2 σ_b Versus Time

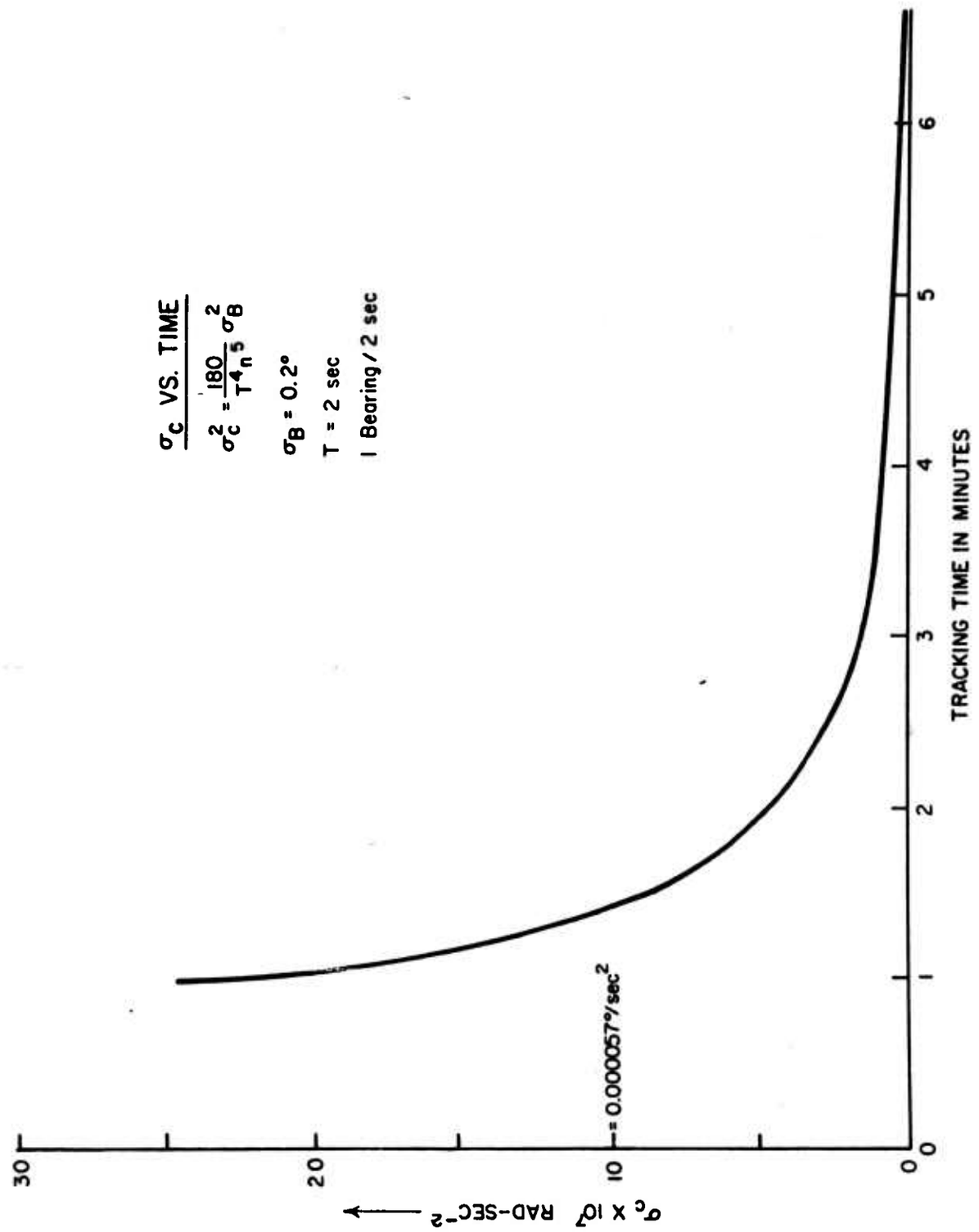

Fig. B-1-3 σ_c Versus Time

Also, from equations (B-1-4) and (B-1-11),

$$\tau_{ab} = -\sqrt{3}/2 = -0.866,$$

$$\tau_{bc} = -\sqrt{15}/4 = -0.970, \qquad \text{(B-1-14)}$$

$$\tau_{ac} = \sqrt{5}/3 = 0.745.$$

Figs. B-1-1, B-1-2, and B-1-3 are plots of the standard deviations of the least square coefficients as functions of time. A bearing sampling interval of two seconds and a sonar bearing standard deviation of 0.2 degrees are used.

2. Variances in Functions of the Coefficients

For a linear combination of the coefficients

$$u = k_1 a + k_2 b + k_3 c,$$

$$\sigma_u^2 = k_1^2 \sigma_a^2 + k_2^2 \sigma_b^2 + k_3^2 \sigma_c^2 + 2\tau_{ab} k_1 k_2 \sigma_a \sigma_b + \qquad \text{(B-2-1)}$$

$$+2\tau_{bc} k_2 k_3 \sigma_b \sigma_c + 2\tau_{ac} k_1 k_3 \sigma_a \sigma_c.$$

For an arbitrary function of the coefficients

$$u = f(a, b, c),$$

$$\sigma_u^2 = \left(\frac{\partial u}{\partial a}\right)^2 \sigma_a^2 + \left(\frac{\partial u}{\partial b}\right)^2 \sigma_b^2 + \left(\frac{\partial u}{\partial c}\right)^2 \sigma_c^2 + 2\tau_{ab} \frac{\partial u}{\partial a} \frac{\partial u}{\partial b} \sigma_a \sigma_b + \qquad \text{(B-2-2)}$$

$$+ 2\tau_{bc} \frac{\partial u}{\partial b} \frac{\partial u}{\partial c} \sigma_b \sigma_c + 2\tau_{ac} \frac{\partial u}{\partial a} \frac{\partial u}{\partial c} \sigma_a \sigma_c$$

to a first order approximation.

Variance expressions for some of the functions of interest are developed in the following pages. Analysis is being continued on several that have not yet been evaluated.

3. Variance in Bearing Rate and Change in Bearing Rate

From equation (A-2-1),

$$\dot{B} = b + 2ct.$$

Therefore, taking $\tau_{bc} = -1$ (equation B-1-14),

$$\sigma_{\dot{B}}^2 = \left(\frac{\partial \dot{B}}{\partial b}\right)^2 \sigma_b^2 + \left(\frac{\partial \dot{B}}{\partial c}\right)^2 \sigma_c^2 - 2 \frac{\partial \dot{B}}{\partial b} \frac{\partial \dot{B}}{\partial c} \sigma_b \sigma_c$$

or

$$\sigma_{\dot{B}} = \left| \frac{\partial \dot{B}}{\partial b} \sigma_b - \frac{\partial \dot{B}}{\partial c} \sigma_c \right|,$$

which results in

$$\sigma_{\dot{B}} = \left| \sigma_b - 2t\sigma_c \right|. \qquad \text{(B-3-1)}$$

From equations (B-1-12),

$$\sigma_b \cong Tn\sigma_c,$$

or, from the definition of T and n,

$$\sigma_b \cong t\sigma_c.$$

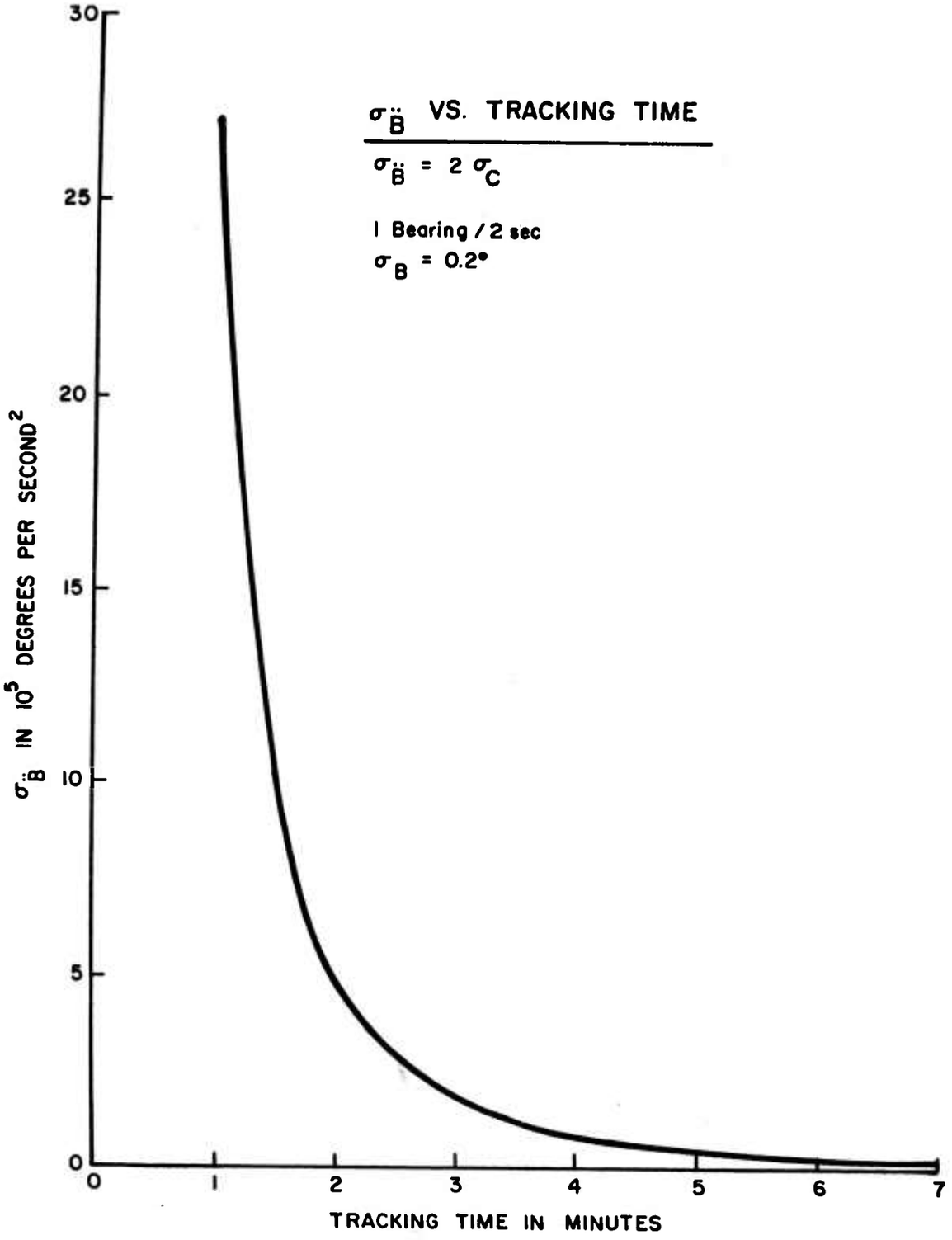

Fig. B-3-1 $\ddot{\sigma}_B$ Versus Time

Therefore,

$$\sigma_{\dot{B}} \cong \sigma_b . \qquad \text{(B-3-2)}$$

Thus Fig. B-1-2 can be interpreted as a plot of $\sigma_{\dot{B}}$ versus tracking time. The time-rate-of-change of bearing-rate is given by

$$\ddot{B} = 2c. \qquad \text{(A-2-2)}$$

Thus, it is obvious that

$$\sigma_{\ddot{B}} = 2\sigma_c . \qquad \text{(B-3-3)}$$

Fig. B-3-1 is a plot of $\sigma_{\ddot{B}}$ versus tracking time.

4. Variances in α_o, α, and θ

From equation (A-3-1)

$$\alpha_o = \tan^{-1}(b^2/c)$$

and

$$\frac{\partial \alpha_o}{\partial b} = \frac{2b/c}{\left[1+(b^2/c\ )^2\right]} = \frac{2bc}{c^2+b^4} ,$$

$$\frac{\partial \alpha_o}{\partial c} = \frac{-b^2/c^2}{\left[1+(b^2/c)^2\right]} = \frac{-b^2}{c^2+b^4} .$$

Using equations (A-1-4) and (A-1-5)

$$\frac{\partial \alpha_o}{\partial b} = 2(U/R_o)^{-1}\cos\ \alpha_o \qquad \text{and} \qquad \frac{\partial \alpha_o}{\partial c} = -\ (U/R_o)^{-2}.$$

Thus, using $\tau_{bc} = -1$,

$$\sigma_{\alpha_o} = \left|2(U/R_o)^{-1}\cos\ \alpha_o\sigma_b+(U/R_o)^{-2}\sigma_c\right|. \qquad \text{(B-4-1)}$$

Consider the ratio of the first term in (B-4-1) to the second term,

$$\frac{2(U/R_o)^{-1}\cos\ \alpha_o\sigma_b}{(U/R_o)^{-2}\sigma_c} = 2(U/R_o)\cos\ \alpha_o\ \frac{\sigma_b}{\sigma_c}\ .$$

Using (B-1-12), the ratio becomes

$$2(U/R_o)\cos\ \alpha_o(Tn) = 2(U/R_o)t\ \cos\ \alpha_o$$

which must be small for the expansion expressed by (A-1-2) to be valid. Thus, to a first order approximation,

$$\sigma_{\alpha_o} \cong (U/R_o)^{-2}\ \sigma_c. \qquad \text{(B-4-2)}$$

It can be shown that

$$\sigma_\alpha = \sigma_{\alpha_o}. \qquad \text{(B-4-3)}$$

From equations (A-3-3) and (A-3-1)

$$\theta = \pi-\tan^{-1}(b^2/c)+a.$$

Also,

$$\frac{\partial\theta}{\partial a} = 1,$$

$$\frac{\partial\theta}{\partial b} = \left(\frac{-1}{1+b^4/c^2}\right)\left(\frac{2b}{c}\right) = \frac{-2bc}{c^2+b^4},$$

and

$$\frac{\partial\theta}{\partial c} = \left(\frac{-1}{1+b^4/c^2}\right)\left(\frac{-b^2}{c^2}\right) = \frac{b^2}{c^2+b^4}.$$

Using $\tau_{ab} = -1$, $\tau_{bc} = -1$, and $\tau_{ac} = +1$,

$$\sigma_\theta = \left|\sigma_a + \frac{2bc}{c^2+b^4}\sigma_b + \frac{b^2}{c^2+b^4}\sigma_c\right|,$$

or

$$\sigma_\theta = \left|\sigma_a + \frac{b}{c^2+b^4}(2c\sigma_b+b\sigma_c)\right|. \qquad \text{(B-4-4)}$$

Consider the ratio of the first term in the above parenthesis to the second term, using equations (A-1-4), (A-1-5), and (B-1-12),

$$\frac{2c\sigma_b}{b\sigma_c} = \frac{2(U/R_o)^2 \sin\alpha_o \cos\alpha_o\, t\sigma_c}{U/R_o \sin\alpha_o \sigma_c} = 2(U/R_o)\cos\alpha_o t$$

which must be small for the bearing expansion to be valid. Therefore, to a first order approximation,

$$\sigma_\theta \cong \left|\sigma_a + \frac{b^2}{c^2+b^4}\sigma_c\right|. \qquad \text{(B-4-5)}$$

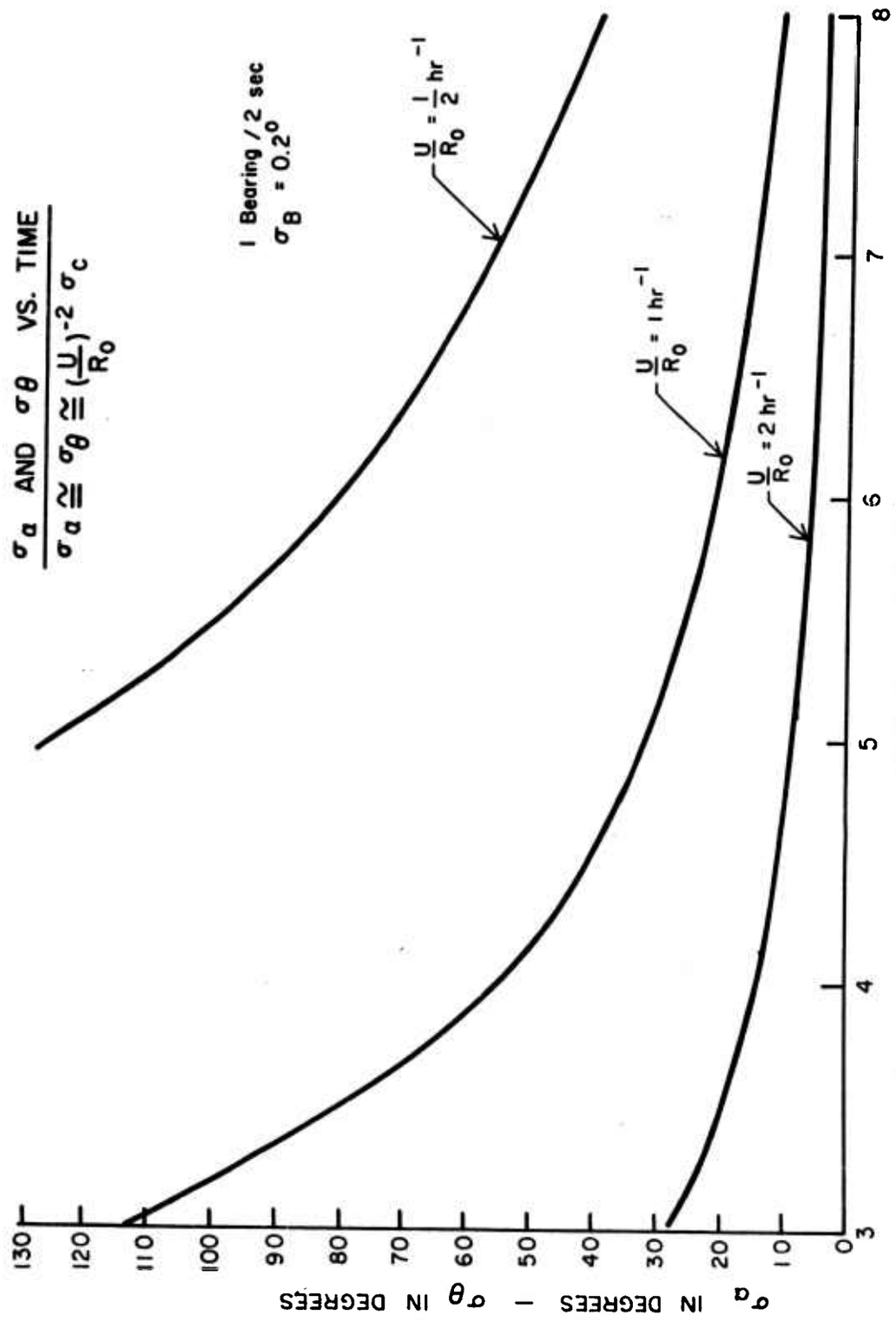

Fig. B-4-1 σ_α and σ_θ Versus Time

Then, from equation (A-3-5),

$$\sigma_\theta \cong \left| \sigma_a + \left(\frac{R_o}{U}\right)^2 \sigma_c \right|. \qquad \text{(B-4-6)}$$

Expressing σ_a in terms of σ_c and using the arguments used above

$$\sigma_\theta \cong \left(\frac{U}{R_o}\right)^{-2} \sigma_c \cong \sigma_\alpha. \qquad \text{(B-4-7)}$$

Fig. B-4-1 is a plot of σ_α and σ_θ versus tracking time for various values of U/R_o.

5. Variance in (U/R_o)

From equation (A-3-5)

$$(U/R_o) = \left[\frac{c^2+b^4}{b^2}\right]^{1/2},$$

Using equations (A-1-4, 5) and the above,

$$\frac{\partial(U/R_o)}{\partial b} = \frac{\sin^2\alpha_o - \cos^2\alpha_o}{\sin\alpha_o}$$

and

$$\frac{\partial(U/R_o)}{\partial c} = \frac{\cos\alpha_o}{b} = (U/R_o)^{-1}\cot\alpha_o.$$

Therefore, taking $\tau_{bc} = -1$,

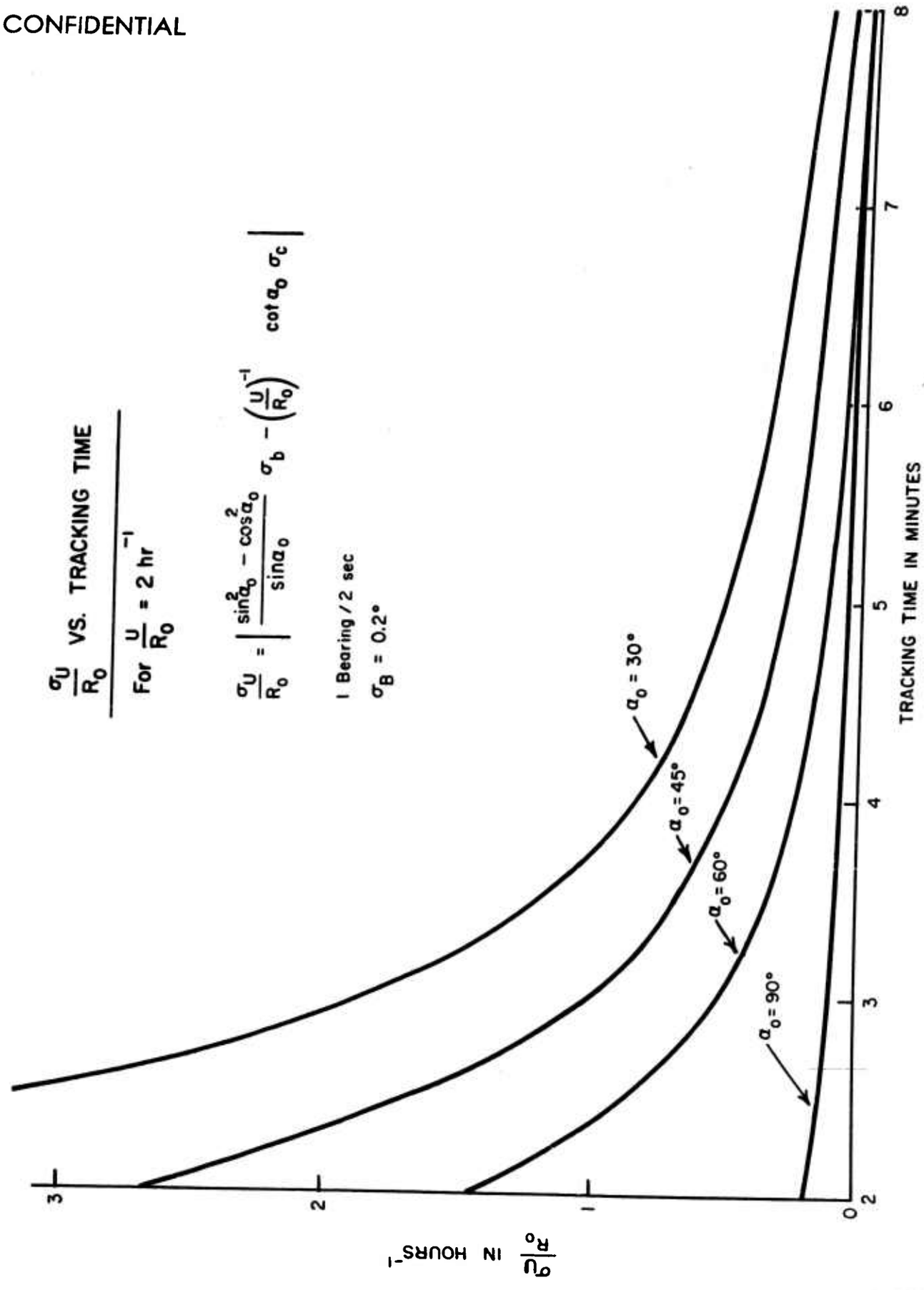

Fig. B-5-1 σ_{U/R_o} Versus Time for U/R_o = 2 hr^{-1}

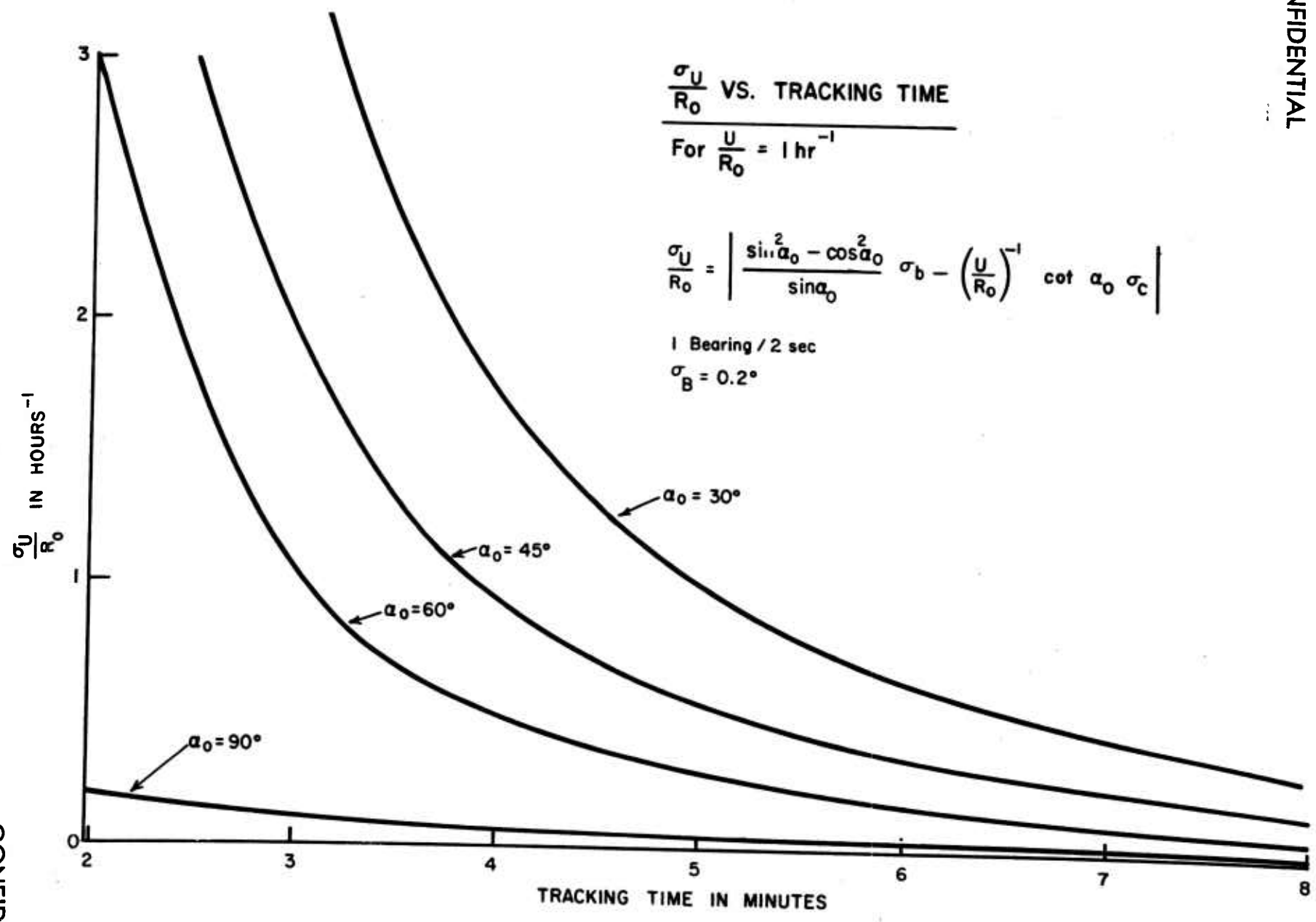

Fig. B-5-2 σ_{U/R_o} Versus Time for U/R_o = 1 hr^{-1}

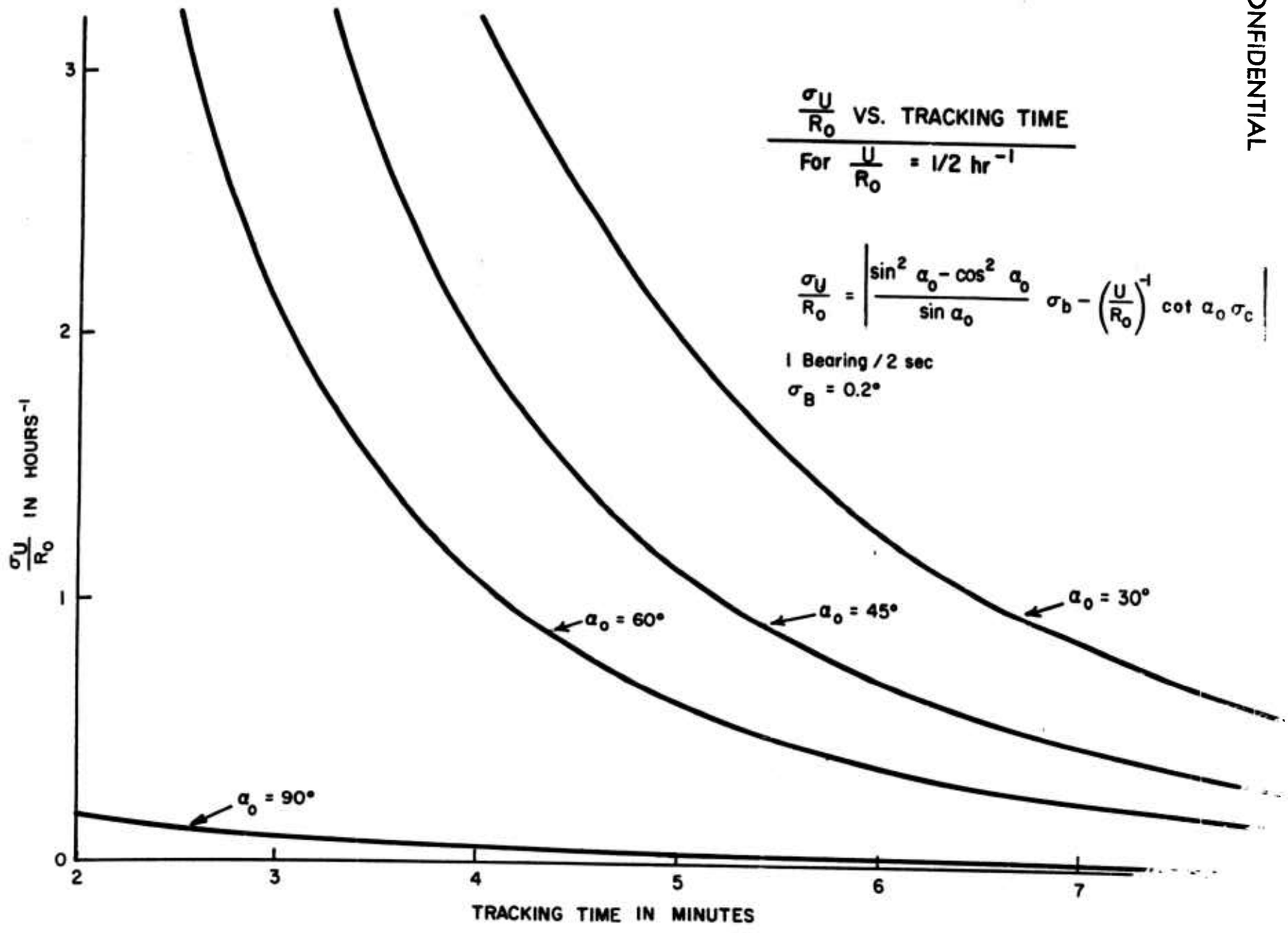

Fig. B-5-3 σ_{U/R_o} Versus Time for U/R_o = 0.5 hr^{-1}

$$\sigma_{U/R_o} \cong \left| \left(\frac{\sin^2\alpha_o - \cos^2\alpha_o}{\sin \alpha_o} \right) \sigma_b - (U/R_o)^{-1} \cot \alpha_o \sigma_c \right| . \qquad \text{(B-5-1)}$$

Figs. B-5-1 through B-5-3 show the variation of σ_{U/R_o} with tracking time for various values of U/R_o and α_o.

For $\alpha_o \cong \pi/2$,

$$\sigma_{U/R_o} \cong \sigma_b . \qquad \text{(B-5-2)}$$

For $\alpha_o \cong 0$,

$$\sigma_{U/R_o} \rightarrow \infty . \qquad \text{(B-5-3)}$$

In this case, however, bearing-rate is zero and the only information which can be derived from the data is,

$$B = \text{constant and } \dot{B} = 0.$$

6. Examples for Particular Geometries and Comparisons of ASP with Manual Plots

The figures of this section give relative motion parameter accuracies as functions of time for the geometries illustrated. The ASP results are based upon a two-second bearing sampling interval with a bearing standard deviation of 0.2 degrees, and the manual-plot results are based upon a one minute bearing sampling interval with a bearing standard deviation of 0.3 degrees. The significance of these figures is discussed in Section 4-A of Part II.

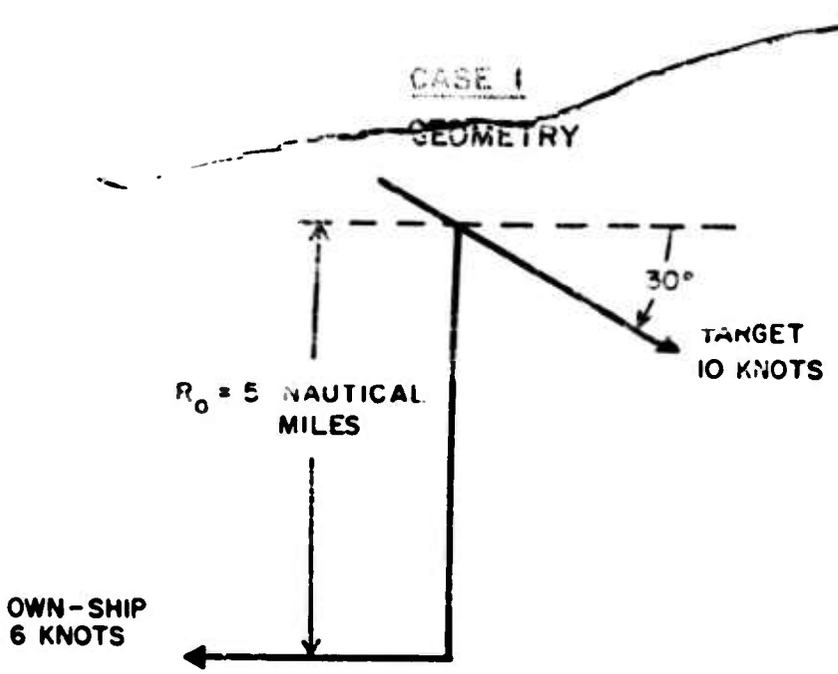

Fig. B-6-1 Case 1 Geometry

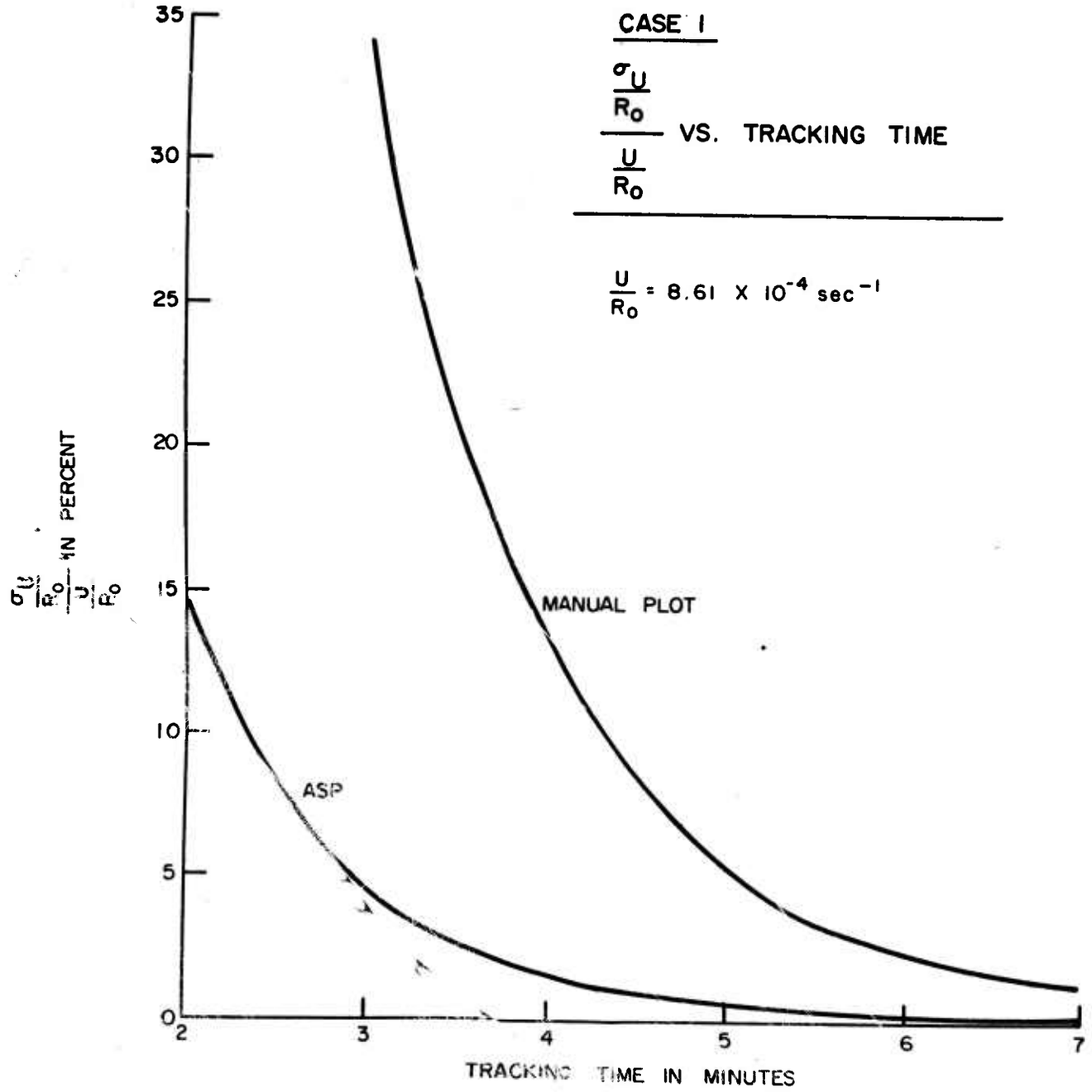

Fig. B-6-2 Case I $\sigma_{\dot{U}/R_o}/\dot{U}/R_o$ Versus Time

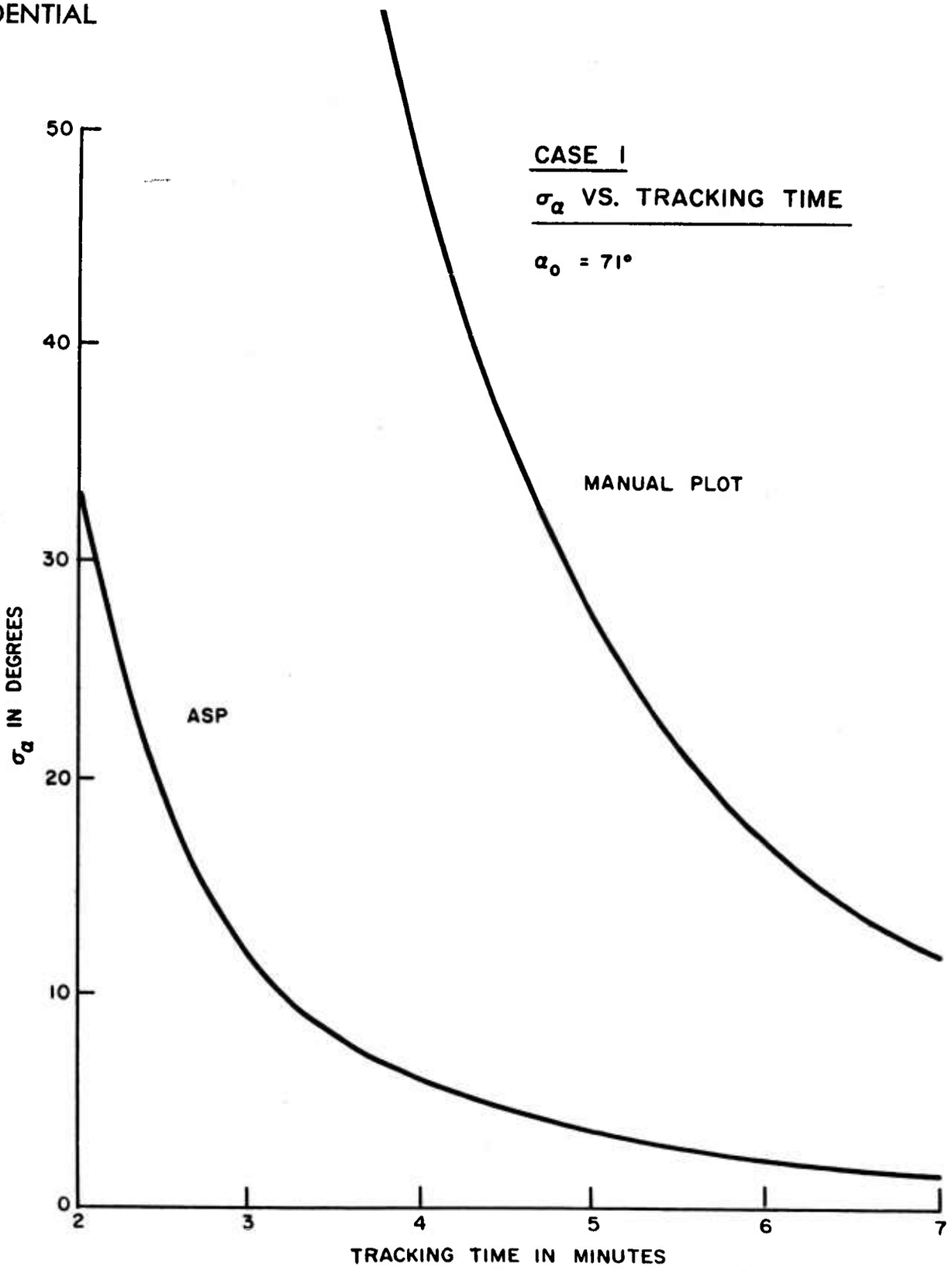

Fig. B-6-3 Case 1 σ_α Versus Time

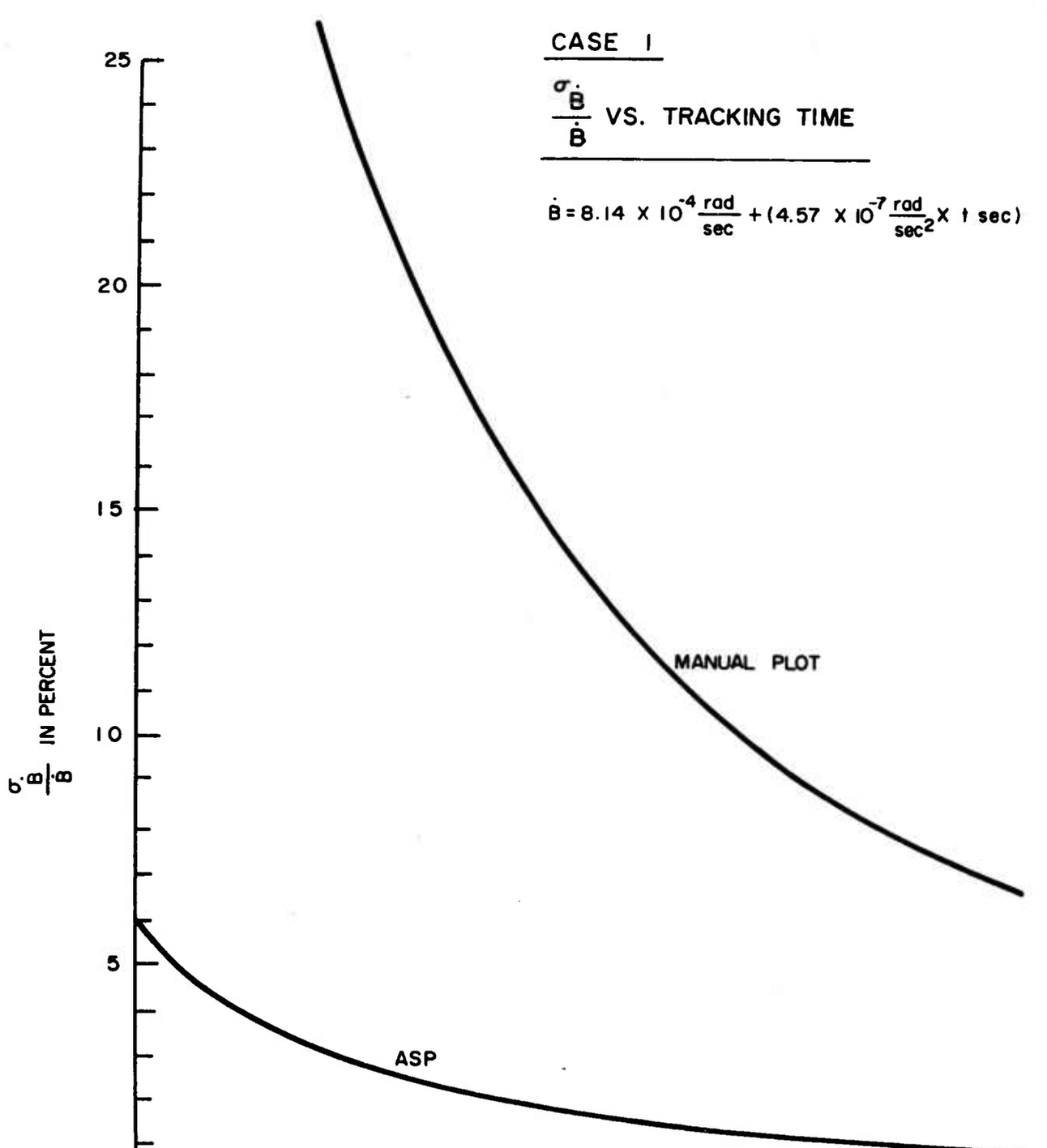

Fig. B-6-4 Case 1 $\sigma_{\dot{B}/\dot{B}}$ Versus Time

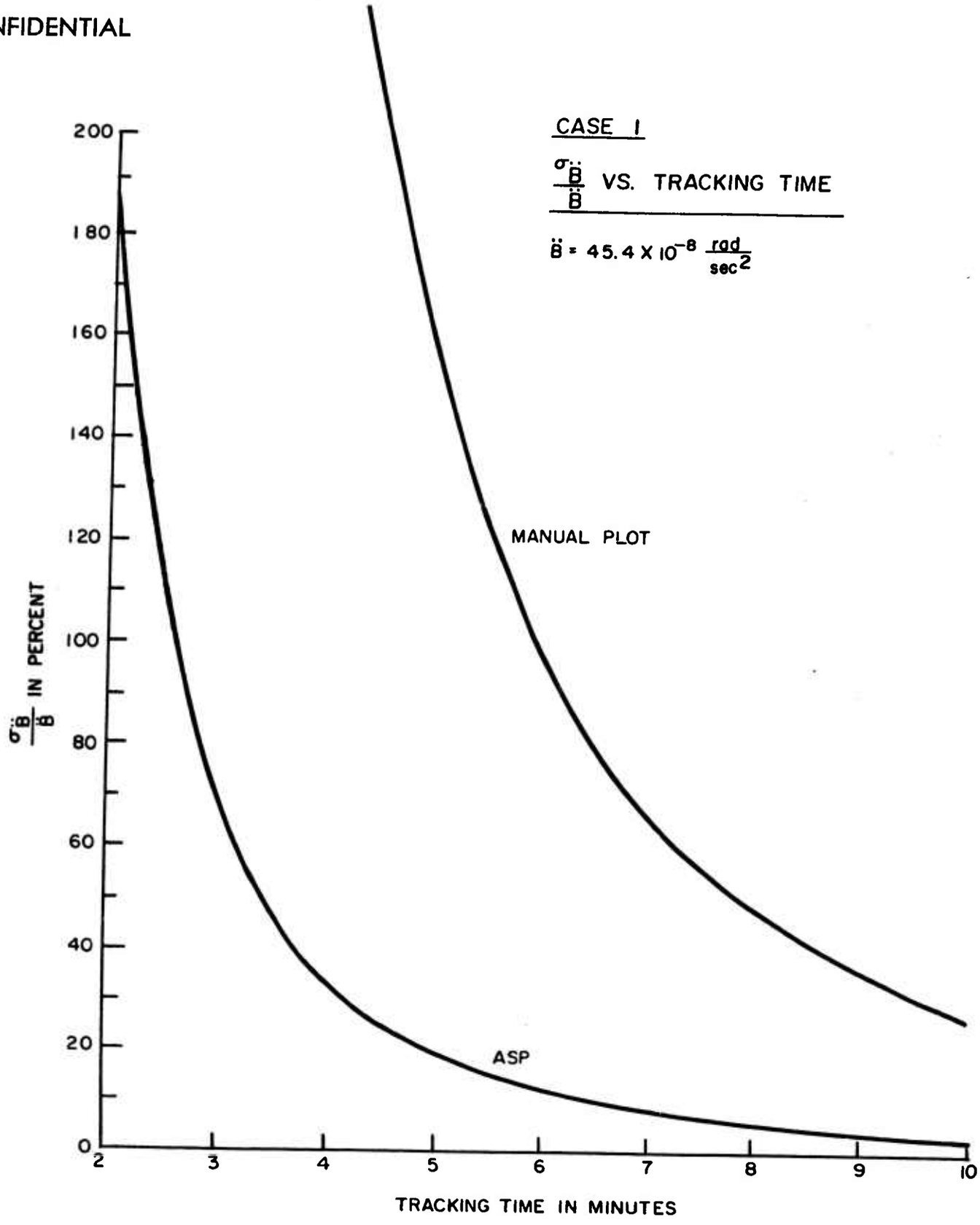

Fig. B-6-5 Case 1 $\sigma_{\ddot{B}/\ddot{B}}$ Versus Time

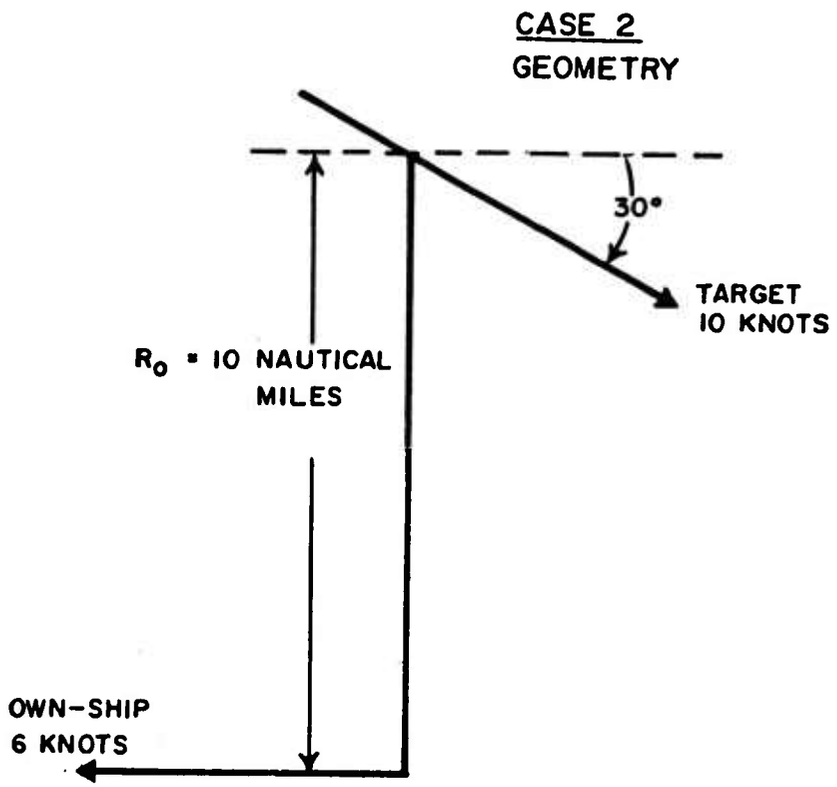

Fig. B-6-6 Case 2 Geometry

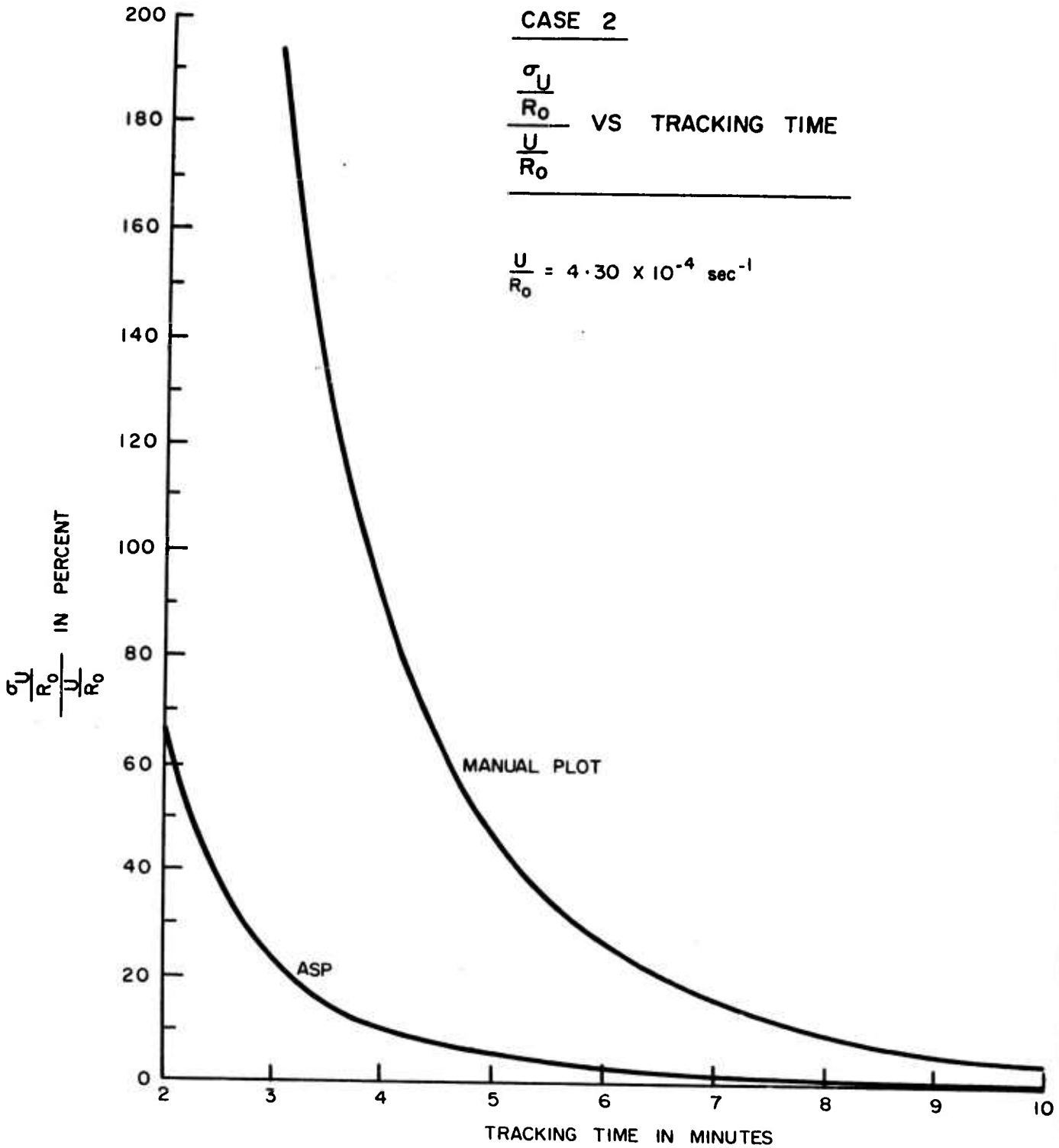

Fig. B-6-7 Case 2 $\sigma_{U/R_o}/U/R_o$ Versus Time

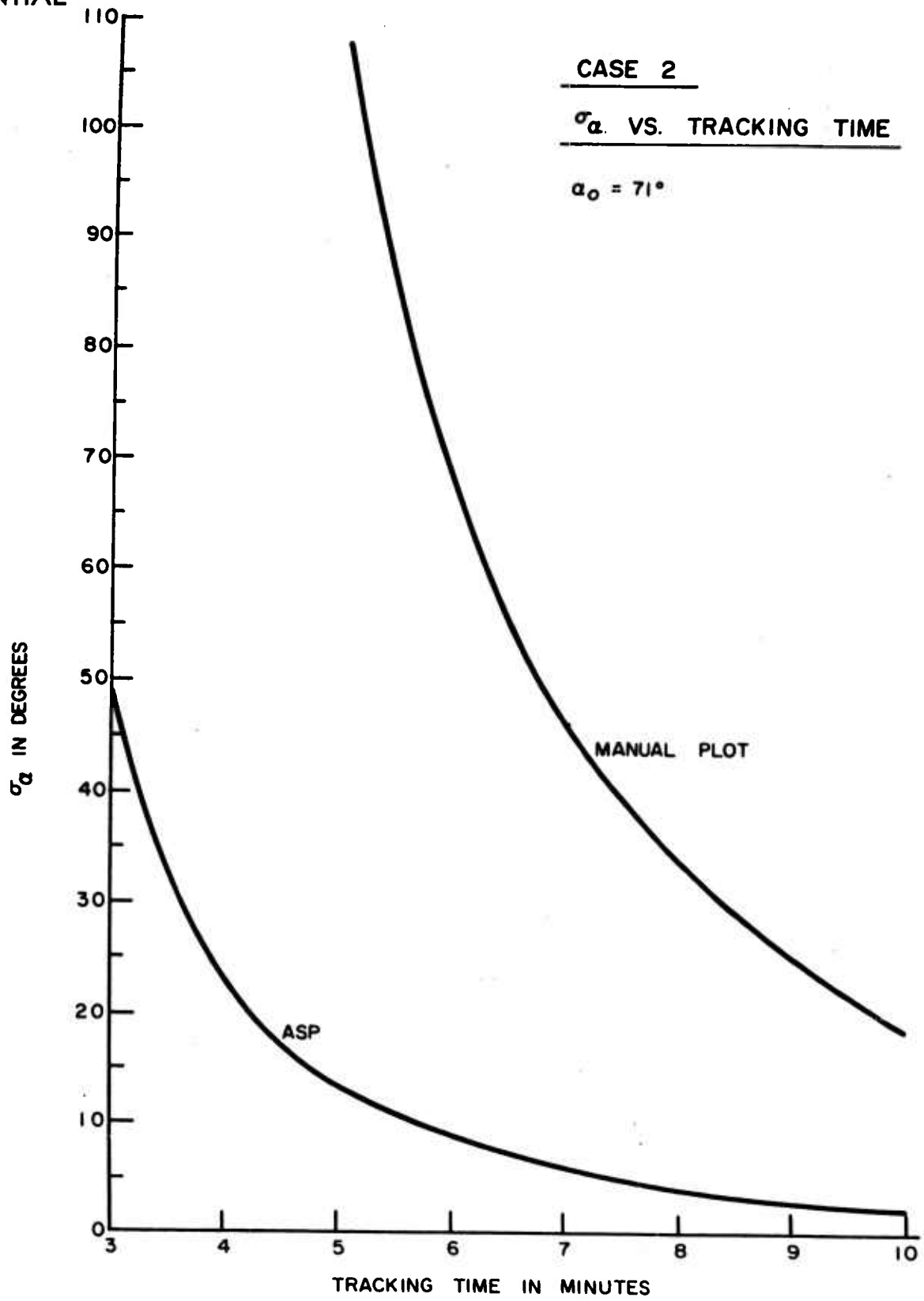

Fig. B-6-8 Case 2 σ_α Versus Time

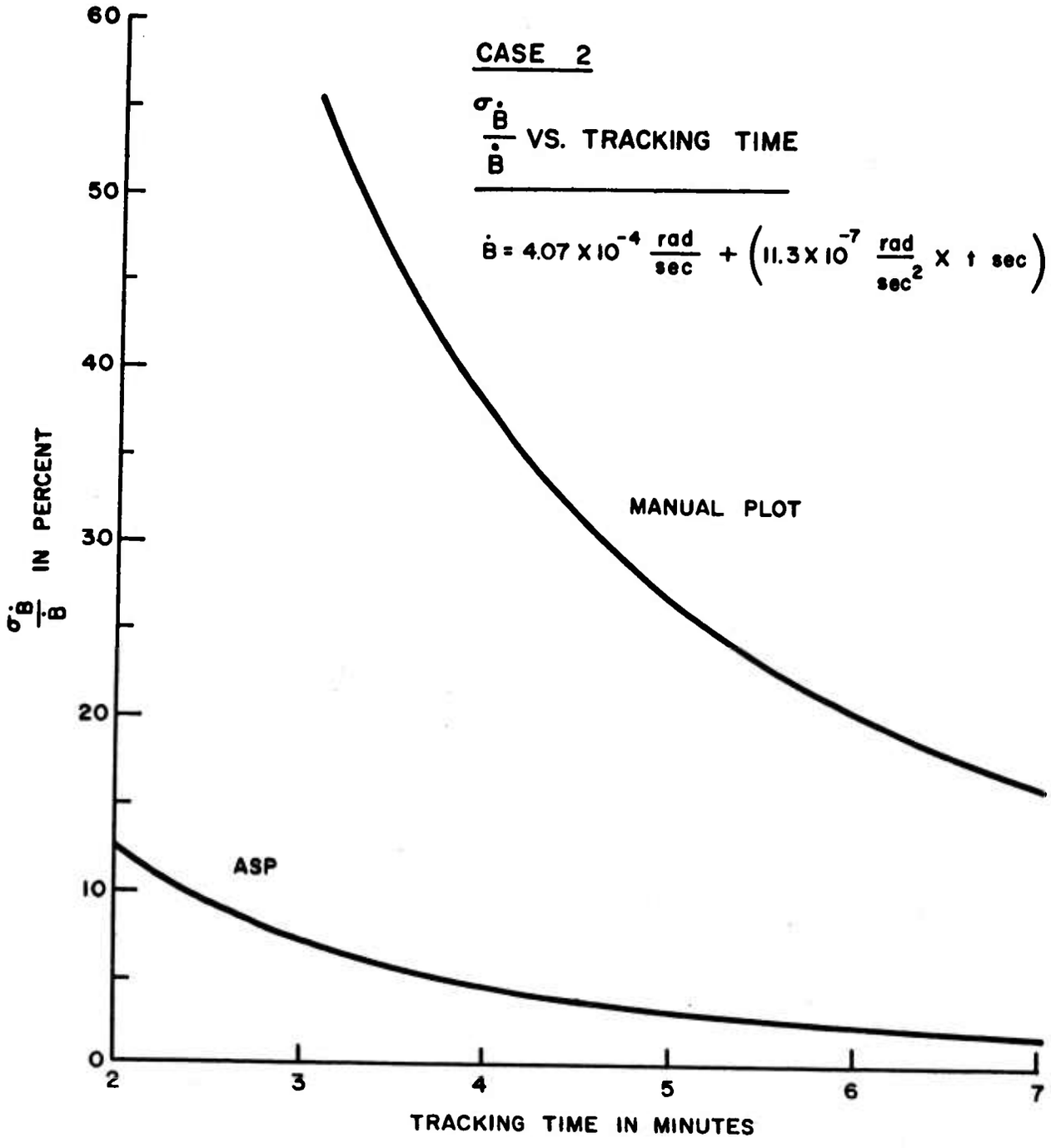

Fig. B-6-9 Case 2 $\sigma_{\dot{B}/\dot{B}}$ Versus Time

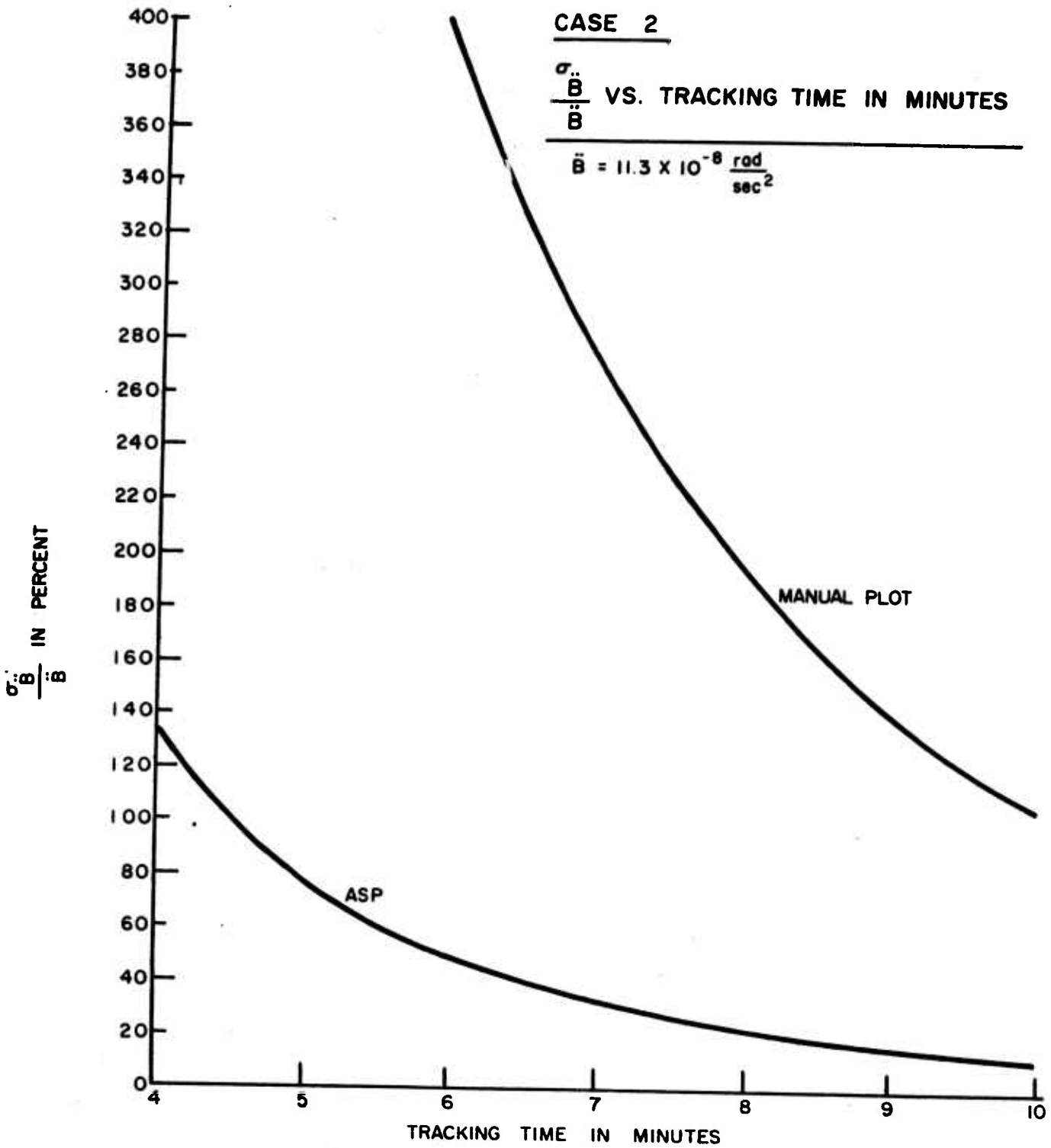

Fig. B-6-10 Case 2 $\sigma_{\ddot{B}/\ddot{B}}$ Versus Time

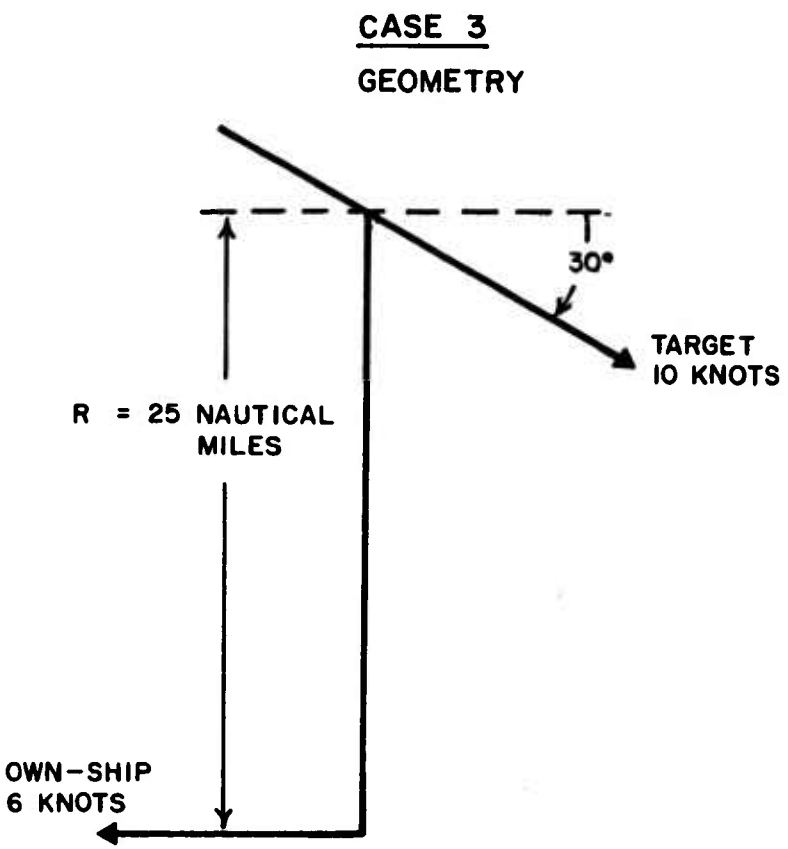

Fig. B-6-11 Case 3 Geometry

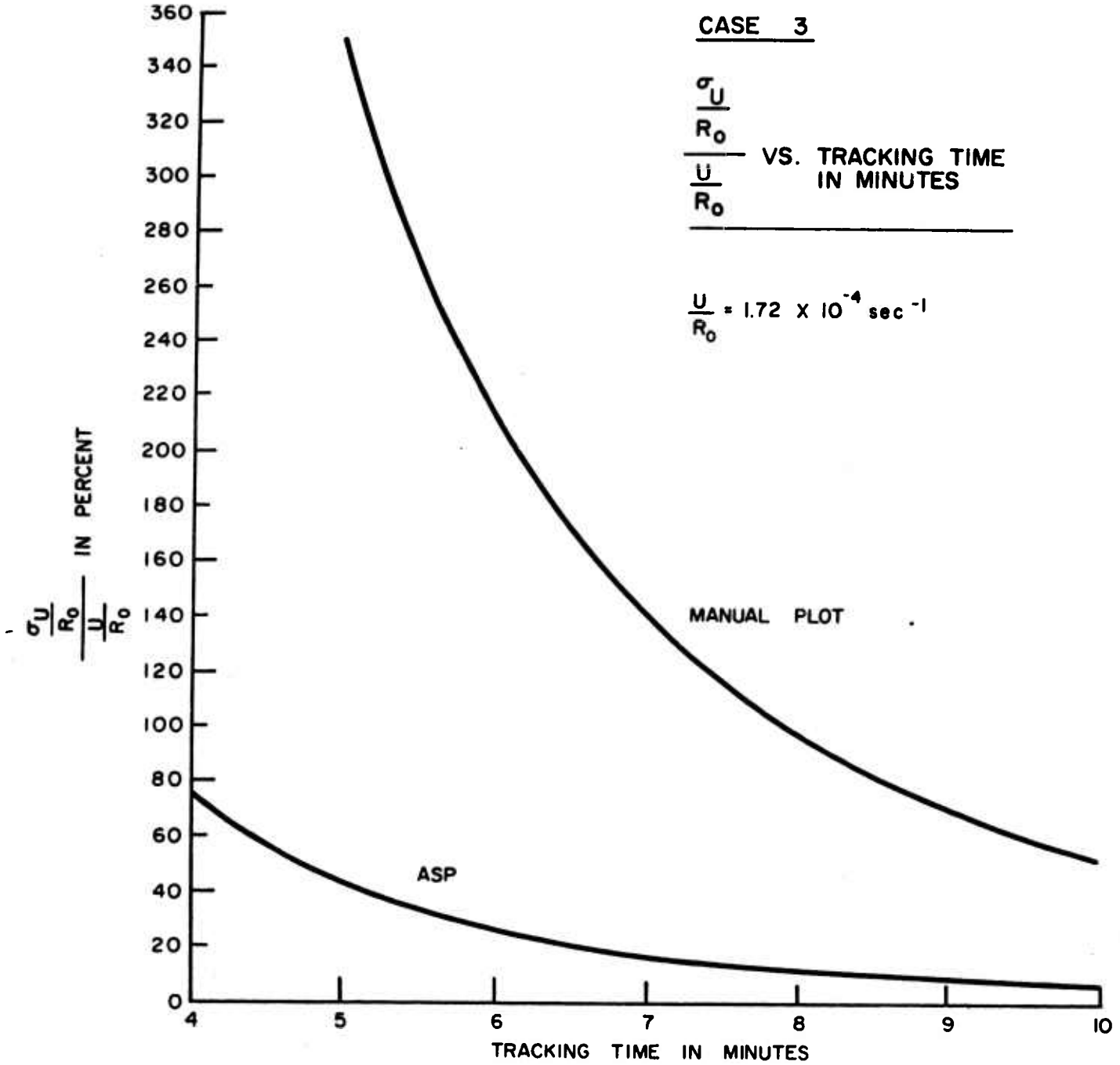

Fig. B-6-12 Case 3 $\sigma_{U/R_o}/U/R_o$ Versus Time

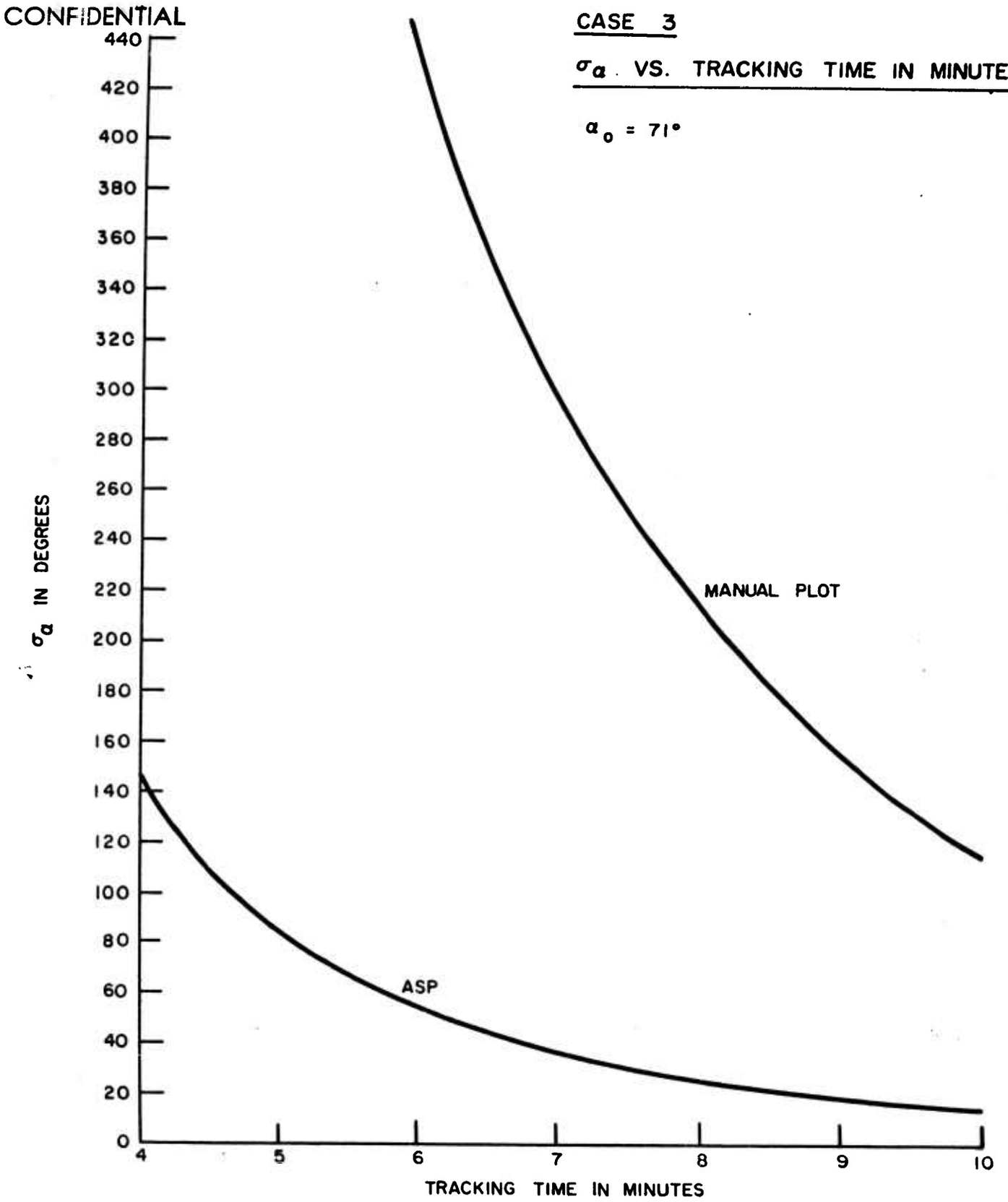

Fig. B-6-13 Case 3 σ_α Versus Time

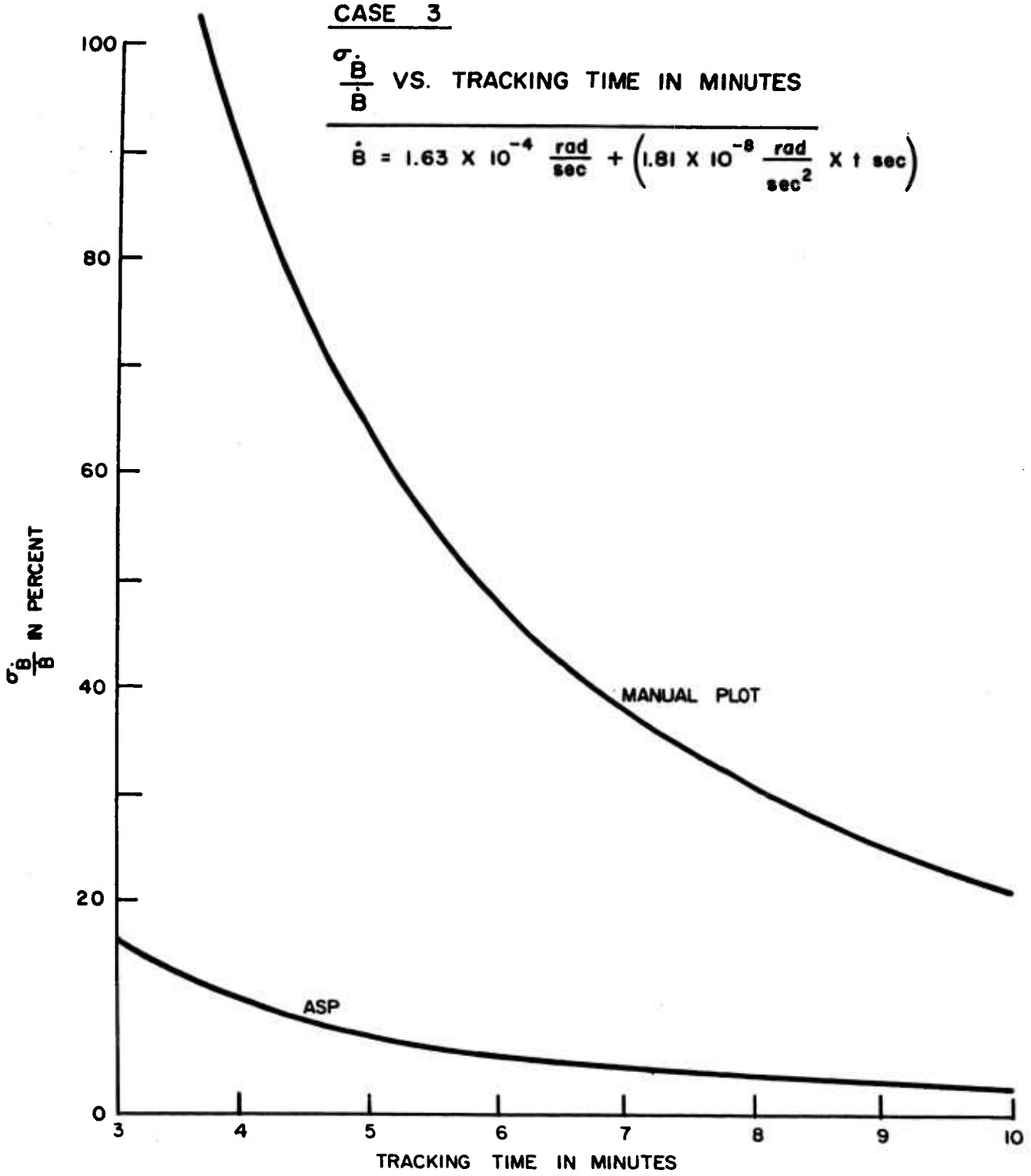

Fig. B-6-14 Case 3 $\sigma_{\dot{B}/\dot{B}}$ Versus Time

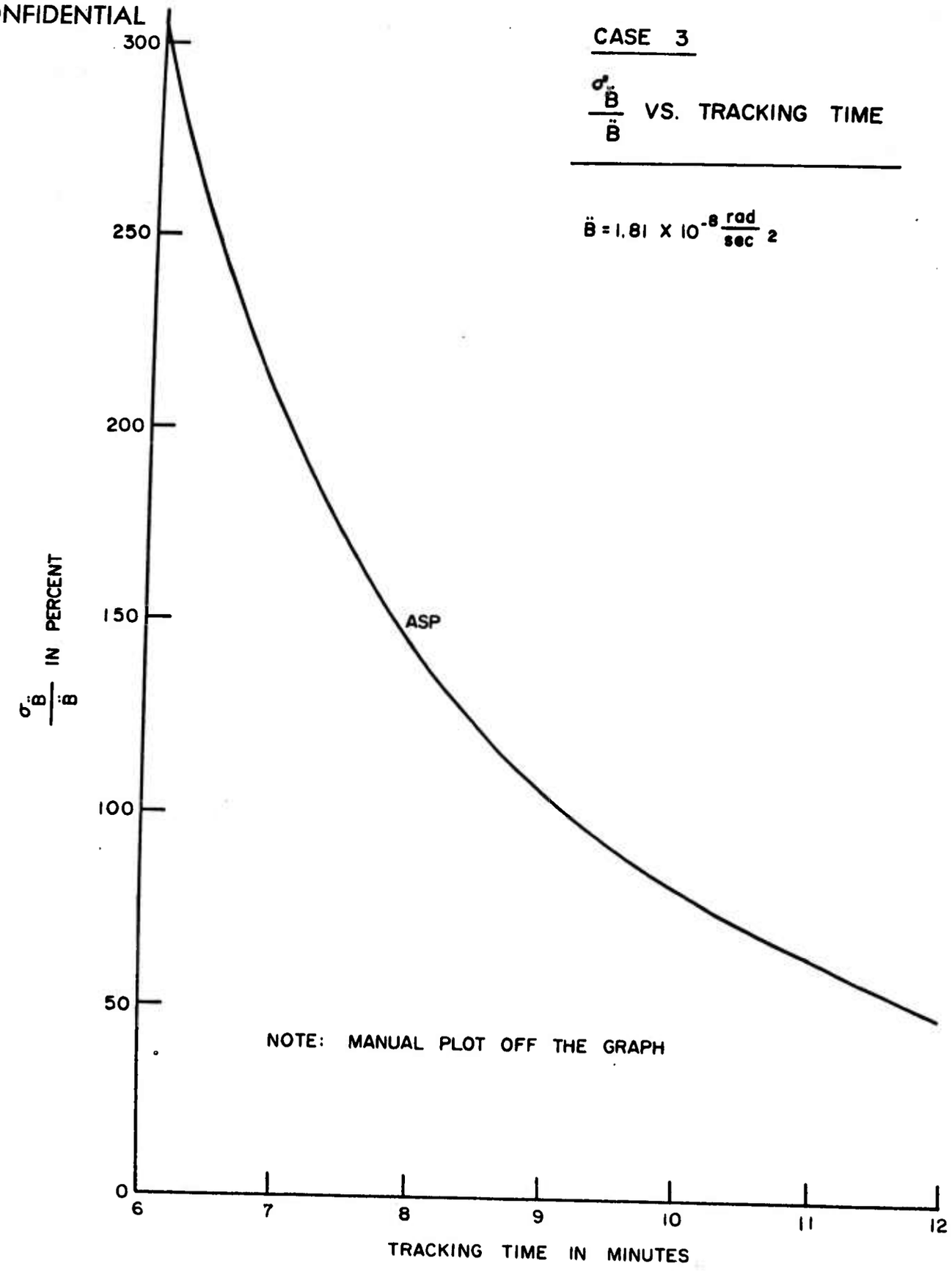

Fig. B-6-15 Case 3 $\sigma_{\ddot{B}/\ddot{B}}$ Versus Time

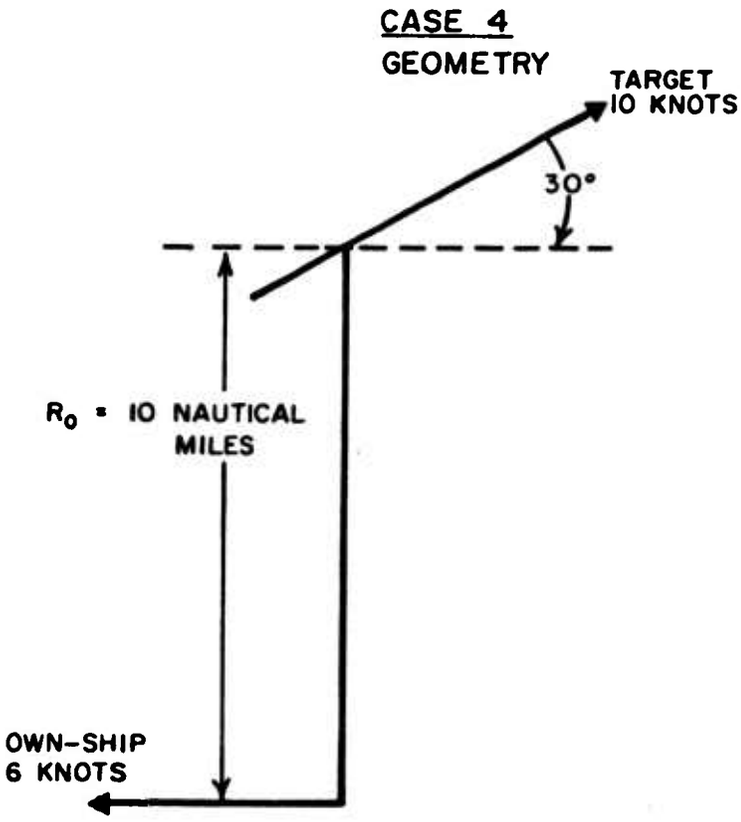

Fig. B-6-16 Case 4 Geometry

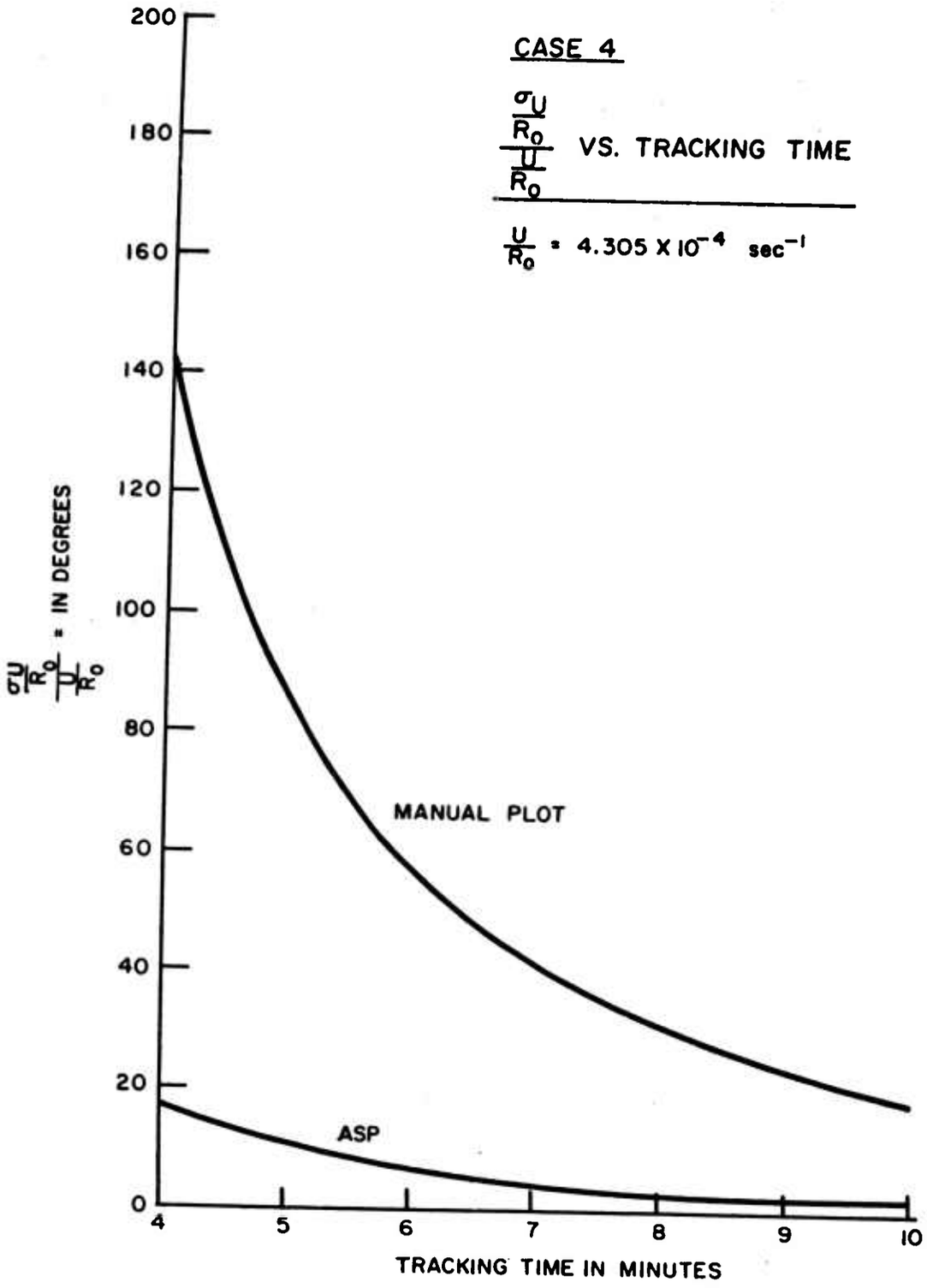

Fig. B-6-17 Case 4 $\sigma_{U/R_o}/U/R_o$ Versus Time

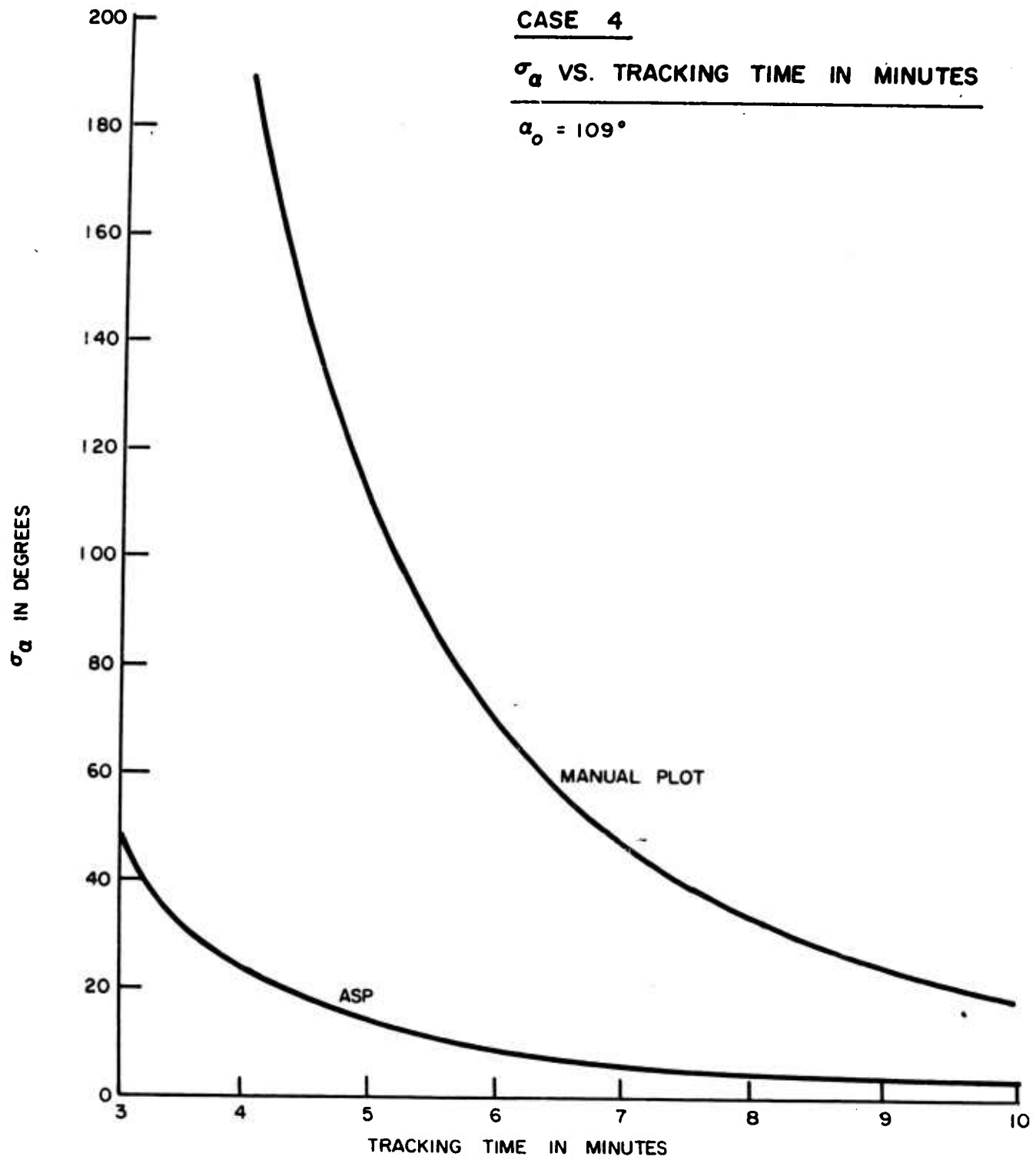

Fig. B-6-18 Case 4 σ_α Versus Time

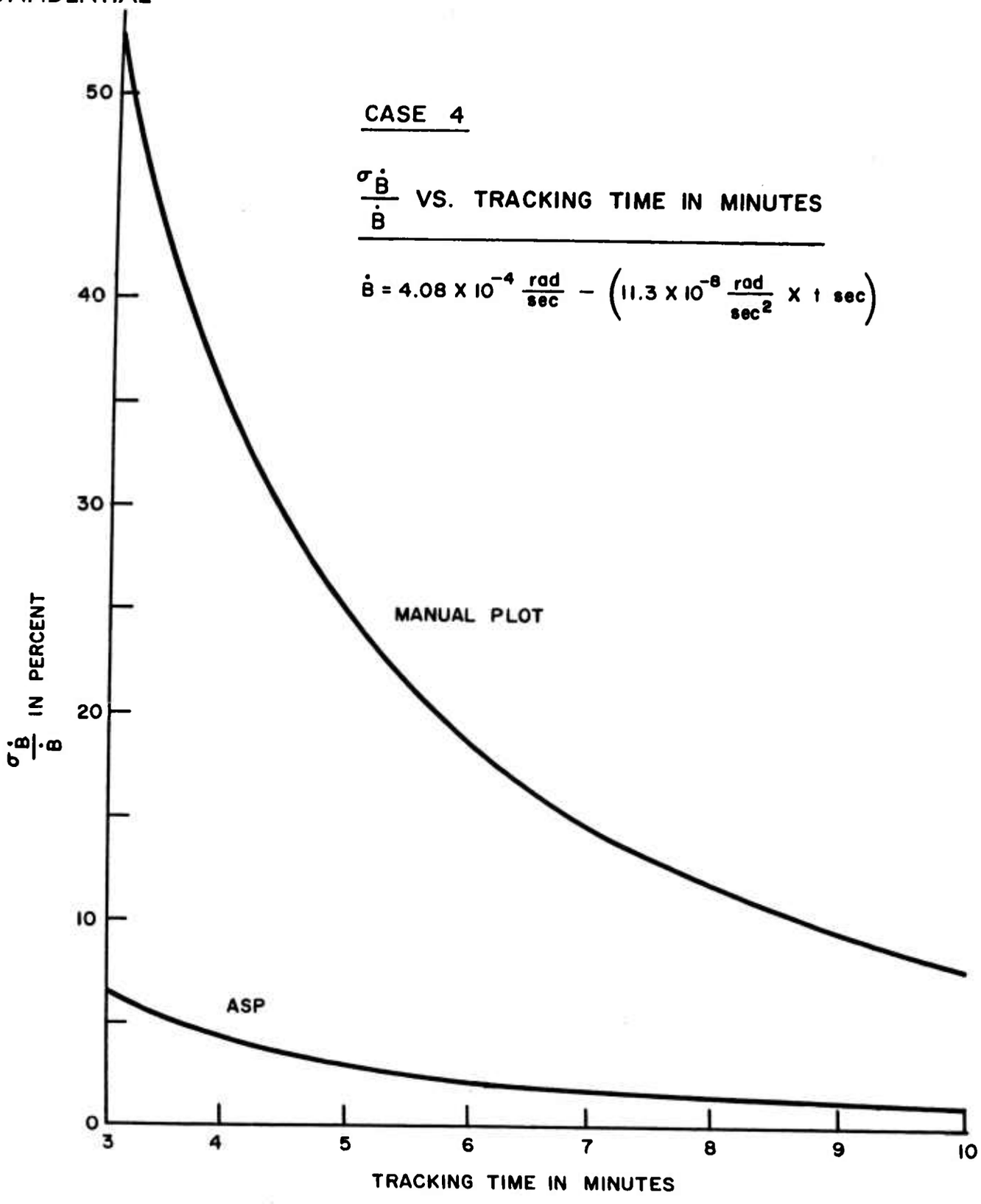

Fig. B-6-19 Case 4 $\sigma_{\dot{B}/\dot{B}}$ Versus Time

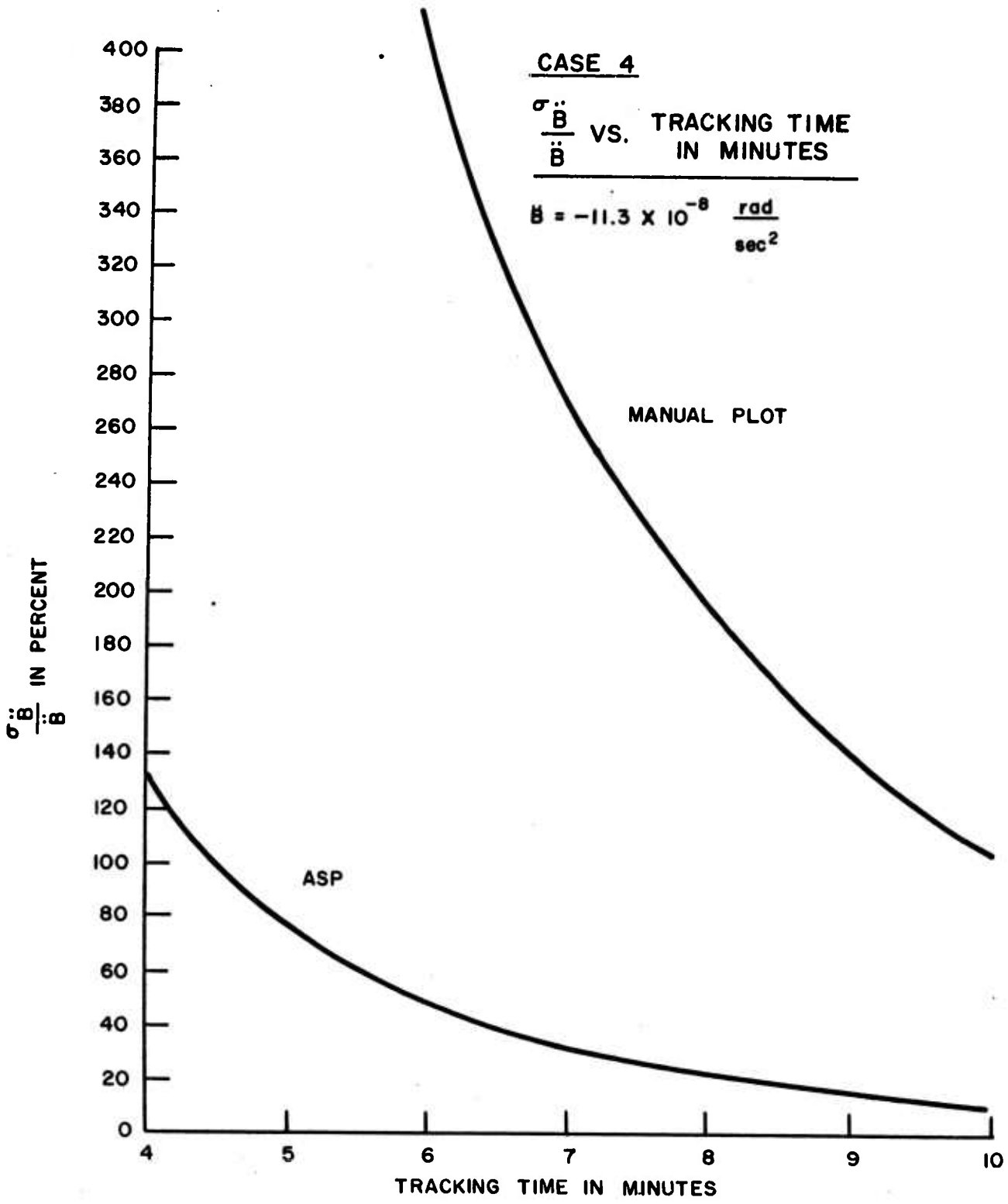

Fig. B-6-20 Case 4 $\sigma_{\ddot{B}/\ddot{B}}$ Versus Time

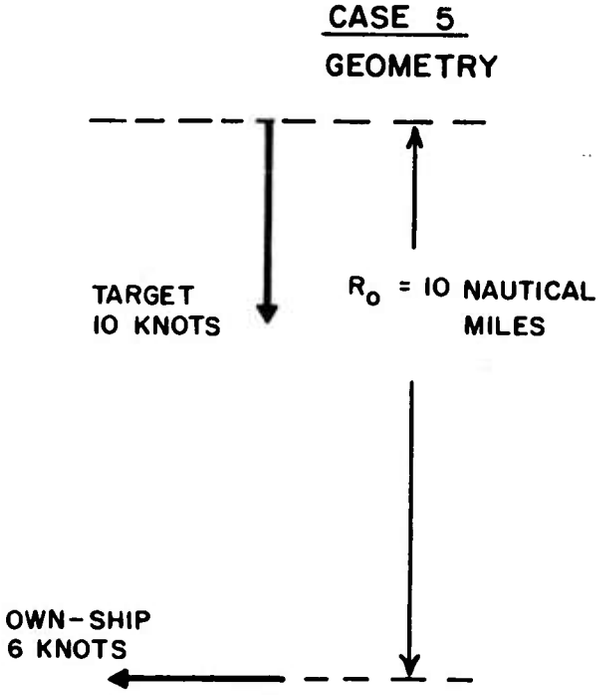

Fig. B-6-21 Case 5 Geometry

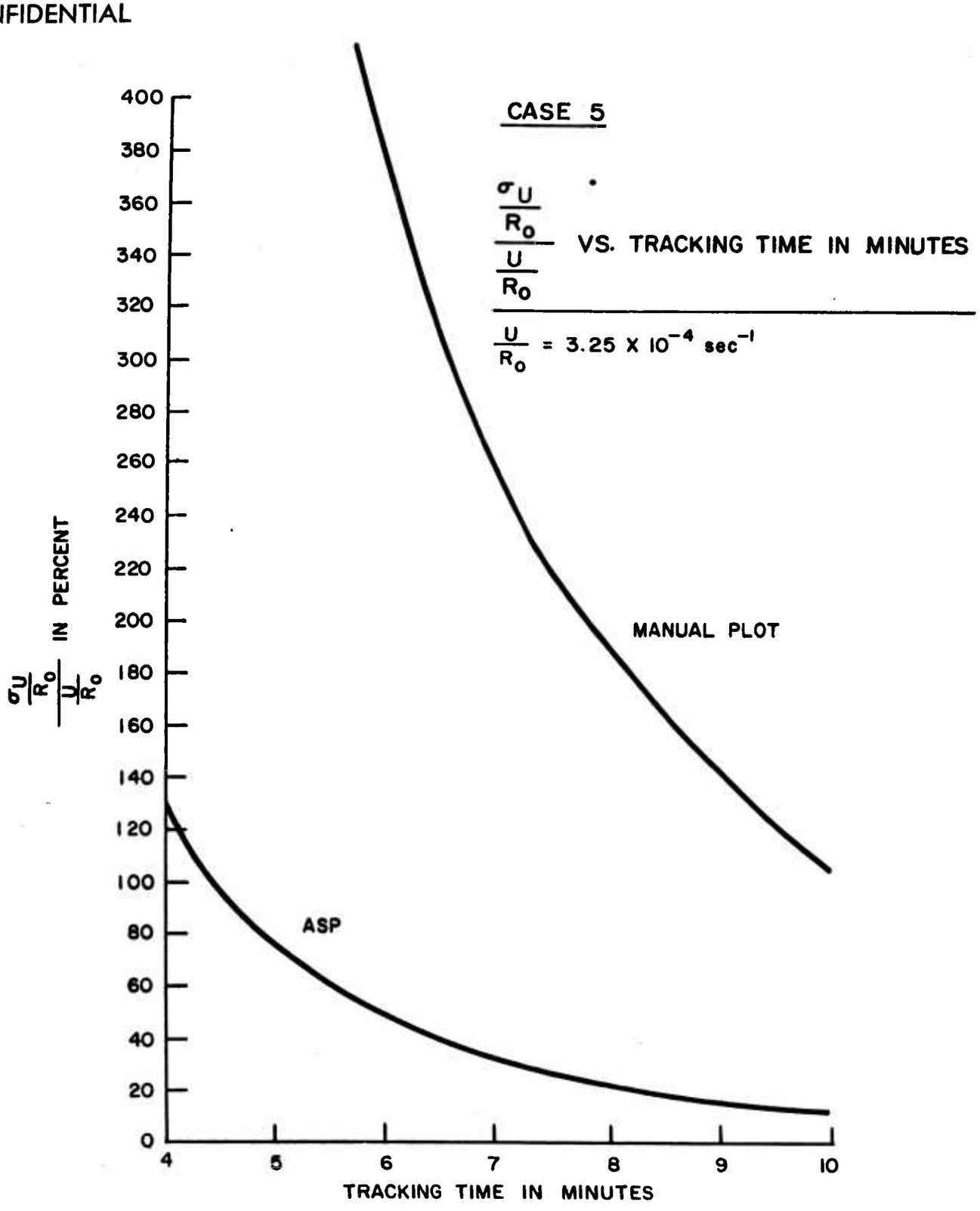

Fig. B-6-22 Case 5 $\sigma_{U/R_o}/U/R_o$ Versus Time

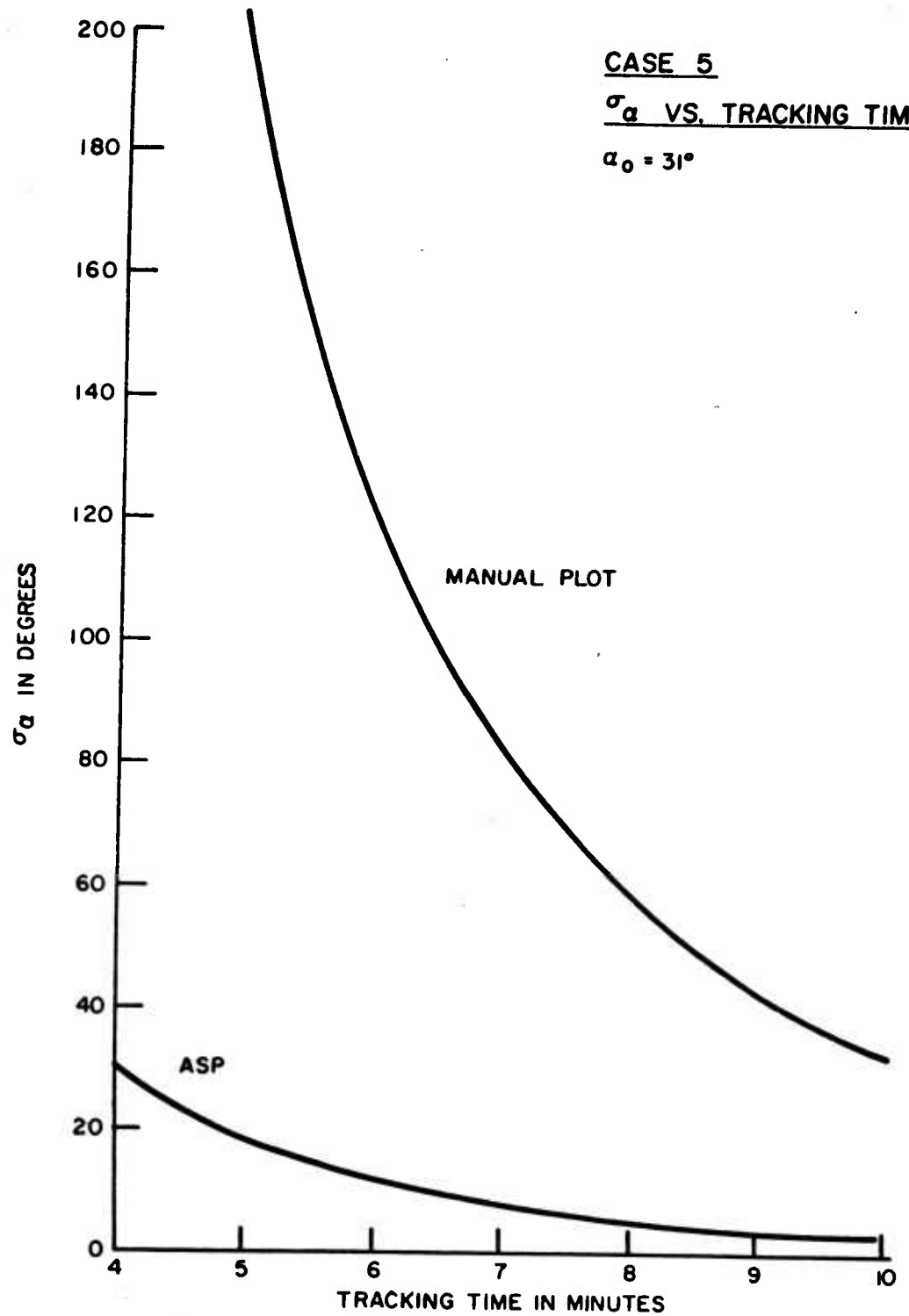

Fig. B-6-23 Case 5 σ_α Versus Time

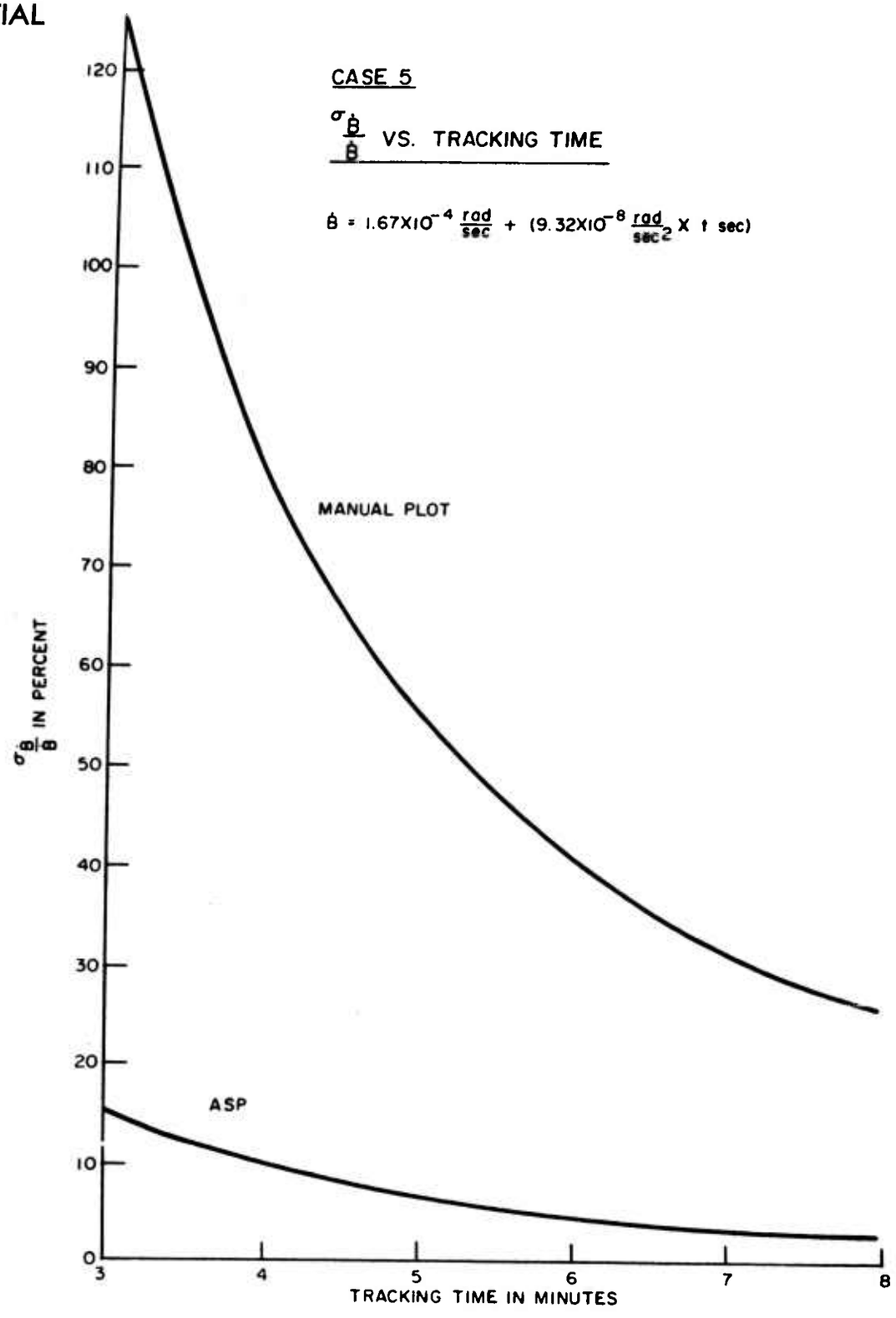

Fig. B-6-24 Case 5 $\sigma_{\dot{B}/\dot{B}}$ Versus Time

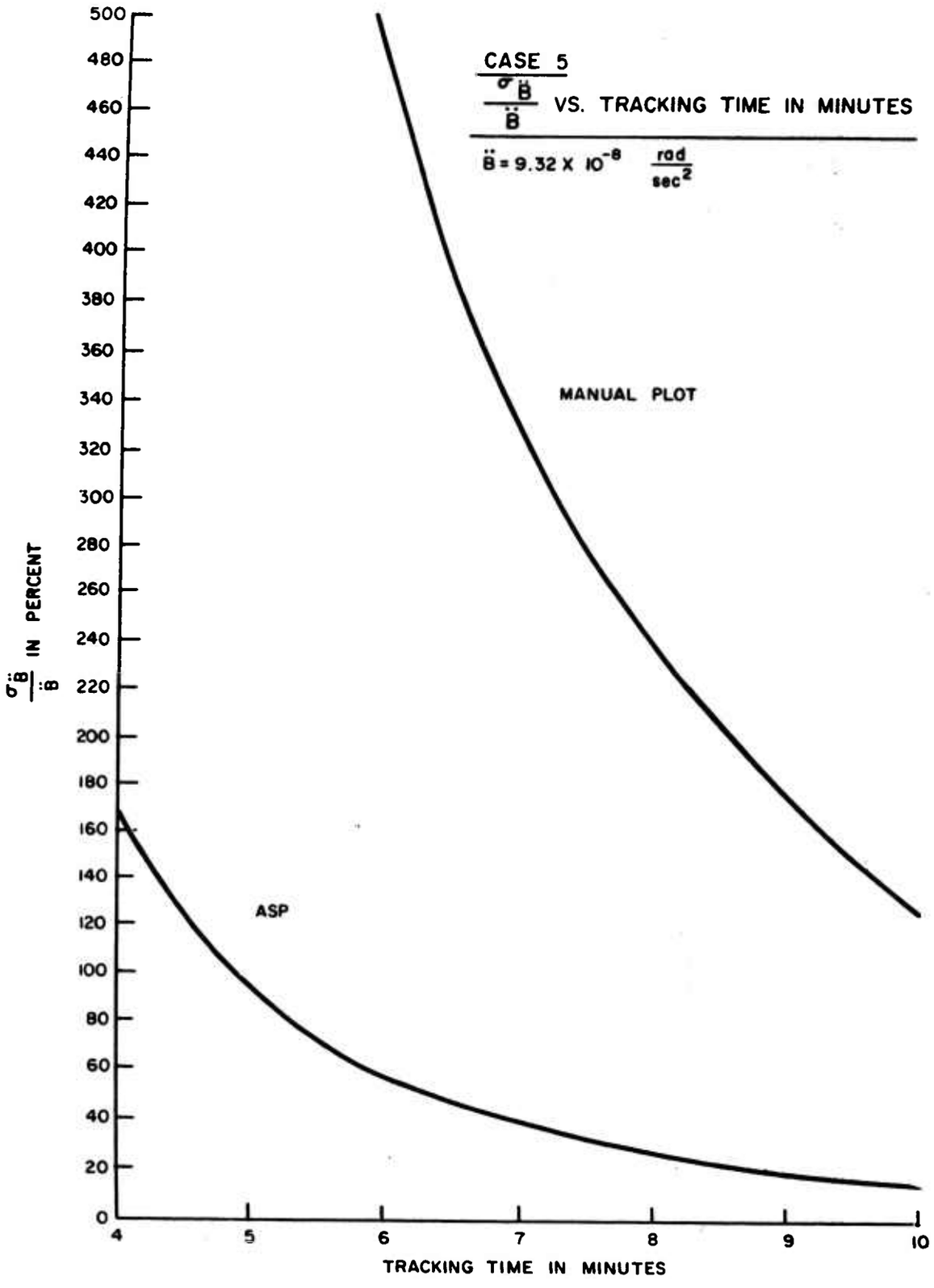

Fig. B-6-25 Case 5 $\sigma_{\ddot{B}/\ddot{B}}$ Versus Time

7. Bearings-Only Range Variance

From equations (A-7-3, 7, 8, 9),

$$R(t) = \frac{\Delta V_x^{(1)}(t')b_2}{\left[b_1+2c_1(t'-t_o)-b_2\right]\left[b_2+c_2(t-t')\right]} . \qquad \text{(B-7-1)}$$

From this equation,

$$\frac{\partial R(t)}{\partial b_2} = \frac{R(t)}{b_2} + \frac{R(t)}{\left[b_1+2c_1(t'-t_o)-b_2\right]} - \frac{R(t)}{\left[b_2+c_2(t-t')\right]} ,$$

$$\frac{\partial R(t)}{\partial c_2} = - \frac{R(t)(t-t')}{b_2+c_2(t-t')} ,$$

$$\frac{\partial R(t)}{\partial b_1} = \frac{-R(t)}{\left[b_1+2c_1(t'-t_o)-b_2\right]} = \frac{R(t)}{\Delta\dot{B}(t')}$$

$$\frac{\partial R(t)}{\partial c_1} = \frac{-2R(t)(t'-t_o)}{\left[b_1+2c_1(t'-t_o)-b_2\right]} = \frac{2R(t)(t'-t_o)}{\Delta\dot{B}(t')} .$$

Own-ship speed and course are assumed to have negligible error and the own-ship track is assumed to be nearly perpendicular to the B(t') bearing line such that

$$V_{jx}^{(1)} = V_j^{(1)} \sin\left[\phi_j^{(1)} - B(t')\right]$$

$$= V_j^{(1)} \sin(A_j + \varepsilon_B)$$

in which $A_j \approx \pi/2$ and ϵ_B represents the error in B(t'). Thus,

$$V_{jx}^{(1)} = V_j^{(1)}\left[\sin A_j + \epsilon_B \cos A_j\right]$$

which, to a first order approximation, is

$$V_{jx}^{(1)} = V_j^{(1)} \sin A_j.$$

Thus, errors arising from resolving own-ship velocity are negligible.

From the above, using $\tau_{b_1c_1} = \tau_{b_2c_2} = -1$, no correlation between first and second leg coefficients and $\sigma_b = t\sigma_c$,

$$\frac{\sigma_{R(t)}^2}{R(t)^2} \cong \frac{\sigma_{b_1}^2}{\Delta\dot{B}^2(t')} + \left(\frac{1}{b_2} - \frac{1}{\Delta\dot{B}(t')}\right)^2 \sigma_{b_2}^2$$

and using

$$\Delta\dot{B} = \dot{B}_2 - \dot{B}_1,$$

$$\dot{B}_2 = b_2;$$

$$\frac{\sigma_{R(t)}}{R(t)} = \frac{1}{|\Delta\dot{B}|}\left[\sigma_{b_1}^2 + \left(\frac{\dot{B}_1}{\dot{B}_2}\right)^2 \sigma_{b_2}^2\right]^{1/2}. \qquad \text{(B-7-2)}$$

Using (B-1-12),

$$\frac{\sigma_{R(t)}}{R(t)} = \left[\frac{T_t^3}{T_1^3} + \frac{T_t^3}{T_2^3}\left(\frac{\dot{B}_1^2}{\dot{B}_2^2}\right)\right]^{1/2} \frac{8\sqrt{3}\, T^{1/2}\sigma_B}{T_t^{3/2}\,|\Delta\dot{B}|} \qquad \text{(B-7-3)}$$

in which T_1 and T_2 are the times on the first and second legs, respectively, and T is the bearing sampling interval. Let the bracketed expression be denoted by z^2, then

$$\frac{\sigma_{R(t)}}{R(t)} = \frac{z\, 8\sqrt{3}\, T^{1/2}\sigma_B}{|\Delta\dot{B}|\, T_t^{3/2}} \,. \qquad \text{(B-7-4)}$$

This equation is similar to that for range variance in Mode 2 (Reference 1). The optimum value of z, however, differs in the two systems.

The tracking time on each leg appears only in z. Now let

$$x = \frac{T_2}{T_t} \quad \text{and} \quad y = \frac{\dot{B}_1}{\dot{B}_1 - \dot{B}_2}$$

in which T_t is the total tracking time. Then,

$$z^2 = \frac{1}{(1-x)^3} + \frac{1}{x^3}\left[\frac{y^2}{(y-1)^2}\right]$$

Minimizing this expression with respect to x gives the optimum time ratio (T_2/T_t) and the minimum z (z-opt). Figs. (B-7-1) and (B-7-2) are graphs of x-opt and z-opt versus y for both this system and Mode 2 (Mark 113). Z-opt and consequently the range error for ASP is about 1.4 times larger than the error for Mode 2.

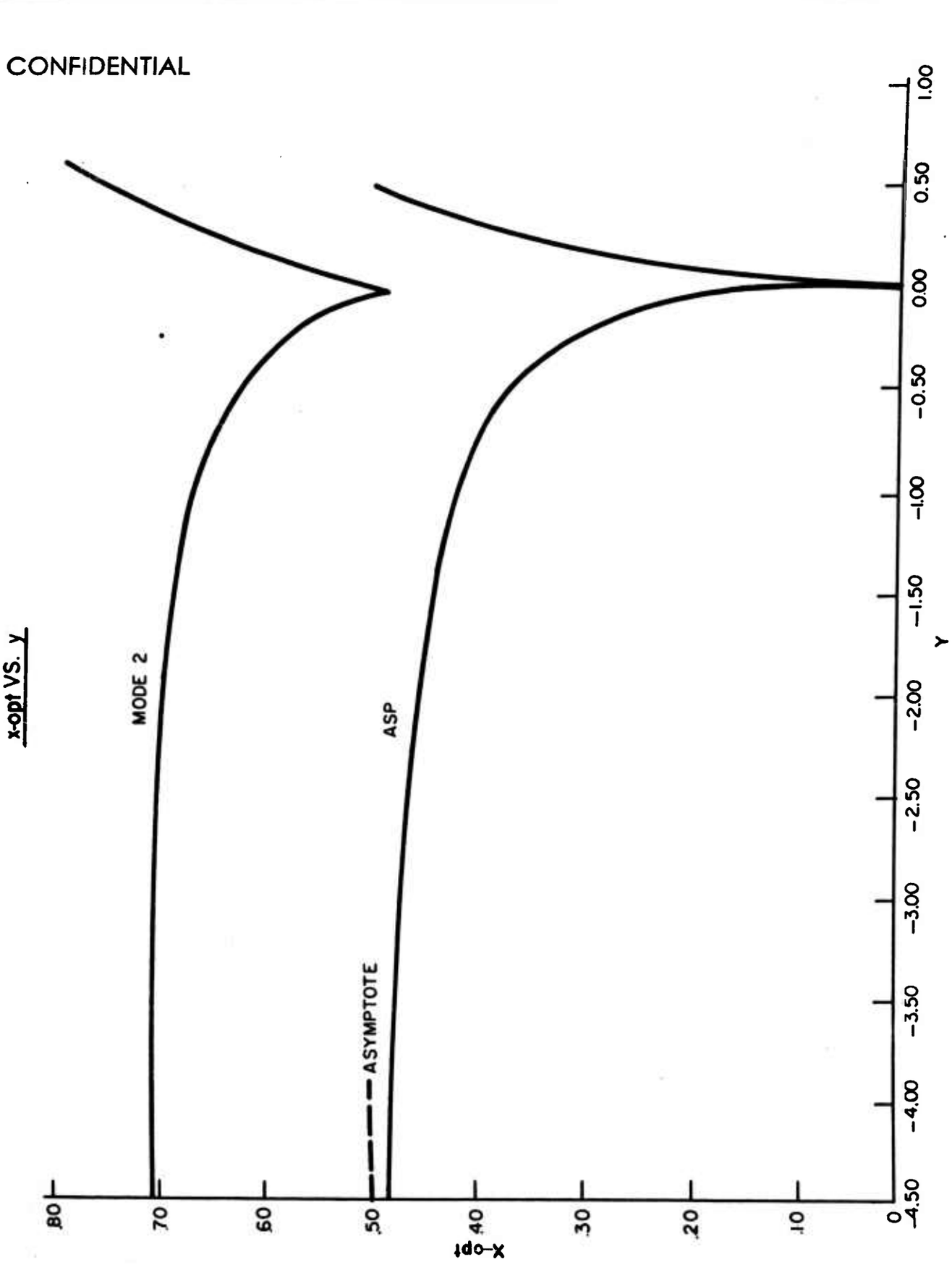

Fig. B-7-1 x-opt Versus y

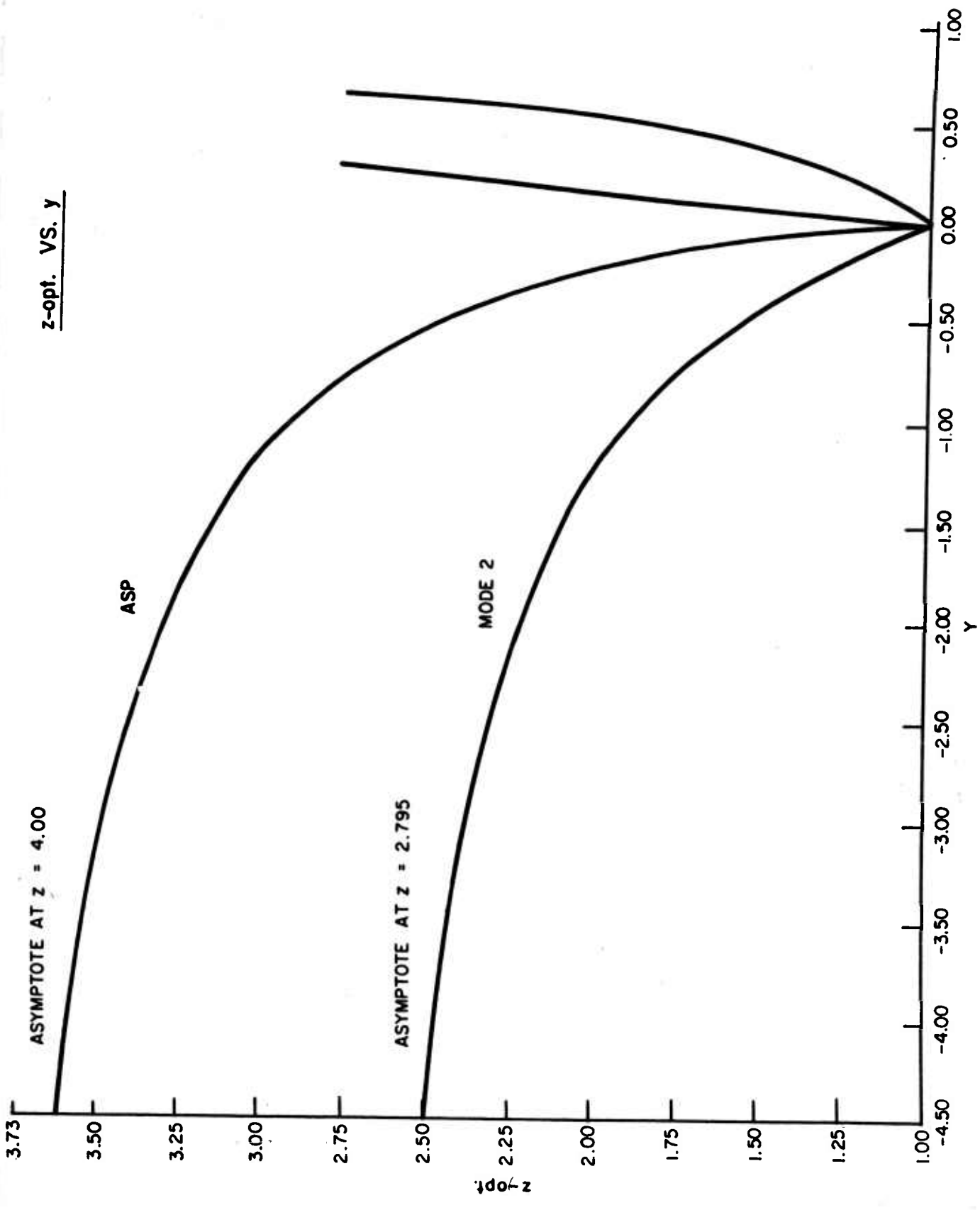

Fig. B-7-2 z-opt Versus y

From equation (B-7-2), it is apparent that if the second leg bearing-rate approaches zero, the range deviation increases without bound. Thus, R(t) may be of no value. However, the range at time of own-ship zig, R(t'), can be used in this situation.

From equations (A-7-3), (A-7-7), and (A-7-8) range at time of own-ship zig is given by

$$R(t') = \frac{V_{1x}^{(1)}(t') - V_{2x}^{(1)}(t')}{\dot{B}_2(t') - \dot{B}_1(t')} = \frac{V_{1x}^{(1)}(t') - V_{2x}^{(1)}(t')}{b_2 - b_1 - 2c_1(t' - t_o)} .$$

From the above equation,

$$\frac{\partial R(t')}{\partial b_1} = \frac{V_{1x}^{(1)}(t') - V_{2x}^{(1)}(t')}{\left[b_2 - b_1 - 2c_1(t' - t_o)\right]^2} = \frac{R(t')}{\left[\Delta\dot{B}(t')\right]} ,$$

$$\frac{\partial R(t')}{\partial b_2} = \frac{-\left(V_{1x}^{(1)}(t') - V_{2x}^{(1)}(t')\right)}{\left[b_2 - b_1 - 2c_1(t' - t_o)\right]^2} = -\frac{R(t')}{\left[\Delta\dot{B}(t')\right]} ,$$

and

$$\frac{\partial R(t')}{\partial c_1} = \frac{2(t' - t_o)\left[V_{1x}^{(1)}(t') - V_{2x}^{(1)}(t')\right]}{\left[b_2 - b_1 - 2c_1(t' - t_o)\right]^2} = \frac{2(t' - t_o)R(t')}{\left[\Delta\dot{B}(t')\right]} .$$

The assumptions which led to (B-7-2) are again used to get

$$\sigma^2_{R(t')} = \left[\frac{R(t')}{\Delta\dot{B}(t')}\,\sigma_{b_1}\right]^2 + \left[\frac{-R(t')}{\Delta\dot{B}(t')}\,\sigma_{b_2}\right]^2 + \left[\frac{2(t'-t_o)R(t')}{\Delta\dot{B}(t')}\,\sigma_{c_1}\right]^2 +$$

$$- 4(t'-t_o)\left[\frac{R(t')}{\Delta\dot{B}(t')}\right]^2 \sigma_{b_1}\sigma_{c_1}.$$

Thus,

$$\sigma^2_{R(t')} = \frac{R^2(t')}{\Delta\dot{B}^2(t')}\left[\sigma^2_{b_1} + \sigma^2_{b_2} + 4(t'-t_o)^2\sigma^2_{c_1} - 4(t'-t_o)\,\sigma_{b_1}\sigma_{c_1}\right].$$

Then, using

$$\sigma_{b_1} = (t'-t_o)\sigma_{c_1}$$

$$\frac{\sigma^2_{R(t')}}{R^2(t')} = \frac{\sigma^2_{b_1}+\sigma^2_{b_2}}{\Delta\dot{B}^2(t')}$$

or

$$\frac{\sigma_{R(t')}}{R(t')} = \left|\frac{\left[\sigma^2_{b_1}+\sigma^2_{b_2}\right]^{1/2}}{\Delta\dot{B}(t')}\right|. \qquad \text{(B-7-5)}$$

Using equations (B-1-12),

$$\frac{\sigma_{R(t')}}{R(t')} = \left[\left(\frac{T_t}{T_1}\right)^3 + \left(\frac{T_t}{T_2}\right)^3\right]^{1/2} \frac{8\sqrt{3}\,T^{1/2}\sigma_B}{T_t^{3/2}\,|\Delta\dot{B}|}\,. \qquad \text{(B-7-6)}$$

APPENDIX C
DERIVATION AND ANALYSIS OF ZIG DETECTION EQUATIONS

1. Predicted Versus Measured Bearings

Let the interval t_o to t_i be such that a quadratic approximation to the bearing-time curve is sufficiently accurate, and let the bearing data from t_o to t_j ($t_o < t_j < t_i$) be least-square fitted to obtain coefficients a_j, b_j, and c_j. The bearing at time t_i can then be obtained from

$$B^*_{ij} = a_j + b_j(t_i - t_o) + c_j(t_i - t_o)^2. \qquad \text{(C-1-1)}$$

The B^*_{ij}'s thus represent predicted bearings based on bearing history from t_o to t_j. When the interval t_o to t_i is further restricted, bearings can be predicted from

$$B^*_{ij} = a'_j + b'_j(t_i - t_o) \qquad \text{(C-1-2)}$$

in which a'_j and b'_j are obtained from a linear least-square fit.

Let

$$r_j = \left| \sum_{i=m_j+1}^{m_j+p+1} (B^*_{ij} - B_{ij}) \right| \qquad \text{(C-1-3)}$$

in which the B_{ij}'s are the bearing data as received from sonar at t_i,

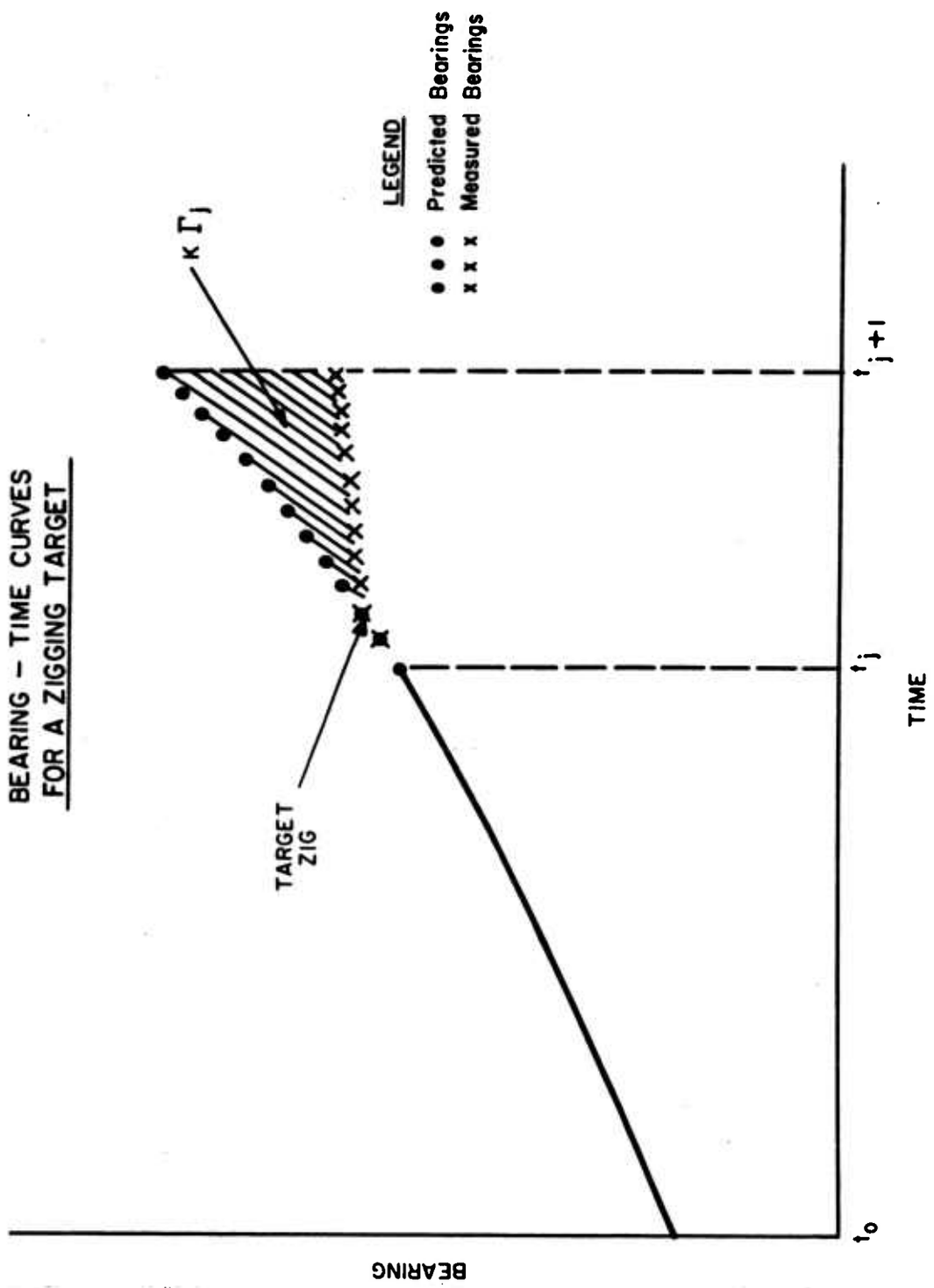

Fig. C-1-1 Bearing-Time Curves for a Zigging Target

m_j is the number of bearings prior to t_j, and p is the number of predicted bearings. It can be seen that r_j represents a quantity proportional to the area between the expected and the true bearing-time curve from t_j to t_{j+1} (see Fig. C-1-1). This area is also approximately proportional to the difference between the expected and the true bearing rates.

The probability of a target zig is found by

$$P_{zj} = \frac{1}{\sqrt{2\pi}\,\sigma_j} \int_{-r_j}^{r_j} \exp\left(-\frac{x^2}{2\sigma_j^2}\right) dx \qquad \text{(C-1-4)}$$

in which σ_j is the standard deviation of r_j and remains to be determined. Zig detection sensitivity will obviously depend upon r_j and σ_j.

2. Linear Least-Square Fit

The primed coefficients of equation (C-1-2) are obtained from

$$u' = c'v' \qquad \text{(C-2-1)}$$

in which

$$u' = \begin{bmatrix} a' \\ b' \end{bmatrix}, \qquad \text{(C-2-2)}$$

$$v' = \begin{bmatrix} \Sigma B_1 \\ \Sigma B_1(t_1 - t_o) \end{bmatrix}, \qquad \text{(C-2-3)}$$

$$c' = (A')^{-1} = \frac{\text{Adj } A'}{\text{Det } A'} \qquad \text{(C-2-4)}$$

and

$$A' = \begin{bmatrix} n & \Sigma (t_i - t_o) \\ \Sigma (t_i - t_o) & \Sigma (t_i - t_o)^2 \end{bmatrix} . \qquad \text{(C-2-5)}$$

The primes are used here to distinguish between the linear and quadratic least-square fits.

From the above

$$\begin{aligned} a' &= c'_{11} \Sigma B_i + c'_{12} \Sigma B_i (t_i - t_o), \\ b' &= c'_{12} \Sigma B_i + c'_{22} \Sigma B_i (t_i - t_o) \end{aligned} \qquad \text{(C-2-6)}$$

and

$$\begin{aligned} \sigma_{a'}{}^2 &= c'_{11} \sigma_B{}^2 , \\ \sigma_{b'}{}^2 &= c'_{22} \sigma_B{}^2 , \\ \tau_{a'b'} \sigma_{a'} \sigma_{b'} &= c'_{12} \sigma_B{}^2 . \end{aligned} \qquad \text{(C-2-7)}$$

From equations (C-2-4, 5),

$$\begin{aligned} \text{Det } A' &= n\Sigma(t_i - t_o)^2 - \left[\Sigma(t_i - t_o)\right]^2 , \\ c'_{11} &= \Sigma(t_i - t_o)^2 / \text{Det } A' , \end{aligned}$$

$$c'_{22} = n/\text{Det } A' \qquad \text{(C-2-8)}$$

and

$$c'_{12} = c'_{21} = -\Sigma(t_i - t_o)/\text{Det } A'.$$

3. Variance of Γ for Quadratic Extrapolation

From equations (C-1-1, 3)

$$\Gamma_j = \left| \Sigma \left\{ a_j + b_j(t_i - t_o) + c_j(t_i - t_o)^2 - B_{ij} \right\} \right| \qquad \text{(C-3-1)}$$

or

$$\Gamma_j = \left| a_j p + b_j \Sigma(t_i - t_o) + c_j \Sigma(t_i - t_o)^2 - \Sigma B_{ij} \right| \qquad \text{(C-3-2)}$$

in which the sums are from $t_i = t_j$ to t_{j+1}. Since the B_{ij} bearings are bearing data obtained after time t_j and the coefficients a_j, b_j, and c_j are derived from bearing data obtained prior to t_j, the B_{ij} bearings are stochastically independent of the coefficients. Also, Γ_j is a linear combination of variates. Thus, the variance of $\Gamma_j (\sigma_j^2)$ is

$$\sigma_j^2 = \left\{ \begin{array}{l} p^2 \sigma_a^2 + \left[\Sigma(t_i - t_o)\right]^2 \sigma_b^2 + \left[\Sigma(t_i - t_o)^2\right]^2 \sigma_c^2 + \\ +2\tau_{ab} p \Sigma(t_i - t_o) \sigma_a \sigma_b + 2\tau_{ac} p \Sigma(t_i - t_o)^2 \sigma_a \sigma_c + \\ +2\tau_{bc} \Sigma(t_i - t_o) \Sigma(t_i - t_o)^2 \sigma_b \sigma_c + p\sigma_B^2 \end{array} \right\}. \qquad \text{(C-3-3)}$$

Now let

$$\sum_{t_i=t_j+T}^{t_{j+1}} (t_i-t_o) = T_{j1}, \qquad \text{(C-3-4)}$$

and

$$\sum_{t_i=t_j+T}^{t_{j+1}} (t_i-t_o)^2 = T_{j2},$$

then, using equations (B-1-2, 3) with t_i replaced by t_j, equation (C-3-3) becomes

$$\sigma_j^2 = \sigma_B^2 \left\{ \begin{array}{l} c_{11}p^2+c_{22}T_{j1}^2+c_{33}T_{j2}^2+2c_{12}T_{j1}p + \\ \\ +2c_{13}T_{j2}p+2c_{23}T_{j1}T_{j2}+p \end{array} \right\} . \qquad \text{(C-3-5)}$$

Let the number of bearings from t_o to t_j be m_j, then the c_{ij}'s of equation (C-3-5) can be replaced by equations (B-1-11) in which $n=m_j$. For $t_o=0$ the expressions (C-3-4) can be written as

$$T_{j1} = T \sum_{i=m_j+1}^{m_j+1+p} i$$

and

$$T_{j2} = T^2 \sum_{i=m_j+1}^{m_j+1+p} i^2.$$

Now let

$$i=K+m_j+1,$$

then for m_j large,

$$T_{j1} = T \sum_{K=0}^{p} (K+m_j) = T\left[m_j p+\Sigma K\right]$$

and

$$T_{j2} = T^2 \sum_{K=0}^{p} (K+m_j)^2 = T^2\left[m_j{}^2 p+2m_j \Sigma K+\Sigma K^2\right].$$

The sums over K can be reduced by

$$\sum_{K=0}^{p} K = p(p+1)/2$$

and

$$\sum_{K=0}^{p} K^2 = p(p+1)(2p+1)/6.$$

Using the above simplifications, equation (C-3-5) becomes

$$\sigma_j{}^2 = \sigma_B{}^2 \left\{ \begin{array}{l} p+\frac{9}{m_j} p^2+\frac{36}{m_j^2} p^2(p+1)+\frac{p^2}{m_j^3} (p+1)(68p+58)+ \\ \\ \frac{30p^2}{m_j^4}(p+1)^2(2p+1)+\frac{5p^2}{m_j^5} (p+1)^2(2p+1)^2 \end{array} \right\}. \quad (C-3-6)$$

This equation was used to obtain the curves of Figure C-3-1.

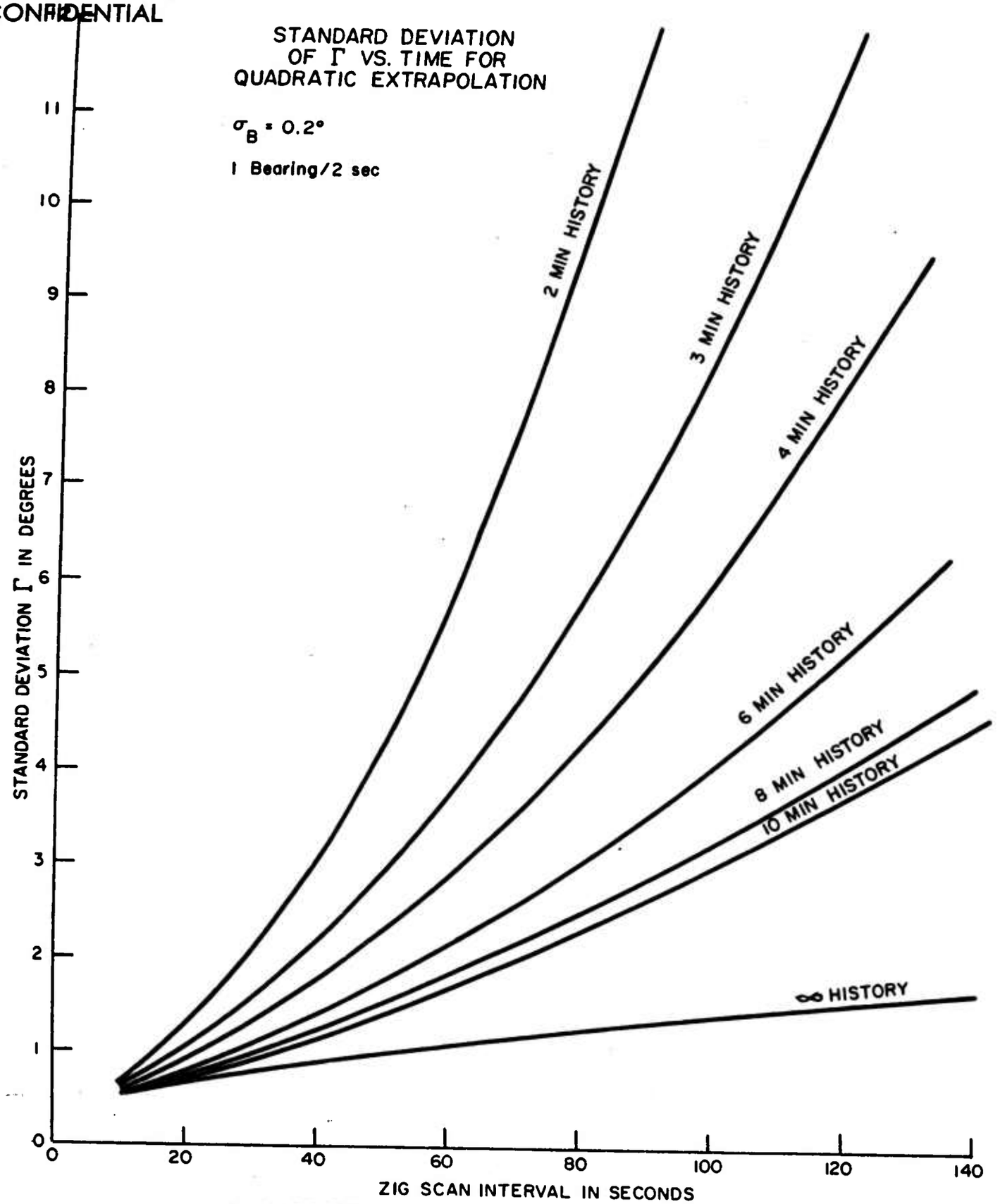

Fig. C-3-1 Standard Deviation of Γ Versus Time for Quadratic Extrapolation

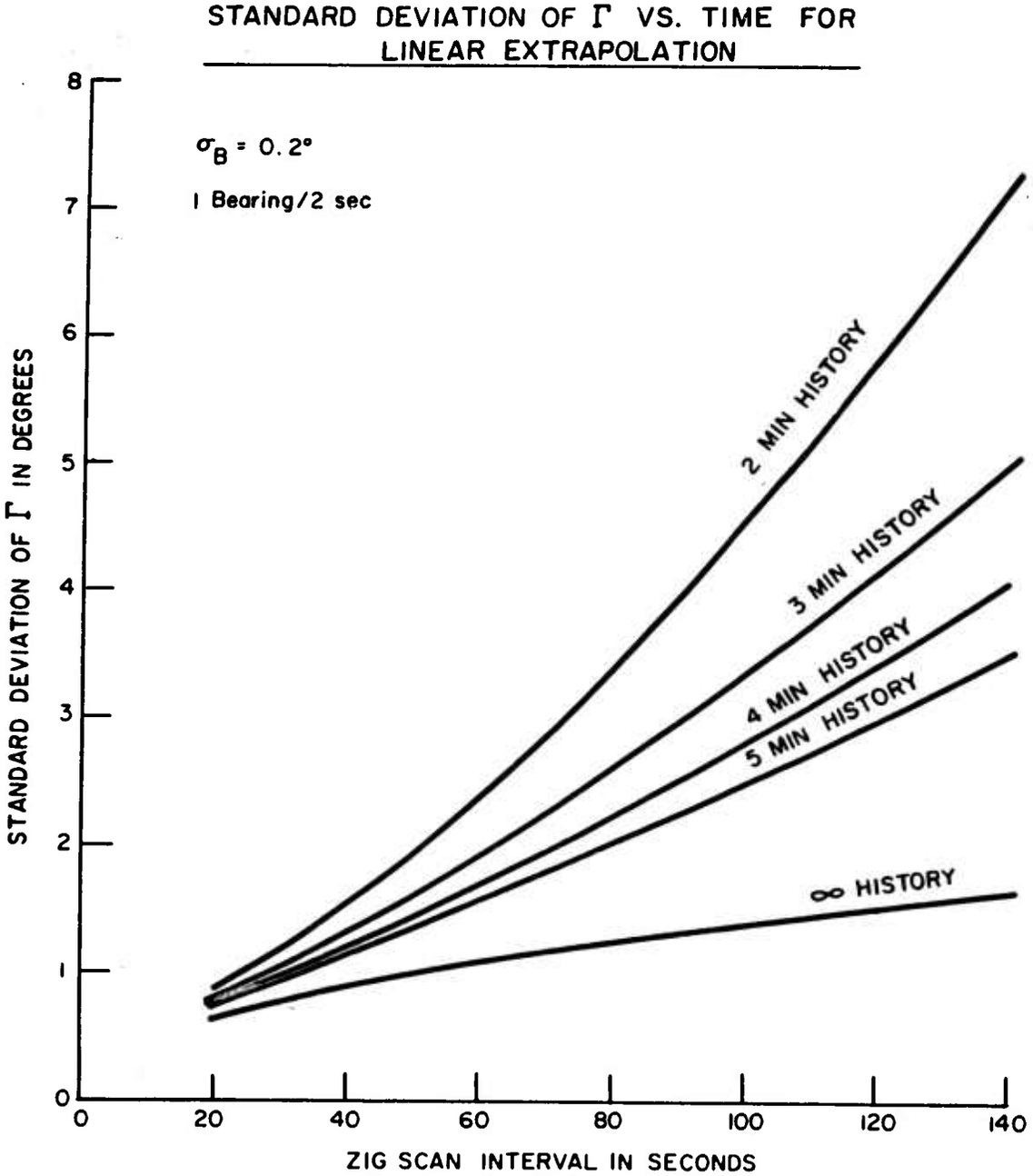

Fig. C-4-1 Standard Deviation of Γ Versus Time for Linear Extrapolation

4. Variance of Γ_j for Linear Extrapolation

From equations (C-1-2, 3)

$$r_j = \left| \Sigma \left\{ a'_j + b'_j (t_i - t_o) - B_{ij} \right\} \right| \qquad \text{(C-4-1)}$$

and in a manner analogous to the previous section.

$$\sigma_j^2 = p^2 \sigma_{a'}^2 + \left[\Sigma (t_i - t_o) \right]^2 \sigma_{b'}^2 + 2\tau_{a'b'} p \Sigma (t_i - t_o) \sigma_{a'} \sigma_{b'} + p \sigma_B^2 \qquad \text{(C-4-2)}$$

$$= \sigma_B^2 \left\{ c'_{11} p^2 + c'_{22} T_{j1}^2 + 2c'_{12} T_{j1} p + p \right\} \qquad \text{(C-4-3)}$$

in which T_{j1} is defined by equation (C-3-4).

The approximation to (C-4-3) analogous to (C-3-6) is

$$\sigma_j^2 = \sigma_B^2 \left\{ p + \frac{4}{m_j} p^2 + \frac{6p^2}{m_j^2} (p+1) + \frac{3p^2}{m_j^3} (p+1)^2 \right\} . \qquad \text{(C-4-4)}$$

Curves of Fig. (C-4-1) were obtained from equation (C-4-4).

5. Approximate Expressions for Γ_j

The analysis of this section is simplified by assuming target zigs to occur instantaneously and without changes in speed for course zigs. The effects of these assumptions must be considered when interpreting the results of the analysis. Thus, a finite zig time will retard

detection while a speed reduction accompanying a course zig will either retard or advance detection depending upon its effect on the change in bearing-rate. The effects can easily be deduced for the particular cases examined.

Consider first the linear extrapolation scheme expressed by equation (C-1-2). This scheme will obviously be suitable for long range targets, but can also be used at the shorter ranges by restricting the time intervals. A target zig is illustrated by the bearing-time curve of Fig. C-5-1. The curve consists of two straight lines (lines 1 and 2) meeting at t_z (the time of target zig). The case where ($t_z < t_j$) will be considered later. The prediction interval (or scan interval) begins at t_j so that ($t_j - t_o$) represents the history interval which contains m_j bearings. The number of bearings from t_j to t_{j+1} is ($m_{j+1} - m_j$) = p and the number from t_o to t_z is N. For further simplification without loss of generality, $B(t_o)$ and t_o are both set to zero. For line 1,

$$B = b_1 t \tag{C-5-1}$$

and for line 2,

$$B = a_2 + b_2 t = B(t_z) + b_2(t - t_z) = (b_1 - b_2)t_z + b_2 t. \tag{C-5-2}$$

Thus,

$$B^*_{ij} = b_1 t_i \text{ for } t_j < t_i \leq t_{j+1} \tag{C-5-3}$$

and

$$B_{ij} = \begin{cases} b_1 t_i & \text{for } t_j < t_i \leq t_z \\ (b_1 - b_2)t_z + b_2 t_i & \text{for } t_z < t_i \leq t_{j+1}. \end{cases} \tag{C-5-4}$$

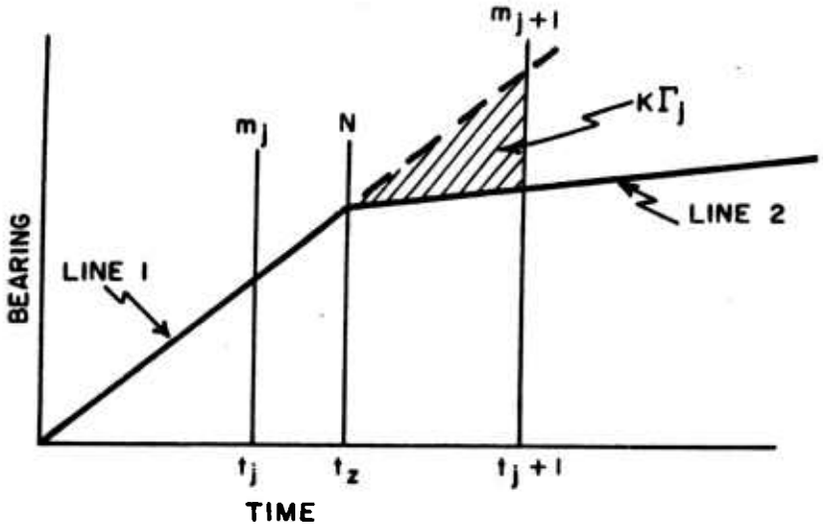

Fig. C-5-1 Linear Bearing-Time Curve for a Zigging Target

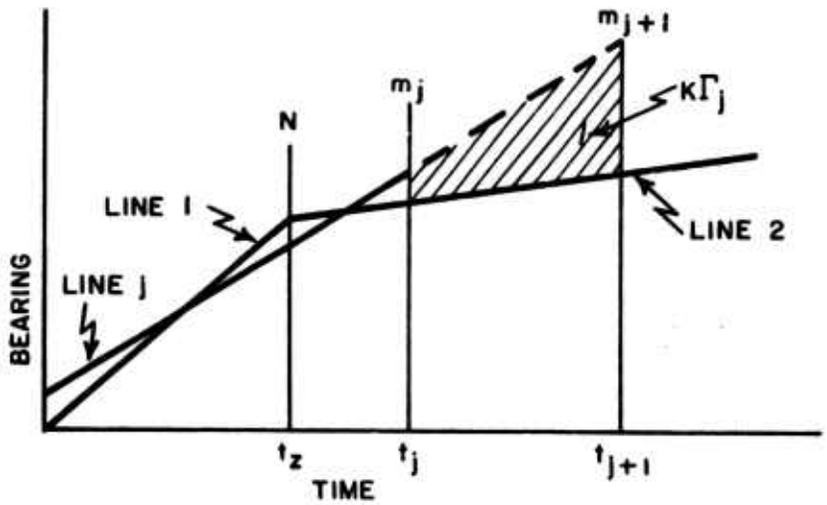

Γ_j For $t_z < t_j$

Fig. C-5-2 Γ_j for $t_z < t_j$

Using equation (C-1-3)

$$r_j = \left| \sum_{i=m_j+1}^{N} (B^*_{ij} - B_{ij}) + \sum_{i=N}^{m_{j+1}} (B^*_{ij} - B_{ij}) \right|$$

in which the first sum is 0 by virtue of (C-5-3) and (C-5-4). Introducing the expressions for B^*_{ij} and B_{ij},

$$r_j = \left| \sum_{t_i=t_z}^{t_j} \left[(b_1 - b_2)(t_i - t_z) \right] \right|. \qquad \text{(C-5-5)}$$

Assuming equal bearing sampling intervals,

$$t_i = iT \text{ and } t_z = NT$$

in which T is the time between samples. Then,

$$r_j = \left| T \sum_{i=N}^{m_{j+1}} \left[(b_1 - b_2)(i - N) \right] \right|.$$

Now let $i = K+N$, then

$$r_j = \left| T \sum_{K=0}^{m_{j+1}-N} \left[(b_1 - b_2)K \right] \right|$$

or

or

$$r_j = \left| T \frac{(b_1-b_2)}{2} (m_{j+1}-N)(m_{j+1}-N+1) \right| . \qquad \text{(C-5-6)}$$

Since $m_{j+1} > N$ by hypothesis, only (b_1-b_2) can be negative. Also, from equations (C-5-1, 2)

$$\left|(b_1-b_2)\right| = \left|\Delta \dot{B}\right|$$

so that (C-5-6) reduces to

$$r_j = \frac{T}{2}\left|\Delta \dot{B}\right|(m_{j+1}-N)(m_{j+1}-N+1)$$

or

$$r_j = \frac{1}{2} \frac{|\Delta \dot{B}|}{T}(t_{j+1}-t_z)(t_{j+1}-t_z+T) \qquad \text{(C-5-7)}$$

for $t_j \leqslant t_z \leqslant t_{j+1}$.

Consider now $t_z < t_j$ as indicated in Fig. C-5-2. The least-square fit of the bearings from t_o to t_j is represented by line j which will intersect line 1 at $t_z/2$ and line 2 at $(t_j-t_z)/2$. The equation of line j is

$$B = \frac{t}{t_j}\left\{(b_1-b_2)t_z+b_2t_j\right\} + \frac{t_z}{2}\left\{(b_1-b_2)\left[1-\frac{t_z}{t_j}\right]\right\} . \qquad \text{(C-5-8)}$$

Using this equation for B^*_{ij} and the equation of line 2 for B_{ij}, equation (C-1-3) reduces to

$$r_j = \frac{1}{2} \frac{|\Delta \dot{B}|}{T} \frac{t_z}{t_j} (t_{j+1}-t_j)(t_{j+1}-t_z+T) \qquad \text{(C-5-9)}$$

for $t_z \leqslant t_j$. This relation reduces to equation (C-5-7) when $t_z = t_j$, as indeed it should.

It will subsequently be seen that for small $\Delta \dot{B}$ the ratio r_j/σ_j decreases with increasing $(t_{j+1}-t_j)$. This merely reflects the results of extrapolation and should be expected. Suppose a zig has occurred in the interval $(t_{j+1}-t_j)$, but that P_{zj} was not of sufficient magnitude to conclude that a zig occurred. Extrapolation is terminated at t_{j+1} whence all of the bearing data prior to t_{j+1} is least-square fitted, and the interval $(t_{j+2}-t_{j+1})$ is scanned using this latter least-square fit, and so on, for the next interval. We would like to determine the behavior of r_j in these subsequent scanning intervals. The situation is illustrated in Fig. C-5-3. r_{j+k} is given by equation (C-5-9). Thus,

$$\frac{r_{j+K}}{r_{j+K-1}} = \frac{t_{j+K-1}(t_{j+K+1}-t_{j+K})(t_{j+K+1}-t_z+T)}{t_{j+K}(t_{j+K}-t_{j+K-1})(t_{j+K}-t_z+T)} .$$

If $t_{j+i+1} - t_{j+i} = \Delta t$ for all i,

$$\frac{r_{j+K}}{r_{j+K-1}} = \frac{(t_{j+K} - \Delta t)\ (t_{j+K}+\Delta t-t_z+T)}{t_{j+K}(t_{j+K}-t_z+T)}$$

which for T small compared to $(t_{j+K}-t_z)$ reduces to

$$\frac{r_{j+K}}{r_{j+K-1}} = 1 + \frac{\Delta t}{t_{j+K}} \left(\frac{t_z-\Delta t}{t_{j+K}-t_z}\right) . \qquad \text{(C-5-10)}$$

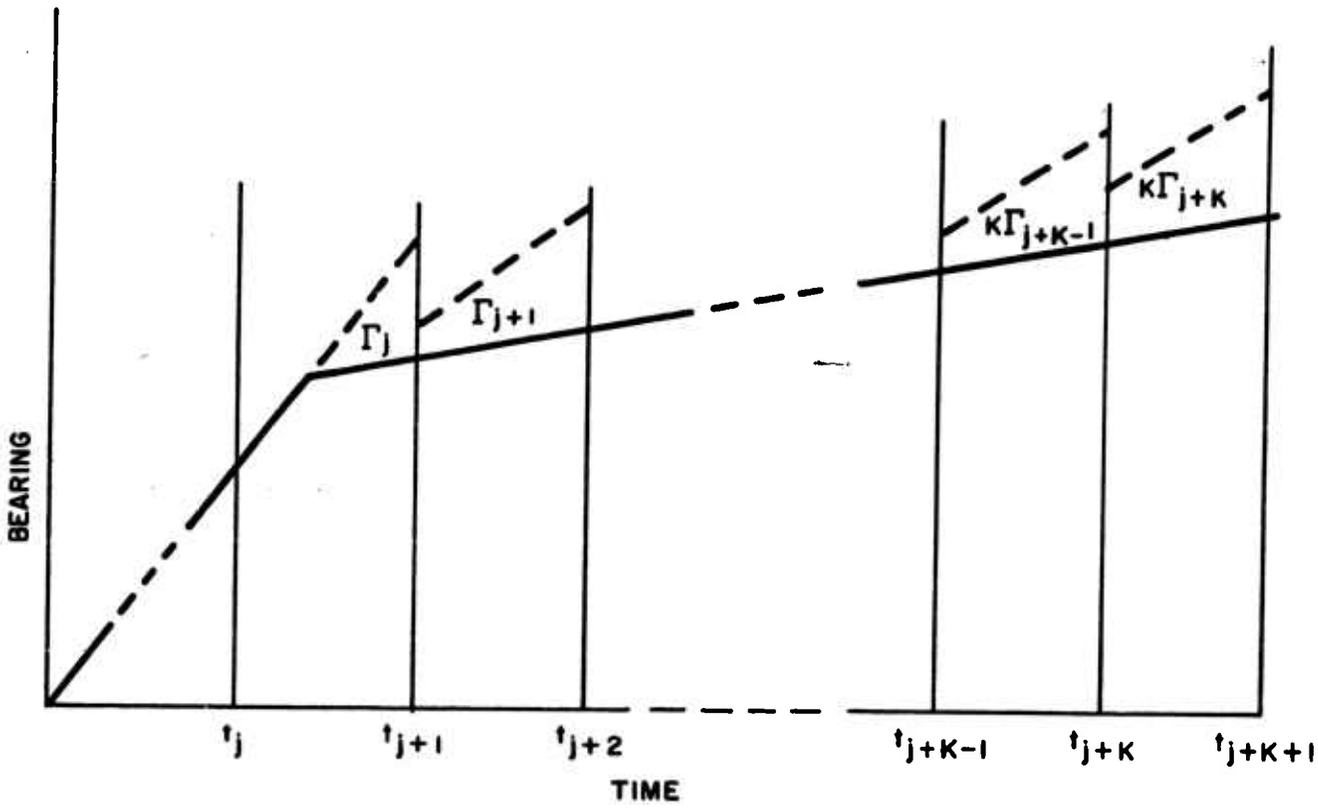

Fig. C-5-3 Behavior of Linear Γ_j in Succeeding Scan Intervals

Since $t_z < t_{j+K}$ for $K \geq 1$,

$$\frac{\Gamma_{j+K}}{\Gamma_{j+K-1}} = \begin{cases} > 1 & \text{for } t_z > \Delta t \\ < 1 & \text{for } t_z < \Delta t \\ = 1 & \text{for } t_z = \Delta t \end{cases} \qquad \text{(C-5-11)}$$

It can thus be concluded that Γ_j increases when we progress to succeeding scan intervals whenever $t_z > \Delta t$, and conversely.

The value of any Γ_{j+K} rapidly approaches its limiting value for a fixed scan interval as $(t_{j+K}-t_z)$ gets large. The limiting value is

$$\lim_{K \to \infty} \Gamma_{j+K} = \frac{1}{2} \frac{|\Delta \dot{B}|}{T} t_z \Delta t. \qquad \text{(C-5-12)}$$

Approximate expressions for $\Delta\dot{B}$ for long ranges can easily be obtained for specific geometries. We assume range to be approximately constant. For Fig. C-5-4

$$\Delta \dot{B} \approx -(V^{(2)} \sin\zeta)/R, \qquad \text{(C-5-13)}$$

and for Fig. C-5-5

$$\Delta \dot{B} \approx V^{(2)}(1 - \cos\zeta)/R. \qquad \text{(C-5-14)}$$

For a speed zig,

$$\Delta \dot{B} \approx \Delta V^{(2)}/R. \qquad \text{(C-5-15)}$$

These equations and the equations for Γ_j were used to obtain Figs. C-5-6 and C-5-8.

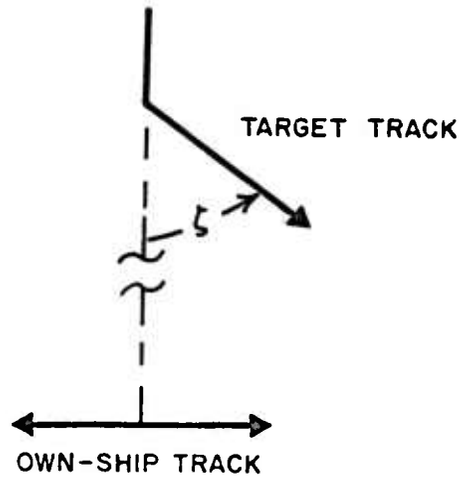

Fig. C-5-4 Zig Geometry No. 1

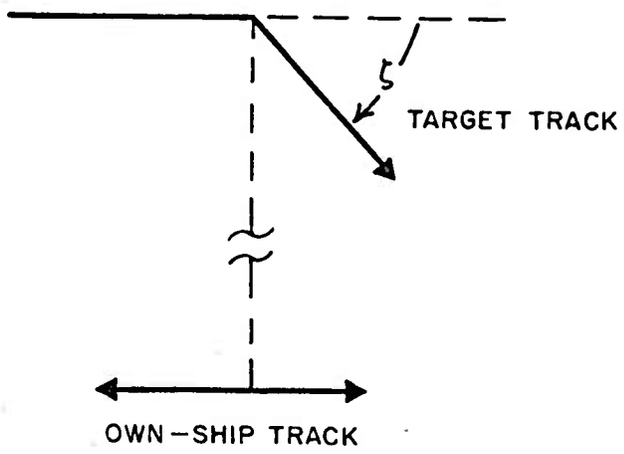

Fig. C-5-5 Zig Geometry No. 2

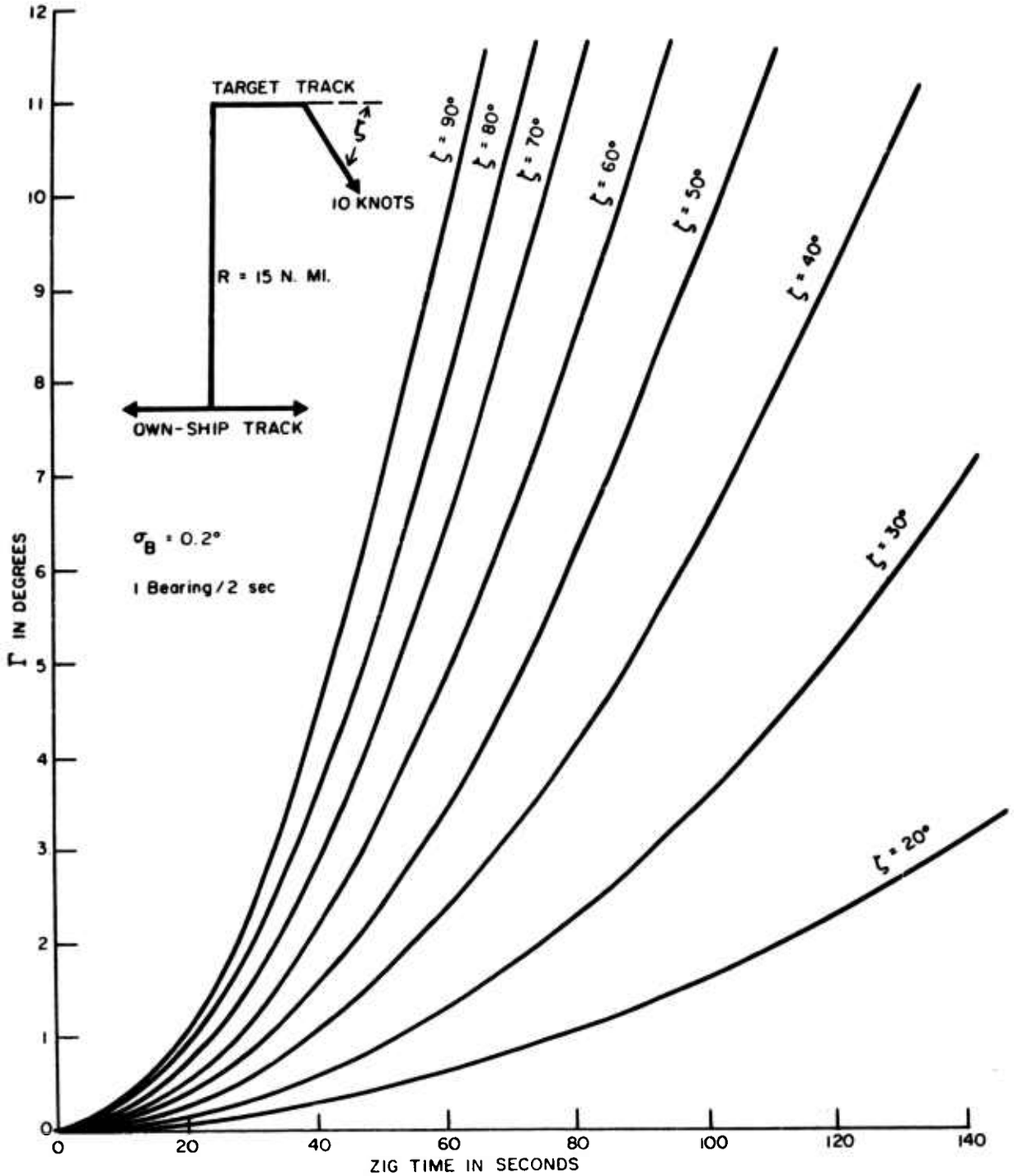

Fig. C-5-6 Γ Linear Versus Zig Time for Given Geometries

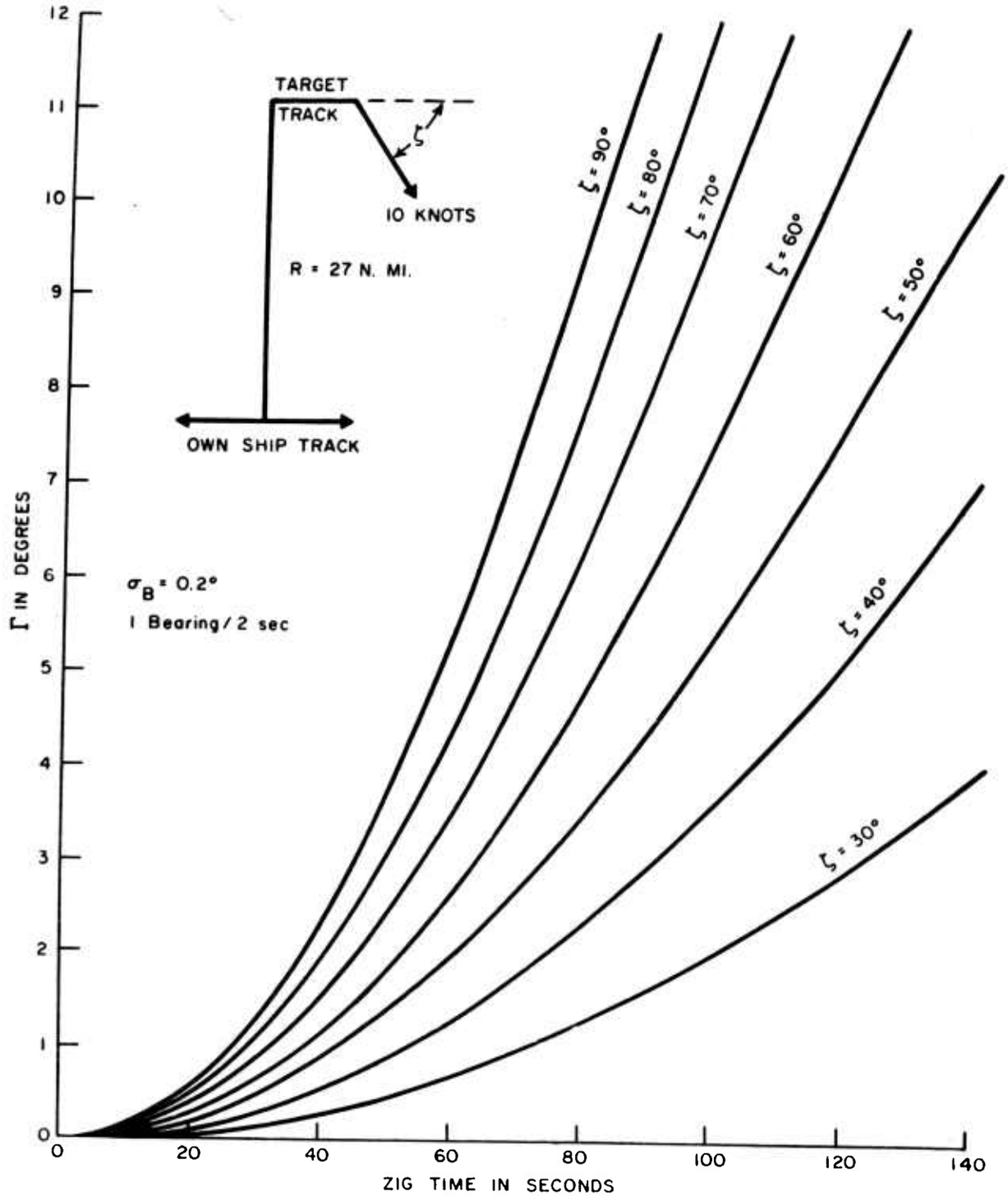

Fig. C-5-7 Γ Linear Versus Zig Time for Given Geometries

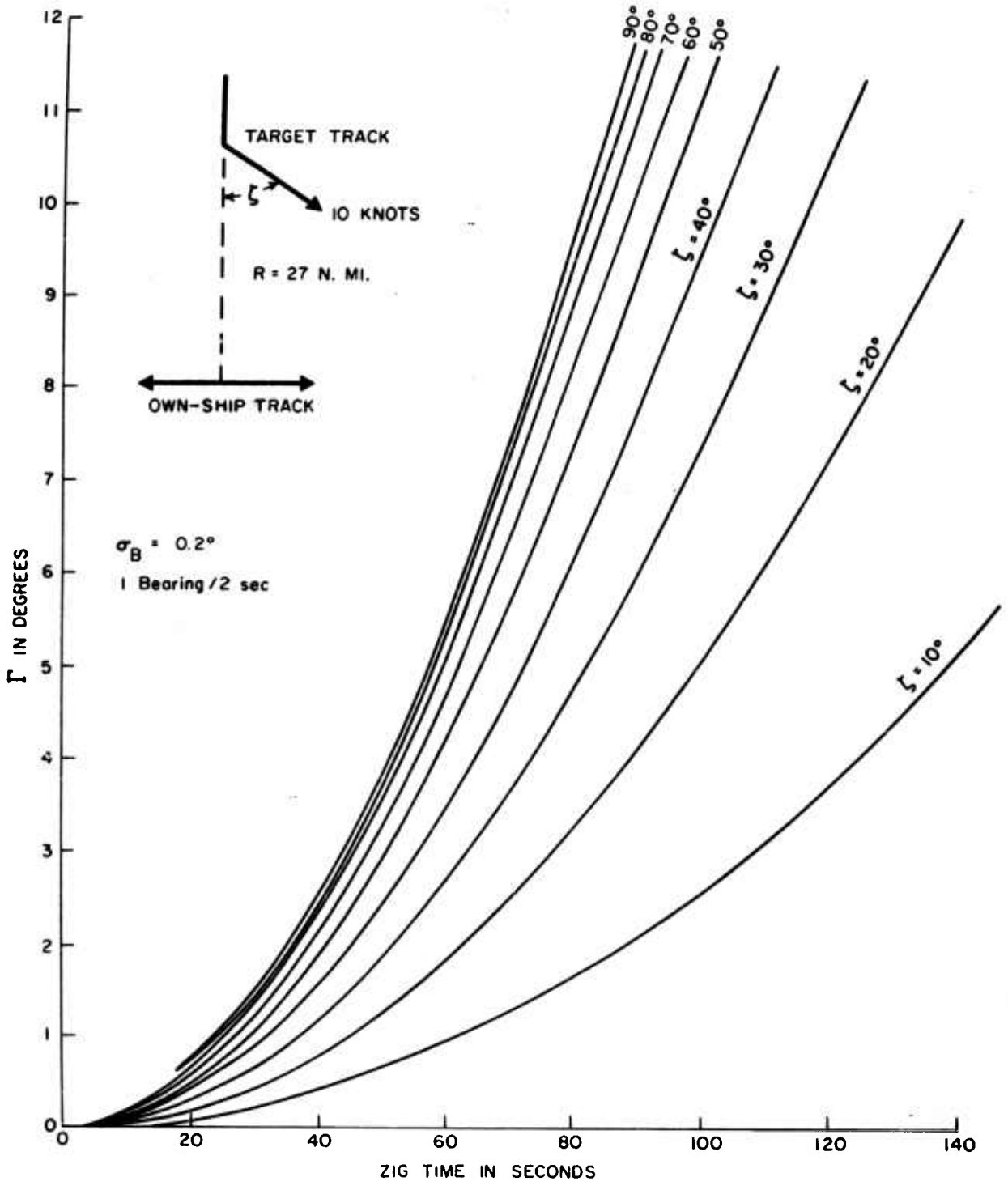

Fig. C-5-8 Γ Linear Versus Zig Time for Given Geometries

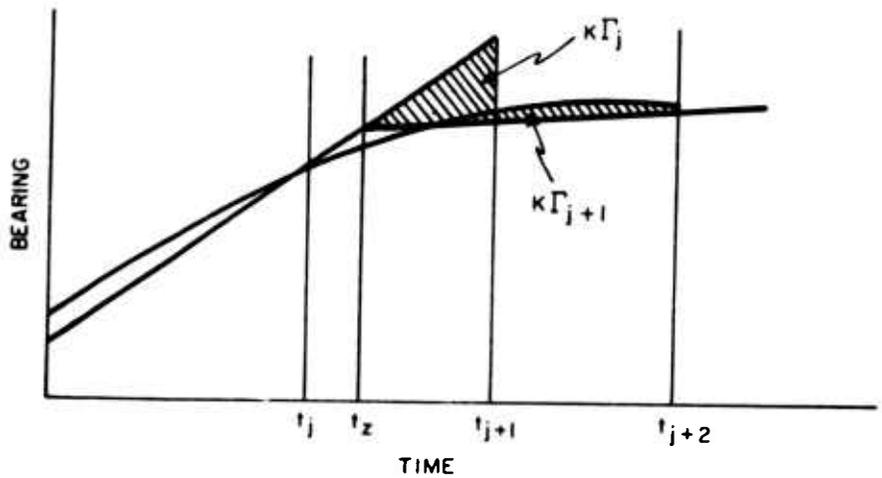

Fig. C-5-9 Behavior of Quadratic Γ_j in Succeeding Scan Interval

The quadratic bearing extrapolation expressed by equation (C-1-1) has the disadvantage of having a much larger σ_j associated with it. Additional difficulties arise when the zig is not detected in the interval in which it occurred. This difficulty arises from the tendency of the quadratic least-square fit to follow the bearing-time curve "knee" caused by the zig. The situation is qualitatively illustrated in Fig. C-5-9 where the parabolic curve represents a least-square fit of the bearing data from t_o to t_{j+1}. It appears that linear extrapolation is superior to quadratic extrapolation for two reasons: 1) for t_z near t_j, r_j for long ranges is approximately the same for both, but the σ_j associated with linear extrapolation is considerably less; and 2) zigs not detected in the interval in which they occurred have a greater probability of being detected in subsequent scans with linear extrapolation. If, however, the interval of validity of the linear equation is comparable to zig execution time, as might occur at short ranges, the quadratic method might be better than the linear method. A detailed study of this situation is needed.

6. Theoretical Zig Probabilities

Graphs of r_j and the associated σ_j based on the approximate equations of the previous sections are presented in this section. Only a few geometries are considered. Zig probability tables accompany each graph; the tables correspond to the graphs bearing the same numbers.

Figs. C-6-1, C-6-2, and the tables illustrate the conclusion arrived at in the previous section. The zig was assumed to occur at the beginning of the scan interval.

Figs. C-6-3 through C-6-5 and their tables illustrate zigs which have small effect on bearing-rate. It is very unlikely that these zigs would be detected using the quadratic method.

In all of the cases considered, speed reductions during the zigs would tend to increase r_j and consequently advance detection time. Finite zig times would, of course, retard detection time.

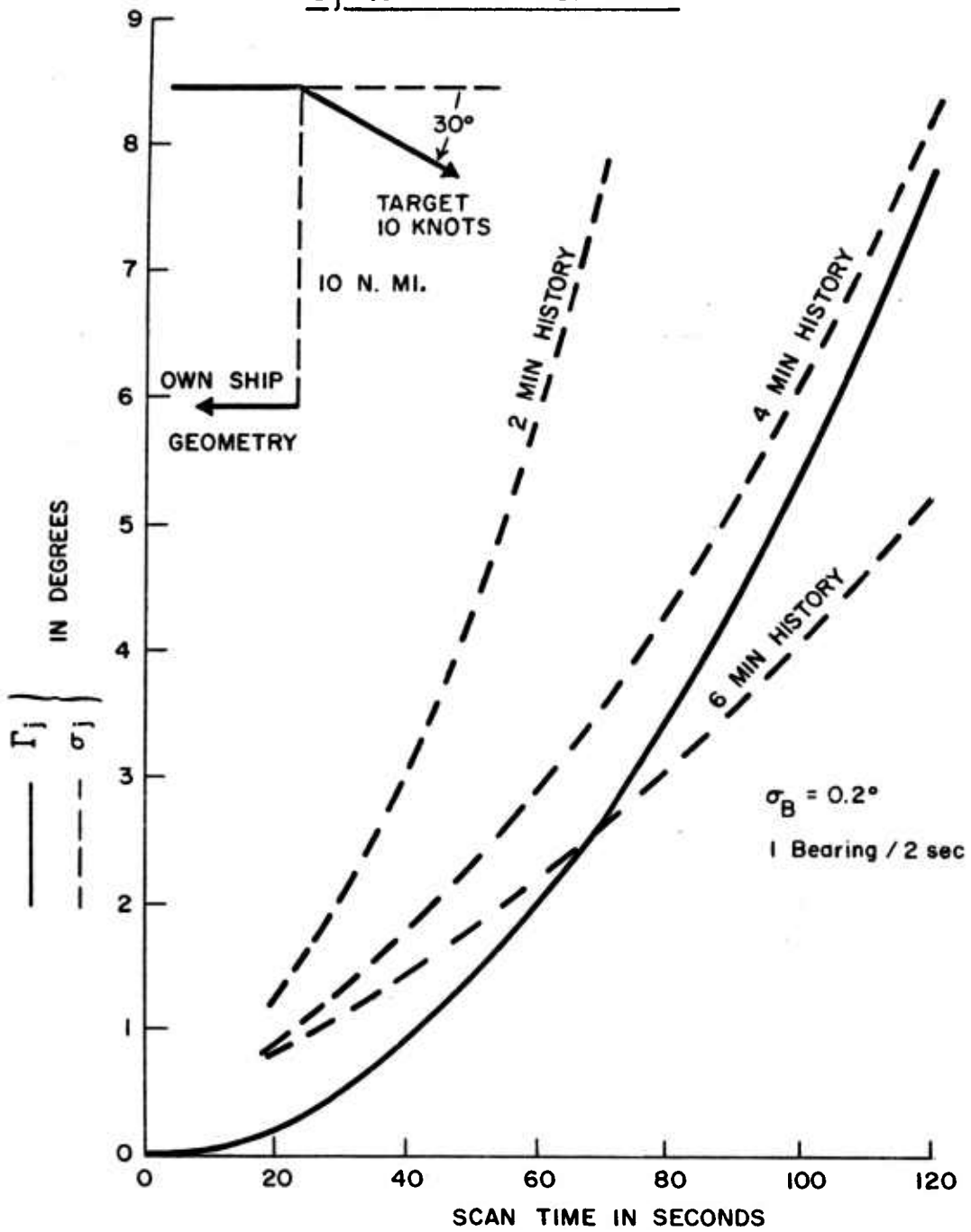

Fig. C-6-1 Γ_j Quadratic Versus Time

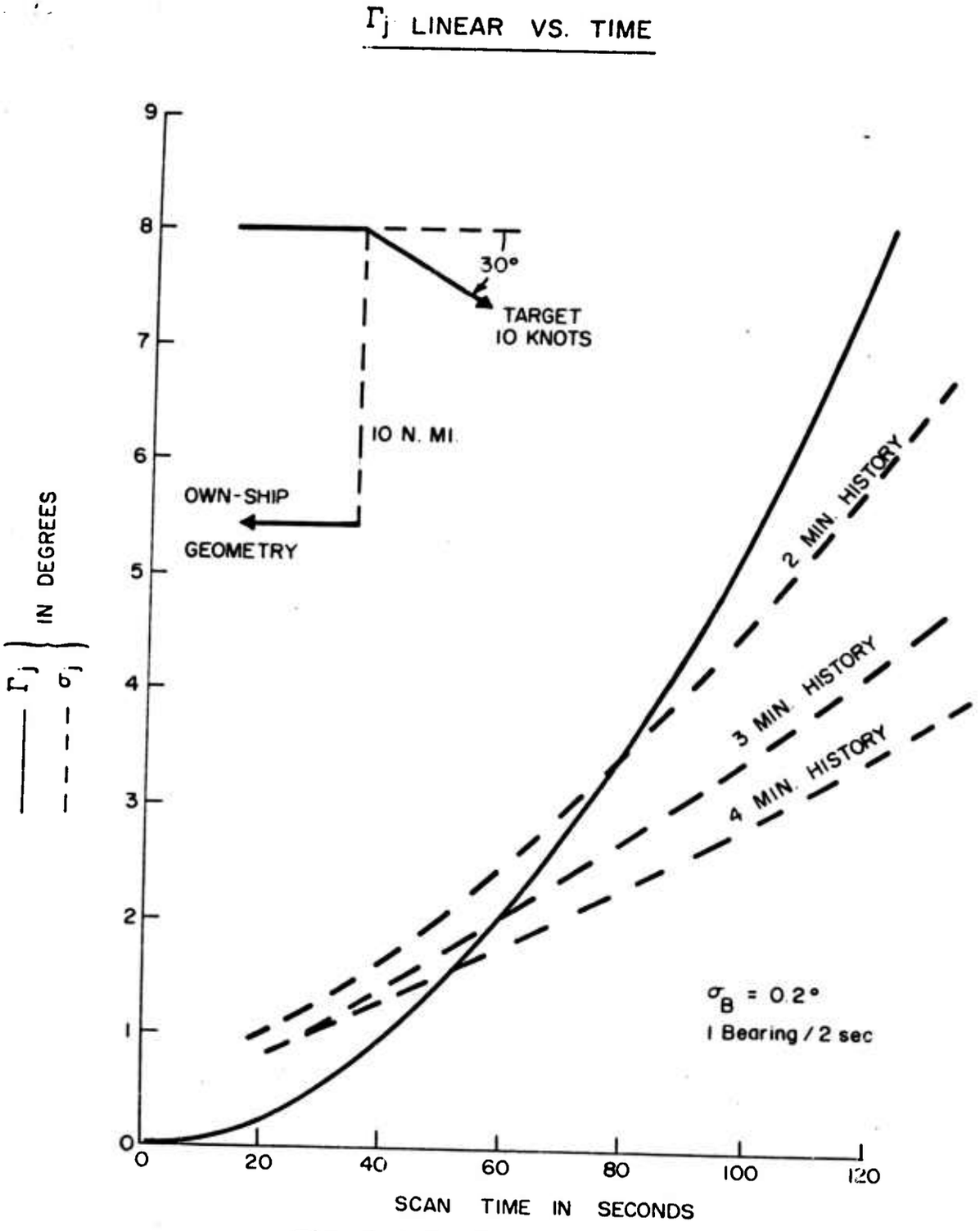

Fig. C-6-2 Γ_j Linear Versus Time

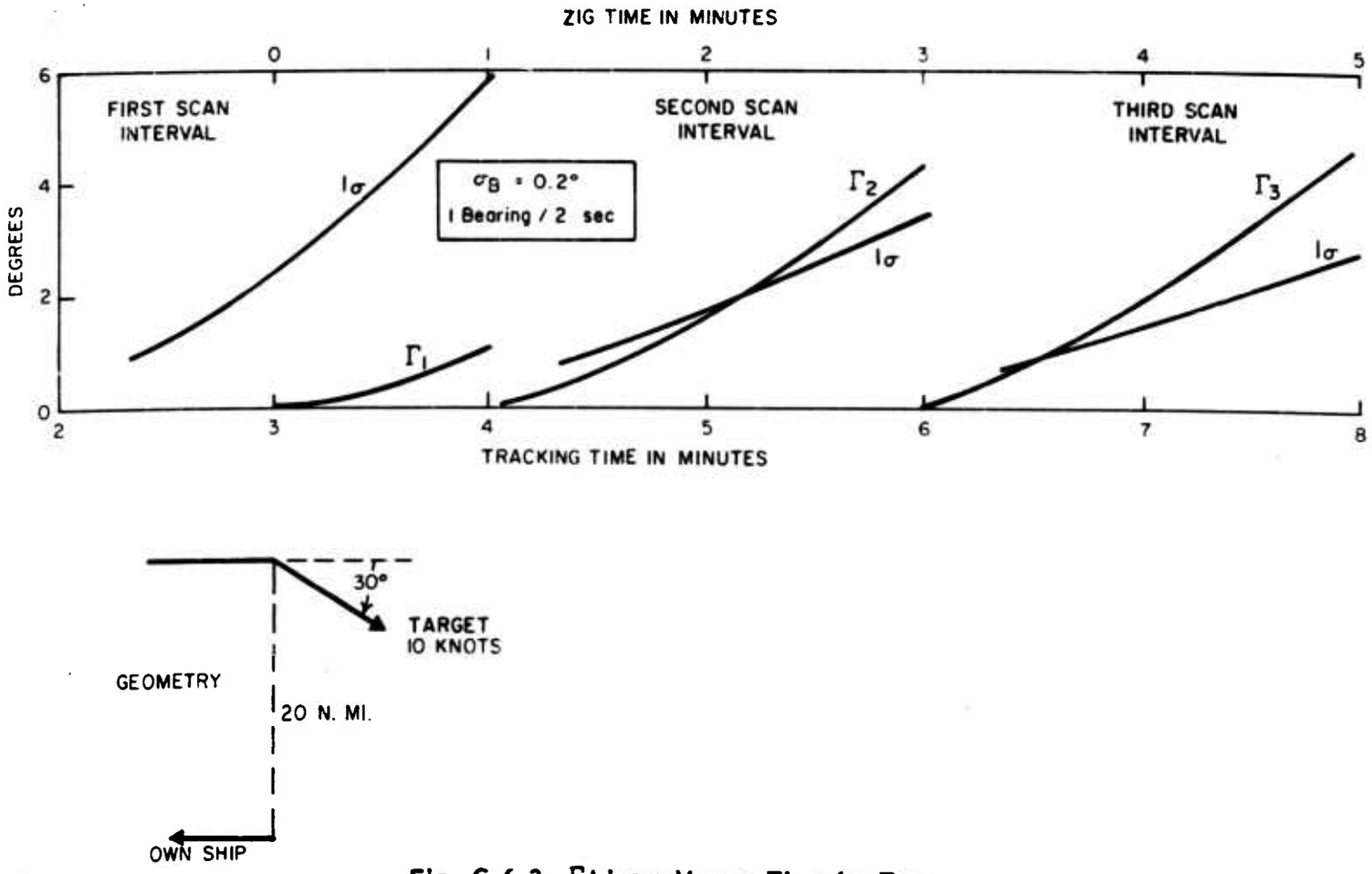

Fig. C-6-3 Γ Linear Versus Time for Two-Minute Scans - 20 Nautical Mile Target

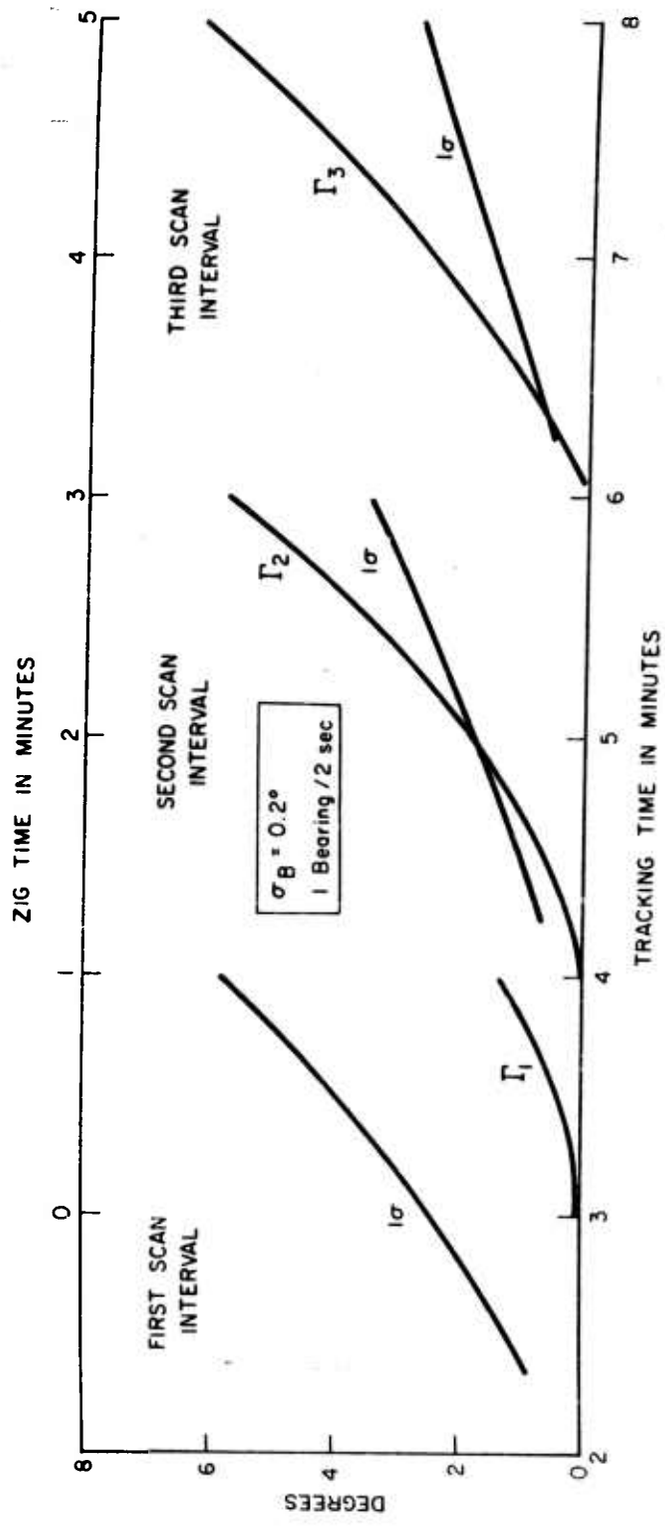

Fig. C-6-4 Γ Linear Versus Time for Two-Minute Scans - 15 Nautical Mile Target

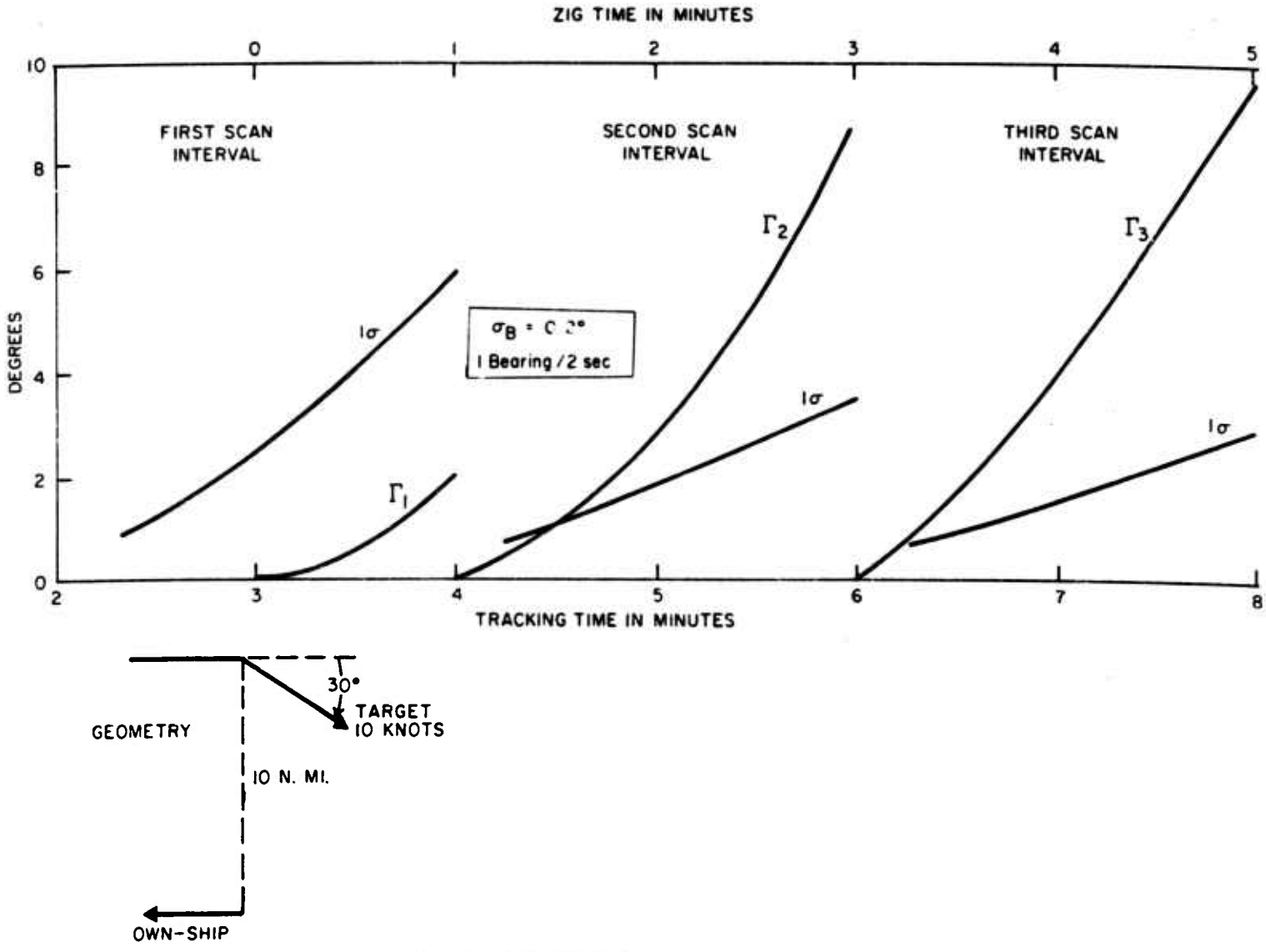

Fig. C-6-5 Γ Linear Versus Time for Two-Minute Scans - 10 Nautical Mile Target

TABLE C-6-1

History (min.)	Time (sec.)	Zig Probability
2	40	.21
2	70	.28
4	60	.50
4	80	.58
4	100	.63
4	120	.65
6	60	.63
6	80	.75
6	100	.82
6	120	.86

TABLE C-6-2

History (min.)	Time (sec.)	Zig Probability
2	60	.59
2	80	.68
2	100	.76
2	120	.74
3	60	.68
3	80	.80
3	100	.89
3	120	.93
4	60	.75
4	80	.87
4	100	.94
4	120	.97

TABLE C-6-3

Zig Time (Min.)	Zig Probability
1	.14
2	.75
3	.79
4	.80
5	.92

TABLE C-6-4

Zig Time (Min.)	Zig Probability
1	.18
2	.73
3	.90
4	.94
5	.97

TABLE C-6-5

Zig Time (Min.)	Zig Probability
1	.26
2	.90
3	.99
4	.99
5	.999

REFERENCES

REPORTS

(1) IBM - "Final Report for SUBIC Weapons Control Information Requirements Study," 1 July 1960, CONFIDENTIAL, C-612-2.

(2) Librascope, Inc. - "SUBROC Fire Control System Mathematical Model," May 1960, CONFIDENTIAL, C-115-3.

TEXTS

(3) Whittaker, Sir Edmund and Robinson, G., The Calculus of Observations. London: Blackie and Son Limited, 1924.

(4) Worthing, Archie G. and Geffner, Joseph., Treatment of Experimental Data. New York: John Wiley and Sons, Inc., 1943.

Office of Naval Research (10 copies)
Navy Department
Washington 25, D.C.
Attn: Code 466
Cdr. F.R. Haselton, Jr.

Chief of Naval Operations
Navy Department
Washington 25, D.C.
Attn: Op-311

Chief of Naval Operations
Navy Department
Washington 25, D.C.
Attn: Op-713

Office of Naval Research
Navy Department
Washington 25, D.C.
Attn: Code 461

Office of Naval Research
Navy Department
Washington 25, D.C.
Attn: Code 463

Bureau of Naval Weapons
Navy Department
Washington 25, D.C.
Attn: RUDC-1

Bureau of Ships
Navy Department
Washington 25, D.C.
Attn: Code 525

Bureau of Ships
Navy Department
Washington 25, D.C.
Attn: Code 450

Chief of Naval Operations
Navy Department
Washington 25, D.C.
Attn: Op-71

Armed Services Technical
Information Agency (10 copies)
Via: Office of Naval Research
Code 466

(With two copies
of Fwd. letter)

Director (6 copies)
Naval Research Laboratory
Washington 25, D.C.
Attn: Code 2000

(With letter explaining 3 copies
are for transmittal to British
Joint Naval Staff

2 copies for transmittal to
Canadian Joint Staff)

Director
David Taylor Model Basin
Washington 25, D.C.
Attn: Code 533

Commandant
Mare Island Naval Shipyard
Vallejo, California
Attn: Design Superintendent

Commandant
Portsmouth Naval Shipyard
Portsmouth, New Hampshire
Attn: Design Superintendent

Director
Aeronautical Instrument Laboratory
Naval Air Development Center
Johnsville, Pennsylvania
Attn: L.S. Guarino

Commanding Officer and Director
U.S. Naval Electronics Lab.
San Diego 52, California
Attn: M.J. Sheehy

Naval Ordnance Test Station
China Lake, California
Attn: Code 1422
LCdr. L.H. Lippincott

U.S. Naval Training Devices Center
Port Washington, L.I., N.Y.
Attn: J. Pecoraro, Head
Exper. Research Div.

Commanding Officer
Office of Naval Research
Branch Office, Navy 100
c/o Fleet Post Office
New York, New York

Commanding Officer
Naval War College
Newport, Rhode Island

Director
Special Projects
Department of the Navy
Washington 25, D.C.

SACLANT
ASW Research Center
Via: Secretariat
State Defense Military
Information Control Comm.
Chief of Naval Operations
Navy Department
Washington 25, D.C.

Bureau of Ships
Navy Department
Washington 25, D.C.
Attn: Code 565R

Bureau of Ships
Navy Department
Washington 25, D.C.
Attn: Code 677

Bureau of Ships
Navy Department
Washington 25, D.C.
Attn: Code 687F

Bureau of Ships
Navy Department
Washington 25, D.C.
Attn: Code 1500

Committee on Undersea Warfare
National Academy of Science
2101 Constitution Avenue
Washington 25, D.C.

Director
U.S. Navy Underwater Sound Lab.
New London, Connecticut

Commander Submarine Force
U.S. Atlantic Fleet
c/o Fleet Post Office
New York, New York

Deputy
ComSubLant
c/o Fleet Post Office
New York, New York

Commander Submarine Force
U.S. Pacific Fleet
c/o Fleet Post Office
San Francisco, Calif.

Commander Antisubmarine Defense
Force
U.S. Pacific Fleet
NAS, Navy No. 128
c/o Fleet Post Office
San Francisco, California

Commander
Submarine Development Group Two
U.S.N. Submarine Base
New London, Connecticut

Commanding Officer
Submarine School
U.S.N. Submarine Base
New London, Connecticut

Office, Chief Signal Officer
Department of the Army
Washington 25, D.C.
Attn: Code SIGRD-5
A. Stombaugh

Technical Library
Room 3E 1065
Pentagon
Washington 25, D.C.

U.S. Naval Ordnance Lab.
White Oak
Silver Spring, Maryland
Attn: Mr. Robert Miller

Commanding Officer
U.S. Naval Ordnance Test Station
Pasadena, California

Bureau of Naval Weapons
Navy Department
Washington 25, D.C.
Attn: Ree
Dr. A. Miller

Commanding Officer
U.S. Naval Ordnance Lab.
White Oak
Silver Spring, Maryland

Bureau of Ships
Navy Department
Washington 25, D.C.
Attn: Mr. Leroy Rosen
Code 361D

Bureau of Ships
Navy Department
Washington 25, D.C.
Attn: Cdr. Richard Aroner
Code 420

Bureau of Ships
Electronics-Electrical Design
Branch - Submarines
Department of the Navy
Washington 25, D.C.
Attn: Mr. N.L. Black
Code 454E

Scripps Institute of Oceanography
Marine Physical Laboratory
San Diego 52, California
Attn: Dr F.N. Spiess

Documentation, Inc.
Man-Machine Information Center
7900 Norfolk Avenue
Washington 14, D.C.
Attn: Mr. A. Keithen

Bell Helicopter Corporation
P.O. Box 482
Fort Worth, Texas
Attn: Mr. O.Q. Niehaus

Douglas Aircraft Company Inc.
El Segundo Division
827 Lapham Street
El Segundo, California
Attn: Dr. H.L. Wolbers

Sperry Gyroscope Company
Surface Armament Division
Great Neck, L.I., New York
Attn: Mr. S. Daunis

C417-61-011
General Dynamics/Electric Boat
Mathematical Concepts of the Automatic Statistical Processing Fire Control Computer
Claude R. Gagnon
Frances R. Callanan
October 1961
145 Pages, 63 Figures

This report is a math model of a simple, statistical fire control scheme. The equations are developed for the determination of relative target motion parameters, a complete bearings-only solution and complete solutions based upon hypothesized inputs of target speed, course or range. The statistical properties of some of the results are analyzed. A method of detecting target zigs is described and statistically evaluated.

C417-61-011
General Dynamics/Electric Boat
Mathematical Concepts of the Automatic Statistical Processing Fire Control Computer
Claude R. Gagnon
Frances R. Callanan
October 1961
145 Pages, 63 Figures

This report is a math model of a simple, statistical fire control scheme. The equations are developed for the determination of relative target motion parameters, a complete bearings-only solution and complete solutions based upon hypothesized inputs of target speed, course or range. The statistical properties of some of the results are analyzed. A method of detecting target zigs is described and statistically evaluated.

C417-61-011
General Dynamics/Electric Boat
Mathematical Concepts of the Automatic Statistical Processing Fire Control Computer
Claude R. Gagnon
Frances R. Callanan
October 1961
145 Pages, 63 Figures

This report is a math model of a simple, statistical fire control scheme. The equations are developed for the determination of relative target motion parameters, a complete bearings-only solution and complete solutions based upon hypothesized inputs of target speed, course or range. The statistical properties of some of the results are analyzed. A method of detecting target zigs is described and statistically evaluated.

C417-61-011
General Dynamics/Electric Boat
Mathematical Concepts of the Automatic Statistical Processing Fire Control Computer
Claude R. Gagnon
Frances R. Callanan
October 1961
145 Pages, 63 Figures

This report is a math model of a simple, statistical fire control scheme. The equations are developed for the determination of relative target motion parameters, a complete bearings-only solution and complete solutions based upon hypothesized inputs of target speed, course or range. The statistical properties of some of the results are analyzed. A method of detecting target zigs is described and statistically evaluated.